REPORT DOCUMENTATION PAGE	Form Approved OMB NO. 0704-0188

The public reporting burden for this collection of information is estimated to average 1 hour per response, including the time for reviewing instructions, searching existing data sources, gathering and maintaining the data needed, and completing and reviewing the collection of information. Send comments regarding this burden estimate or any other aspect of this collection of information, including suggesstions for reducing this burden, to Washington Headquarters Services, Directorate for Information Operations and Reports, 1215 Jefferson Davis Highway, Suite 1204, Arlington VA, 22202-4302. Respondents should be aware that notwithstanding any other provision of law, no person shall be subject to any oenalty for failing to comply with a collection of information if it does not display a currently valid OMB control number.
PLEASE DO NOT RETURN YOUR FORM TO THE ABOVE ADDRESS.

1. REPORT DATE (DD-MM-YYYY) 15-02-2013	2. REPORT TYPE Final Report	3. DATES COVERED (From - To) 1-Jul-2003 - 30-Jun-2012

4. TITLE AND SUBTITLE	5a. CONTRACT NUMBER
Integrated Desert Terrain Forecasting for Military Operations	DAAD19-03-1-0159
	5b. GRANT NUMBER
	5c. PROGRAM ELEMENT NUMBER 611102

6. AUTHORS	
Eric McDonald, Steven Bacon, Sophie Baker, Rivka Amit, Jose Luis Antinao, Marcus Berli, Tom Bullard, Todd Caldwell, Onn Crouvi, Yehouda Enzel, Heather Green, Fabio Iwashita, Darko Koracin, Jerrold	5d. PROJECT NUMBER
	5e. TASK NUMBER
	5f. WORK UNIT NUMBER

7. PERFORMING ORGANIZATION NAMES AND ADDRESSES	8. PERFORMING ORGANIZATION REPORT NUMBER
Desert Research Institute - Reno 2215 Raggio Parkway Reno, NV 89512 -	

9. SPONSORING/MONITORING AGENCY NAME(S) AND ADDRESS(ES)	10. SPONSOR/MONITOR'S ACRONYM(S) ARO
U.S. Army Research Office P.O. Box 12211 Research Triangle Park, NC 27709-2211	11. SPONSOR/MONITOR'S REPORT NUMBER(S) 45410-EV.58

12. DISTRIBUTION AVAILIBILITY STATEMENT

Approved for Public Release; Distribution Unlimited

13. SUPPLEMENTARY NOTES

The views, opinions and/or findings contained in this report are those of the author(s) and should not contrued as an official Department of the Army position, policy or decision, unless so designated by other documentation.

14. ABSTRACT

The goal of this project was to develop an integrated, predictive tool for forecasting desert terrain conditions (soils, vegetation, dust emission potential, trafficability) to support military activities in desert environments. Results have led to the development of multiple approaches to utilize basic terrain data, including space borne and airborne remote-sensing data and imagery, to rapidly predict surface and subsurface terrain conditions over a wide range of scales.

15. SUBJECT TERMS

deserts, terrain conditions, mobility, remote sensing, modeling, soils, geology

16. SECURITY CLASSIFICATION OF:			17. LIMITATION OF ABSTRACT	15. NUMBER OF PAGES	19a. NAME OF RESPONSIBLE PERSON Eric McDonald
a. REPORT UU	b. ABSTRACT UU	c. THIS PAGE UU	UU		19b. TELEPHONE NUMBER 775-673-7302

Standard Form 298 (Rev 8/98)
Prescribed by ANSI Std. Z39.18

Integrated Desert Terrain Forecasting for Military Operations

ABSTRACT

The goal of this project was to develop an integrated, predictive tool for forecasting desert terrain conditions (soils, vegetation, dust emission potential, trafficability) to support military activities in desert environments. Results have led to the development of multiple approaches to utilize basic terrain data, including space borne and airborne remote-sensing data and imagery, to rapidly predict surface and subsurface terrain conditions over a wide range of scales.

During FY2012, progress was made in the following areas:

1.Empirical research to directly study the impact of military vehicle activity on desert soils, and the changes in soil and surface structure that occur with increasing levels of use;

2.Ongoing research to further examine the sources of dust in Israel;

3.Further development of new more automated approaches for landform mapping, to offer faster and more objective alternatives to the standard expert-based methods;

4.Further development and application of soft computing methods for modeling dust emission potential and other soil properties on desert landforms;

5.Ongoing application of developed predictive mapping techniques, including creating maps of: a) salt-rich dust content for the entire country of Afghanistan; and b) PM10 dust emission flux from undisturbed surfaces across all USCENTCOM (U.S. Central Command) countries.

Enter List of papers submitted or published that acknowledge ARO support from the start of the project to the date of this printing. List the papers, including journal references, in the following categories:

(a) Papers published in peer-reviewed journals (N/A for none)

Received		Paper
02/14/2013	57.00	Netra Regmi, Eric McDonald, Steven Bacon. Mapping Quaternary Alluvial Dans in the Southwestern United States based on Multi-Parameter Surface Roughness of LiDAR Topographic Data, Journal of Geophysical Research-Earth Surface, (01 2013): 0. doi:
12/16/2012	12.00	E. McDonald, A. R. Gillespie, R. Amit, Y. Enzel, O. Crouvi, O. Simhai, A. Matmon, N. Porat. The role of the Nile in initiating a massive dust influx to the Negev late in the middle Pleistocene, Geological Society of America Bulletin, (01 2011): 0. doi: 10.1130/B30241.1
12/16/2012	21.00	Sophie Baker, John Gosse, Eric McDonald, Edward Evenson, Oscar Martinez. Quaternary history of the piedmont reach of Río Diamante, Argentina, Journal of South American Earth Sciences, (01 2009): 0. doi:
12/16/2012	19.00	Steven Bacon, Eric McDonald, Todd Caldwell, Graham Dalldorf. Timing and distribution of alluvial fan sedimentation in response to strengthening of late Holocene ENSO variability in the Sonoran Desert, southwestern Arizona, USA, Quaternary Research, (03 2010): 0. doi:
12/16/2012	18.00	Steven Bacon, Eric McDonald, Sophie Baker, Todd Caldwell, Graham Stullenbarger. Desert terrain characterization of landforms and surface materials within vehicle test courses at U.S. Army Yuma Proving Ground, USA, Journal of Terramechanics, (09 2008): 0. doi:
12/16/2012	17.00	Steven Bacon, Eric McDonald, Rivka Amit, Yehouda Enzel, Onn Crouvi. Total suspended particulate matter emissions at high frictionvelocities from desert landforms, Journal of Geophysical Research, (01 2011): 0. doi:
12/16/2012	16.00	Jose Luis Antinao, Eric McDonald. A reduced relevance of vegetation change for alluvial aggradation inarid zones, Geology, (05 2012): 0. doi:
12/16/2012	15.00	Rivka Amit, Ori Simhai, Ayalan Avner, Yehouda Enzel, Ari Matmon, Onn Crouvi, Naomi Porat, Eric McDonald. Transition from arid to hyper-arid environment in the southern Levantdeserts as recorded by early Pleistocene cummulic Aridisols, Quaternanry Science Review , (01 2011): 0. doi:
12/16/2012	14.00	Rivka Amit, Yehouda Enzel, David Sharon. Permanent Quaternary hyperaridity in the Negev, Israel, resulting from regional tectonics blocking Mediterranean frontal systems, Geology, (06 2006): 0. doi: 10.1130/G22354.1
12/16/2012	13.00	Rivka Amit, Yehouda Enzel, Tamir Grodek, Onn Crouvi, Naomi Porat, Avner Ayalon. The role of rare rainstorms in the formation of calcic soil horizons on alluvial surfacesin extreme deserts, Quaternary Research, (03 2010): 0. doi:
12/16/2012	22.00	R. Boroda, R. Amit, A. Matmon, ASTER Team, R. Finkel, N. Porat, Y. Enzel, Y. Eyal. Quaternary-scale evolution of sequences of talus ?atirons in the hyperarid Negev, Geomorphology, (12 2010): 0. doi:
12/19/2012	35.00	Yehouda Enzel, Rivka Amit, Onn Crouvi, Naomi Porat. Abrasion-derived sediments under intensified winds at the latest Pleistocene leading edge of the advancing Sinai–Negev erg, Quaternary Research, (07 2010): 0. doi: 10.1016/j.yqres.2010.04.002
12/19/2012	34.00	Onn Crouvi, Kerstin Schepanski, Rivka Amit, Alan R. Gillespie, Yehouda Enzel. Multiple dust sources in the Sahara Desert: The importance of sand dunes, Geophysical Research Letters, (07 2012): 0. doi: 10.1029/2012GL052145

12/19/2012   33.00   Onn Crouvi, Rivka Amit, Naomi Porat, Alan R. Gillespie, Eric V. McDonald, Yehouda Enzel. Significance of primary hilltop loess in reconstructing dust chronology, accretion rates, and sources: An example from the Negev Desert, Israel,
Journal of Geophysical Research, (05 2009): 0. doi: 10.1029/2008JF001083

12/19/2012   36.00   Yehouda Enzel, Rivka Amit, Uri Dayan, Onn Crouvi, Ron Kahana, Baruch Ziv, David Sharon. The climatic and physiographic controls of the eastern Mediterranean over the late Pleistocene climates in the southern Levant and its neighboring deserts,
Global and Planetary Change, (02 2007): 0. doi: 10.1016/j.gloplacha.2007.02.003

12/19/2012   25.00   Todd Caldwell, Eric McDonald, Steven BAcon, Graham Stullenbarger. The performance and sustainability of vehicle dust courses for desert military testing,
Journal of Terramechanics, (10 2008): 0. doi:

12/19/2012   31.00   Onn Crouvi, Rivka Amit, Yehouda Enzel, Naomi Porat, Amir Sandler. Sand dunes as a major proximal dust source for late Pleistocene loess in the Negev Desert, Israel,
Quaternary Research, (09 2008): 0. doi: 10.1016/j.yqres.2008.04.011

12/19/2012   26.00   Todd Caldwell, Eric McDonald, Michael Young. Soil disturbance and hydrologic reponse at the National Training Center, Ft. Irwin, California,
Journal of Arid environments, (12 2005): 0. doi:

12/19/2012   27.00   Michael Young, Eric McDonald, Todd Caldwell. The seedbed microclimate and active revegetation of disturbed lands in the Mojave Desert,
Journal of Arid environments, (11 2008): 0. doi:

12/19/2012   28.00   Todd Caldwell, Michael Young, Eric McDonald, Jinating Zhu. Soil heterogeneity in Mojave Desert shrublands: Biotic and abiotic processes,
Water Resources Research, (07 2012): 0. doi:

12/19/2012   29.00   Todd G. Caldwell, Michael H. Young, Jianting Zhu, Eric V. McDonald. Spatial structure of hydraulic properties from canopy to interspace in the Mojave Desert,
Geophysical Research Letters, (10 2008): 0. doi: 10.1029/2008GL035095

12/19/2012   30.00   Onn Crouvi, Rivka Amit, Yehouda Enzel, Alan R. Gillespie. Active sand seas and the formation of desert loess,
Quaternanry Science Review , (08 2010): 0. doi: 10.1016/j.quascirev.2010.04.026

12/19/2012   32.00   Onn Crouvi, Eyal Ben-Dor, Michael Beyth, Dov Avigad, Rivka Amit. Quantitative mapping of arid alluvial fan surfaces using field spectrometer and hyperspectral remote sensing,
Remote Sensing of Environment, (09 2006): 0. doi: 10.1016/j.rse.2006.05.004

12/19/2012   37.00   Y. Enzel, R. Amit, T. Grodek, A. Ayalon, J. Lekach, N. Porat, P. Bierman, J. D. Blum, Y. Erel. Late Quaternary weathering, erosion, and deposition in Nahal Yael, Israel: An "impact of climatic change on an arid watershed"?,
Geological Society of America Bulletin, (02 2012): 0. doi: 10.1130/B30538.1

12/19/2012   38.00   V. Etyemezian, G. Nikolich, S. Ahonen, M. Pitchford, M. Sweeney, R. Purcell, J. Gillies, H. Kuhns. The Portable In Situ Wind Erosion Laboratory (PI-SWERL): A new method to measure PM10 windblown dust properties and potential for emissions,
Atmospheric Environment, (06 2007): 0. doi: 10.1016/j.atmosenv.2007.01.018

12/19/2012   39.00   Gerald Flerchinger, Todd Caldwell, Jaepil Cho, Stuart Hardegree. SIMULTANEOUS HEAT AND WATER (SHAW)MODEL: MODEL USE, CALIBRATION, AND VALIDATION,
American Society of Agrcultural and Biological Engineers, (10 2012): 0. doi:

12/19/2012   40.00   Yehouda Enzel, Mordechai Stein, Yonaton Goldsmith. Systematic Mn fluctuations in laminated rock varnish developed on coeval early Holocene flint artifacts along a climatic transect, Negev desert, Israel,
Quaternary Research, (11 2012): 0. doi: 10.1016/j.yqres.2012.07.009

12/19/2012   41.00   Yael Jacoby, Tamir Grodek, Yehouda Enzel, Naomi Porat, Eric V. McDonald, Ofer Dahan. Late Holocene upper bounds of flood magnitudes and twentieth century large floods in the ungauged, hyperarid alluvial Nahal Arava, Israel,
Geomorphology, (03 2008): 0. doi: 10.1016/j.geomorph.2007.06.008

12/19/2012   42.00   A.S. Jayko, Steve Bacon. Late Quaternary MIS 6-8 shoreline features of pluvial Owens Lake, Owens Valley, eastern California,
The geological society of america, (01 2008): 0. doi:

12/19/2012   43.00   Claudia J. Lewis, Eric V. McDonald, Carlos Sancho, José Luis Peña, Edward J. Rhodes. Climatic implications of correlated Upper Pleistocene glacial and fluvial deposits on the Cinca and Gállego Rivers (NE Spain) based on OSL dating and soil stratigraphy,
Global and Planetary Change, (06 2009): 0. doi: 10.1016/j.gloplacha.2009.01.001

12/19/2012   44.00   A. Matmon, O. Simhai, R. Amit, I. Haviv, N. Porat, E. McDonald, L. Benedetti, R. Finkel. Desert pavement-coated surfaces in extreme deserts present the longest-lived landforms on Earth,
Geological Society of America Bulletin, (04 2009): 0. doi: 10.1130/B26422.1

12/19/2012   45.00   J. McAlpine, Darco Koracin, K. Veropoulos, Doug Boyle, Eric McDonald, Greg Lamorey. Determining Atmospheric Dust Concentrations During Strong Flow Perturbations Using a Digital-Optical Technique,
Lecture Notes in Computer Science, (01 2007): 0. doi:

12/19/2012   46.00   Jerrold D. McAlpine, Darko R. Koracin, Douglas P. Boyle, John A. Gillies, Eric V. McDonald. Development of a rotorcraft dust-emission parameterization using a CFD model,
Environmental Fluid Mechanics, (08 2010): 0. doi: 10.1007/s10652-010-9191-y

12/19/2012   47.00   Joseph R. McAuliffe, Eric V. McDonald. Holocene environmental change and vegetation contraction in the Sonoran Desert,
Quaternary Research, (03 2006): 0. doi: 10.1016/j.yqres.2005.11.006

12/19/2012   48.00   Darren G. Meadows, Michael H. Young, Eric V. McDonald. A Laboratory Method for Determining the Unsaturated Hydraulic Properties of Soil Peds,
Soil Science Society of America Journal, (01 2005): 0. doi: 10.2136/sssaj2004.0191

12/24/2012   50.00   Darren G. Meadows, Michael H. Young, Eric V. McDonald. Influence of relative surface age on hydraulic properties and infiltration on soils associated with desert pavements,
Catena, (01 2008): 0. doi: 10.1016/j.catena.2007.05.009

12/24/2012   49.00   Darren G. Meadows, Michael H. Young, Eric V. McDonald. Estimating the Fine Soil Fraction of Desert Pavements Using Ground Penetrating Radar,
Vadose Zone Journal, (01 2006): 0. doi: 10.2136/vzj2005.0095

12/24/2012   51.00   A. Mushkin, A.R. Gillespie. Estimating sub-pixel surface roughness using remotely sensed stereoscopic data,
Remote Sensing of Environment, (11 2005): 0. doi: 10.1016/j.rse.2005.02.018

12/24/2012   53.00   Bryan Stevenson, Eric McDonald, Todd Caldwell. Root patterns for Larrea tridentata in relation to soil morphology in Mojave desert soils of different ages,
The Mojave Desert: Ecosystem Processes and Sustainability, (01 2009): 0. doi:

12/24/2012   54.00   Mark Sweeney, Vic Etyemezian, Torin Macpherson, William Nickling, John Gillies, George Nikolich, Eric McDonald. Comparison of PI-SWERL with dust emission measurements from a straight-line field wind tunnel,
Journal of Geophysical Research, (02 2008): 0. doi: 10.1029/2007JF000830

TOTAL: **40**

Number of Papers published in peer-reviewed journals:

(b) Papers published in non-peer-reviewed journals (N/A for none)

Received   Paper

  TOTAL:

Number of Papers published in non peer-reviewed journals:

(c) Presentations

Ben-Israel, M., Erel, Y., Enzel, Y., and Amit, R., 2012, Geochemical proxies for changes in dust sources in Negev desert loess, Goldschmidt: Montreal, Canada.

Caldwell, T.G., McDonald, E., Bacon, S., Young, M., and Lin, H., 2012, Hydropedology and ecosystem response on an arid soil chronosequence, 2nd International Conference on Hydropedology: Leipzig, Germany.

Caldwell, T.G., Wohling, T., Flerchinger, M.H., Young, E.V., and MCDonald, S.P., 2011, Inverse Modeling water contents of semiarid soils using multiobjective parameter optimization, ASA-CSSA-SSSA International Annual Meeting: San Antonio, TX.

Goldsmith, Y., Stein, M., and Enzel, Y., 2012, Characterizing rock varnish developed on earliest Holocene Negev flint artifacts as a potential environmental or climatic indicator, Israel Geological Society Annual Meeting: Ashkelon, Israel.

Goldsmith, Y., Stein, M., and Enzel, Y., 2012, Rock varnish as a potential environmental or climatic indicator, The Geological Survey of Israel Annual Meeting: Jerusalem.

Harel, M., Amit, R., Enzel, Y., and Porat, N., 2012, Complex landscape evolution of the central Coastal Plain (Israel) based on buried and relict surfaces, Israel Geological Society Annual Meeting: Ashkelon.

McAlpine, J.D., Koracin, D., Bacon, S., Baker, S., and McDonald, E., 2012, Development of an operational predictive tool for visibility degradation and brownout caused by rotorcraft dust emissions., 2012 Weather Impacts Decision Aids (WIDA) Workshop: Reno, NV.

McDonald, E., Spears, L., Fleming, S.D., and Bacon, S., 2012, Developing science-based testing – characterizing the physical environment with enough detail to support test procedures, 28th Annual National Test and Evaluation Conference: Hilton Head, South Carolina.

Number of Presentations: 8.00

Non Peer-Reviewed Conference Proceeding publications (other than abstracts):

Received   Paper

  TOTAL:

Number of Non Peer-Reviewed Conference Proceeding publications (other than abstracts):

Peer-Reviewed Conference Proceeding publications (other than abstracts):

Received   Paper

TOTAL:

Number of Peer-Reviewed Conference Proceeding publications (other than abstracts):

(d) Manuscripts

Received   Paper

TOTAL:

Number of Manuscripts:

Books

12/16/2012   20.00   Steven Bacon, Eric McDonald, Graham Dalldorf, Sophie Baker, Don Sabol,, Tim Minor, Scott Bassett, Shawn MacCabe, Tom Bullard. Predictive soil maps based on geomorphic mapping, remote sensing, and soil databases in the desert southwest, New York: Springer Science+ Business Media, (01 2010)

12/18/2012   23.00   Thomas Bullard, Steven Bacon, Philippe Canonne, Neil Smith, Charles Queen, Lane Ruehlen, Joseph Ormond. Geology, Geomorphology and the Vertical Dimension of the World War II Battlefield, Vienna, Austria: Arbeitsgemeinschaft Truppendienst, Ministry of Defence and Sports, (01 2011)

12/24/2012   52.00   David Schafer, Michael Young, Stephen Zitzer, Eric McDonald, Todd Caldwell. Coupled environmental processes in the Mojave Desert and implications for ET covers as stable landforms., Reston, VA: American Society of Civil Engineers, (01 2006)

12/24/2012   55.00   Douglas R. Caldwell, Judy Ehlen, Russell S. Harmon. Studies in Military Geography and Geology, Dordrecht: Springer Netherlands, (01 2004)

12/24/2012   56.00   Eric McDonald, Todd Caldwell. Geochemical and Physical Characteristics of Iraqi Dust and Soil Samples, Nottingham: Land Quality Press, (01 2008)

TOTAL: **5**

Patents Submitted

Patents Awarded

Awards

Graduate Students

NAME	PERCENT_SUPPORTED	Discipline
Todd Caldwell	0.15	
FTE Equivalent:	**0.15**	
Total Number:	**1**	

Names of Post Doctorates

NAME	PERCENT_SUPPORTED
Fabio Iwashita	0.55
Netra Regmi	0.60
FTE Equivalent:	**1.15**
Total Number:	**2**

Names of Faculty Supported

NAME	PERCENT SUPPORTED	National Academy Member
Jose Luis Antinao	0.23	
Steve Bacon	0.23	
Sophie Baker	0.14	
Tom Bullard	0.10	
Todd Caldwell	0.15	
Russ Cullison	0.01	
Heather Green	0.29	
Elizabeth Huenupi Pena	0.16	
Janis Klimowicz	0.02	
Darko Koracin	0.09	
Eric McDonald	0.35	
George Nikolich	0.09	
Don Sabol	0.12	
Rina Schumer	0.12	
FTE Equivalent:	**2.10**	
Total Number:	14	

Names of Under Graduate students supported

NAME	PERCENT SUPPORTED
FTE Equivalent:	
Total Number:	

Student Metrics
This section only applies to graduating undergraduates supported by this agreement in this reporting period

The number of undergraduates funded by this agreement who graduated during this period: 0.00

The number of undergraduates funded by this agreement who graduated during this period with a degree in science, mathematics, engineering, or technology fields: 0.00

The number of undergraduates funded by your agreement who graduated during this period and will continue to pursue a graduate or Ph.D. degree in science, mathematics, engineering, or technology fields: 0.00

Number of graduating undergraduates who achieved a 3.5 GPA to 4.0 (4.0 max scale): 0.00

Number of graduating undergraduates funded by a DoD funded Center of Excellence grant for Education, Research and Engineering: 0.00

The number of undergraduates funded by your agreement who graduated during this period and intend to work for the Department of Defense 0.00

The number of undergraduates funded by your agreement who graduated during this period and will receive scholarships or fellowships for further studies in science, mathematics, engineering or technology fields: 0.00

Names of Personnel receiving masters degrees

NAME
Total Number:

Names of personnel receiving PHDs

NAME
Todd Caldwell
Total Number: 1

Names of other research staff

NAME	PERCENT_SUPPORTED
Marie DelGrego	0.46
Kopila Regmi Paudel	0.18
FTE Equivalent:	**0.64**
Total Number:	**2**

Sub Contractors (DD882)

Inventions (DD882)

Scientific Progress

See Attachment

Technology Transfer

Integrated Desert Terrain Forecasting for Military Operations

Final Report - Scientific Progress and Accomplishments

Reporting Period: July 1, 2003 to June 30, 2012

Eric McDonald, Steven Bacon, Sophie Baker, Rivka Amit, Jose Luis Antinao, Marcus Berli, Tom Bullard, Todd Caldwell, Onn Crouvi, Yehouda Enzel, Heather Green, Fabio Iwashita, Darko Koracin, Jerrold D. McAlpine, Tim Minor, Netra Regmi and Don Sabol.

Prepared by

Desert Research Institute,
Nevada System of Higher Education

Prepared for

U.S. Army Research Office

Integrated Desert Terrain Forecasting for Military Operations

Eric McDonald, Steven Bacon, Sophie Baker, Rivka Amit, Jose Luis Antinao, Marcus Berli, Tom Bullard, Todd Caldwell, Onn Crouvi, Yehouda Enzel, Heather Green, Fabio Iwashita, Darko Koracin, Jerrold D. McAlpine, Tim Minor, Netra Regmi and Don Sabol.

Final Report: Scientific progress

and accomplishments

Funding No.: DAAD19-03-1-0159

Reporting Period

July 1, 2003 to June 30, 2012

Prepared by:

Desert Research Institute

2215 Raggio Parkway, Reno NV 89512

Prepared for:

U.S. Army Research Office

P.O. Box 12211

Research Triangle Park, NC 27709-2211

ABSTRACT

The goal of this project has been to develop an integrated, predictive tool for forecasting desert terrain conditions (soils, vegetation cover, dust emission potential, mobility hazards) to support military activities in desert environments. Project results have led to the development of a geographic information system (GIS) platform to predict essential surface and subsurface terrain parameters through the integration of data on the spatial distribution, age, and geology of desert landforms. Multiple approaches have been developed to utilize basic terrain data, including space borne and airborne remote-sensing data and imagery, to predict detailed surface and subsurface terrain conditions over a wide range of scales in near real-time.

During FY2012, progress was made in the following areas:

1. ***Empirical research to directly study the impact of military vehicle activity on desert soils, and the changes in soil and surface structure that occur with increasing levels of use.*** These experiments are important not only to determine how desert soil conditions influence operational mobility, but also to evaluate the potential emissivity of these soils following various degrees of disturbance, and to enhance our understanding of the mid- to long-term recoverability of desert soil surfaces following military operations including testing and training. The research has included the establishment of a continual study site, named a Master Environmental Reference Site (MERS), located at YPG where it will be protected indefinitely for current and future analyses. As part of this project, the process of military vehicle-related surface deterioration, especially rut formation, has been modeled numerically. Model validation has been carried out using measurements made at the MERS site. This work has elucidated the details of the surface deterioration process, and the soil mechanical properties that most influence soil surface resilience or fragility.

2. ***Ongoing research to further examine the sources of dust in Israel.*** Dust plays multiple roles in mediating physical and biogeochemical exchanges among the atmosphere, land, and ocean, as well as having a huge impact on military activity. However, even after decades of research, the sources and formation processes of dust and loess in deserts are still unclear. A major goal of this project was to examine the sources and formation processes of dust in Israel and its surroundings. Two projects finalized this year involve: a) examining the use of geochemical proxies (Sr and Nd isotopes) to trace changes in dust sources through time in the Negev, and; b) investigating buried soils as samplers of Quaternary dust in the central coastal plain of Israel. Results of these and previous related projects indicate that sand dunes are an important dust source, and eolian abrasion is a key process for generating coarse and fine dust grains in deserts. This differs from the previously widely-held hypothesis that the main sources of loess and fine dust are playas and fluvial deposits.

3. ***Further development of new more automated approaches for landform mapping, to offer faster and more objective alternatives to the standard expert-based methods.*** This year, an automated, algorithm-based, semi-quantitative model has been refined to allow the detailed differentiation of

landforms, including alluvial fan surfaces of different ages. The model comprises a five step process of analyzing the morphological characteristics of the land surface at multiple scales, and was applied in Cadiz Valley in the Mojave Desert, California.

4. ***Further development and application of soft computing methods for modeling dust emission potential and other soil properties on desert landforms.*** This method, which combines an often sparse field data set with a complete regional data set of geomorphic parameters generated from DEM- and ASTER-derived spectral data, provides a low cost method of creating soil property maps similar to those produced by expert-based mapping methods. This year's work included application of the method to predict soil properties across a range of landform types in Cadiz Valley, California.

5. ***Ongoing application of developed predictive mapping techniques, that includes creating maps of: a) salt-rich dust content for the entire country of Afghanistan; and b) PM10 dust emission flux from undisturbed surfaces across all USCENTCOM (U.S. Central Command) countries.*** The first involved the integration of landform mapping, soil property predictions (derived from the global soils database developed as part of this project), climate data, and bedrock geology data. The second integrated landform mapping data with data derived from field measurements of dust emission potential. Both of these tasks provide important resources for the US military, and also contribute to our understanding of the relationships between readily determinable environmental parameters and the dust content and emission potential of desert soils.

Table of Contents

List of Figures

List of Tables

PROJECT OVERVIEW

Overall Goal and Objectives

The primary goal of this multi-year project was to develop an integrated, predictive, numerical model for forecasting terrain conditions and surface responses affecting trafficability and mobility at different scales in desert regions to support military tactical operations, testing, and training.

Key objectives included the following:

- Development and validation of conceptual and numerical models for predicting terrain conditions, particularly in international settings that represent critical desert terrain types not found in the U.S.

- Development of an extensive soil and terrain database to include the most critical terrain types common to desert areas of strategic interest

- Integration of knowledge of desert surficial processes and remote-sensing to develop dynamic models for predicting desert terrain conditions and associated terrain hazards

- Development of prototype visualization modules to support testing and training in desert terrains

Significance and Army Value

Deserts are—and will continue to be—strategic sites for military operations, and the U.S. armed forces have been called upon repeatedly to operate in the deserts of the Middle East and central Asia. Military success in desert conditions requires familiarity with these environments, as well as appropriate training and testing. Specifically, the need for mobility, flexibility, and rapid deployment of forces requires the ability to predict diverse conditions—a challenge in deserts which are extreme environments characterized by rapid change in local conditions. For example, sudden loss of visibility from dust emissions caused by military operations can result in damage or loss of tactical vehicles and aircraft; and the emission of large dust plumes also discloses vehicle activity and location. Another risk is that dust-rich soils can become incohesive and impassable when wet, drastically reducing mobility.

Avoiding locations susceptible to extreme dust emissions and other terrain-related hazards requires the ability to predict soil and terrain conditions, a difficult task due to limited information and adverse circumstances. The results of this project provide the U.S. military with scientific tools for rapid and efficient forecasting of desert terrain that is required prior to deployment of personnel, vehicles, and weapons. These new tools will significantly enhance intelligence gathering, guide tactical operational planning, and benefit battlefield readiness requirements for the twenty-first century U.S. military.

Further, and nearly as important to Army Research Office (ARO) and Department of Defense (DoD) mission statements, results from this project support efforts to enhance stewardship of DoD installations through careful analysis of the impact of U.S. Army activities on the natural environment. Research from this project will increase knowledge of the role of desert surficial processes in the sustainability and use of military lands.

Approach

Our research strategy to develop and validate a dynamic predictive terrain model for diverse desert conditions was designed to be interdisciplinary, integrating advanced knowledge of surface processes (pedologic, hydrologic, geomorphic, engineering), remote-sensing, numerical modeling, and visualization for desert regions.   Development of new technology, along with innovative application of existing analytical tools, has been undertaken to characterize and monitor desert processes. Primary research strategies consisted of:

Predicting terrain conditions through image analysis and inversion of geomorphic models—Widely available geographic data sources (e.g., digital elevation maps, geologic maps, satellite and aerial imagery) can provide some information regarding terrain conditions but are insufficient for predicting trafficability. These sources do not provide detailed spatial information on the desert surface and immediate subsurface (<100 cm depth), information that now can be provided by linking geomorphic modeling with image analysis. We have developed methods for predicting terrain conditions that start with available imagery (i.e., airborne, satellite, existing maps), and assign soil and surface physical properties to produce output with terrain prediction capabilities that range from terrain favorability maps to input parameters for numerical simulations and visualizations. Soil and surface physical properties are assigned through systematic integration of data on the spatial distribution, age, and geology of desert landforms with data on their associated soil and surface features, as well as through geomorphic models linking observable surface features (e.g., soil cover, landscape position, parent material) with conceptual models of soil formation.

Acquiring soil-surface data to model potential dust emission—Understanding critical relationships between desert soils, their surface conditions (e.g., roughness, vegetation cover), and their emission of dust (airborne particulate matter) as a result of military activities is critical to successful execution of military operations in desert terrain. Information about the dust emission potential of desert soils is required to forecast terrain conditions and develop realistic visualizations supporting military operations. We have gathered critical field data on the dust characteristics (e.g., physical, chemical, hydrologic properties) and emission potential of desert soils from key locations across the southwestern U.S., the Middle East, and Central Asia, which provide strong analogs to identified dust-producing soils. Multiple field measurements across diverse desert soils have been conducted using DRI's Portable In-Situ Wind Erosion Laboratory (PI-SWERL): a small, portable, prototype wind tunnel for evaluating emissions created by aerodynamic forces. Use of this instrument results in the generation of wind shear close to the ground.   The wind shear forces soil particles to begin to move along the ground

surface, causing PM_{10} and $PM_{2.5}$ dust particles to be dislodged and emitted. These dust studies are important for assessing the relationship between the soil and surface properties of a landform and its dust emission potential, and also serve to identify similarities and differences in the dust emission potentials of soils available for testing and training in the U.S. and those found within strategically sensitive areas outside the U.S., such as in the Middle East.

Developing a global database of critical soil and terrain features—Soil and terrain data are commonly unavailable for areas of strategic interest and military operation. We have developed a database of global desert terrain conditions, which includes data on physiography, soil, surface cover, and dust content for specific locations.   Data collection focused on identifying attributes that typify the most critical (in terms of potential terrain hazards affecting mobility and dust emission), and common, physiographic units that occur in deserts encountered during military operations across the globe. These data provide proxy soil and dust characterization in areas where existing data are not available, particularly in international settings.

Advancing remote-sensing strategies—Pre-existing remote-sensing technology required modification and testing to enhance mapping of lithology, surface moisture, and surface roughness. Testing and refinement of remote-sensing techniques—including ASTER, MASTER, and LIDAR—that can aid in rapid classification of desert terrain (in terms of surface age, micro-topography/surface roughness, surface moisture, bedrock composition etc.) have been conducted. Remote-sensing data has been integrated into the GIS platform to aid image analysis for predicting terrain properties.

Implementing an integrated modeling approach—Advancement of desert terrain predictive modeling required the incorporation of data on rapidly changing soil and surface conditions and their effect on surface mobility and tactical operations. We have applied recent developments in the application of the USGS Modular Modeling System (MMS) framework, an object-oriented framework for environmental simulation models. An integrative modeling approach is required to quickly couple a variety of new and existing numeric models of important soil, surface, and climate processes— thereby linking terrain properties with past and predicted environmental conditions. An example of this approach is modeling dust emission generated by either wheeled or tracked vehicles. Field data and conceptual knowledge of key desert processes and properties—primarily soil moisture, dust emission and wind erosion, soil compaction, and shear strength—have been used to selectively correlate the most appropriate process algorithms from applicable models to create an "optimal" model for the desired application. Where existing algorithms were not appropriate, new algorithms have been developed and added to the system. This modular approach to model development and application provides a flexible method for identifying the most appropriate approaches given a specific set of user needs and constraints.

Developing advanced environmental modeling and visualization—The overall objective of this task was to advance environmental modeling and visualization in an interactive virtual environment for use in a variety of defense and environmental applications. Our goal has been to determine if terrain predictive capabilities can be incorporated into an effective simulation tool to serve as a platform for training purposes or for testing operation tactics and procedures. Often referred to by the trademarked designation *CAVE™*, this emerging technology has the capability to provide visual, aural, and even tactile presentation

of complex data in scientific research applications. It may simulate real-world environments for training applications that would otherwise be unavailable or costly. The first simulation in this project was based on a three-dimensional representation of a complex desert terrain at the US Army National Training Center (Ft. Irwin CA), and was complete with interactive soil surfaces capable of dust emission and other changes that may limit operational mobility.

SCIENTIFIC ACCOMPLISHMENTS

1. Determination of Predictive Relations between Landscape, Soil, and Surface Parameters

1.1 Summary of overall accomplishments

The terrain forecasting model that we have developed relies heavily on being able to predict the relationships between climatic conditions, physiographic setting (landform), bedrock geology, and the age of the landscape. It has therefore been crucial to expand our knowledge of these systematic relationships. To this end, extensive research has been done on geomorphic processes in a variety of settings around the world, with a main focus on arid and semi-arid zones. The following paragraphs summarize the main areas of accomplishment related to this goal.

a) **Development of chronosequences**

Multiple chronosequences have been developed whereby an assemblage of landforms (mostly alluvial landforms) in an area have been mapped and their soils characterized in detail using both field description and extensive laboratory analysis. Geochronological techniques have also been applied in many key locations to determine the absolute ages of the landforms and their related soils, so that certain soil characteristics can be linked to age, and the rate of geomorphic and soil development processes can be determined. This work not only gives insight into what terrain characteristics to expect in different aged landscapes, but also into paleoclimate, and the climate related factors that drive geomorphic processes (e.g., McAuliffe and McDonald, 2006; Enzel et al., 2008; Jacoby et al., 2008; Jayko and Bacon, 2008; Baker et al., 2009; Lewis et al., 2009; Matmon et al., 2009; Stevenson et al., 2009; Bacon et al., 2010; Boroda et al., 2011; Enzel et al., 2012; Goldsmith et al., 2012; Antinao and McDonald, 2013). Such chronosequence development efforts have been carried out in multiple locations that span different climatic and physiographic settings both within the US – in the Sonoran Desert (e.g. the Cibola Range Fans) and the Mojave Desert (the Providence Mountains, Owens Valley, Death Valley, and Panamint Valley) – and outside of the US – in Baja California, Argentina, northern Spain, and Israel. Both Pleistocene and Holocene landforms have been dated using a variety of methods including Terrestrial In-Situ Cosmogenic Nuclides (TCN), luminescence dating, and radiocarbon dating.

Furthermore, because much soil-geomorphic work being carried out in arid zones focuses on alluvial landforms (including much of the work described in the last paragraph), considerable effort has been made to characterize the soil-landscape relations in other key landforms that

15

occur in deserts and are subject to military use both in testing/training facilities and in areas of deployment. The most important of these landform types is playas. Results indicate that the assessment of microtopography yields valuable information about the firmness or hardness of the playa surface, which is critical for military vehicle operation. Ultimately, this work shows that visual assessment of the playa surface using satellite or aerial imagery can be used to establish the suitability of playa surfaces for military operations. Additionally, research was conducted to better understand, and hence increase our prediction capability of, common soil characteristics in the areas marginal to desert playas. Soils marginal to playas have not previously been extensively studied, and our work indicates that these soils have a diverse range of properties that can severely impact military operations.

b) Measuring and modeling hydrologic properties of soils

In order to predict terrain related hazards, especially those related to dust emission and trafficability, it is crucial to understand the response of various land surfaces and soils to precipitation and to disturbance of different durations (both natural and anthropogenic). Because these responses are intrinsically linked to soil moisture content and the hydraulic characteristics of the soil, much work has been undertaken to characterize and model the hydrologic properties of various soils, as they relate to plant health, dust emission, trafficability, and flooding (e.g., Caldwell et al., 2008).

c) Experiments to analyze the trafficability of desert surfaces

Empirical research has been carried out to directly study the impact of military vehicle activity on desert soils, and the changes in soil and surface structure that occur with increasing levels of use. These experiments are important not only to determine how desert soil conditions influence operational mobility, but also to evaluate the potential emissivity of these soils following varying degrees of disturbance, and to enhance our understanding of the mid- to long-term recoverability of desert soil surfaces following military maneuvers, including training and testing. The research has included the establishment of a continual study site named a Master Environmental Reference Site (MERS) located in the YPG where it will be protected indefinitely for current and future analyses. Furthermore, attempts have been made to simulate using numerical modeling the process of military vehicle related surface deterioration, specifically due to rut formation. Model validation was carried out using measurements made at the MERS site. While the models failed to simulate the process accurately, this work has elucidated the details of the process and the soil mechanical properties that most influence soil surface resilience or fragility.

d) Amassing terrain and soil data via field samples, remote-sensing data, and published literature

In addition to the detailed field based studies listed above, much effort has been put into collecting geomorphic and terrain data for large areas of the globe, with a particular focus on the US southwest and SW Asia. Landform mapping of Afghanistan, Iraq, Iran, Pakistan, Syria, Jordan, Lebanon, and Israel has been carried out from satellite imagery; published data on bedrock geology and climate has been gathered; and whenever possible soil samples from these areas have been procured and put through extensive laboratory analysis (including sample sets from Iraq, Afghanistan, and Egypt). In this way we have amassed a huge amount of soil and terrain data and expertise, which ameliorates our understanding of the systematic relationships between soil characteristics and specific environmental parameters in various settings, especially those not well represented in the US.

1.2 Accomplishments during FY2012

1.2.1 Desert Pavement Deterioration due to Heavy Vehicle Traffic – Soil Mechanical Measurements and Model Calculations

(Markus Berli, Todd Caldwell, Eric McDonald, Daniel Gilewitch)

Desert pavement deterioration from military off-road vehicle operations is of increasing interest for military training purposes as well as for soil protection and remediation activities. The goal of this study was to mechanically measure and model the deterioration due to heavy vehicle traffic of fine-textured desert pavement with distinct secondary structure. For this purpose, traffic experiments were carried out with an eight-wheeled "Stryker" Light Armored Vehicle III at Yuma Proving Ground (YPG). The soil bearing capacity and shear strength of undisturbed and disturbed desert pavement were determined using a pocket penetrometer (Geotest Instrument Corp. Evanston, IL) and shear vane tester (Humboldt H-4212MH), respectively. Analytical Terzaghi- and Bekker-, as well as cone-index-, based models (hereafter referred as WES models) were used to predict the onset and evolution of rut formation for single and multiple passes of a "Stryker" vehicle (Figure 1). Bearing capacity and shear strength were employed as mechanical measures of soil structure. Rut depth and soil bulk density measurements were used for evaluating the rut formation models. We found that shear strength and bearing capacity of desert pavement decrease with increasing number of vehicle passes, reaching their respective detection limit concurrent to a complete loss of the secondary structure. The onset of rut formation under a "Stryker" agrees with bearing capacity measurements of the undisturbed desert pavement and can be predicted reasonably well employing Terzaghi and Bekker-type as well as the WES models based on shear strength measurements. For multiple passes, rut depth increases linearly at an average rate of 0.75 mm per wheel and 3 mm per vehicle pass, respectively (Figure 2). None of the employed models were able to simulate the measured increases in rut depth accurately. Comparison of rut depth and bulk density measurements with respective model calculations indicate that rut formation on desert pavement probably consists of two processes: (1) compaction of the soil due to the first vehicle pass and (2) soil surface wear ("abrasion") due to shear stresses at the tire-soil interface for subsequent passes.
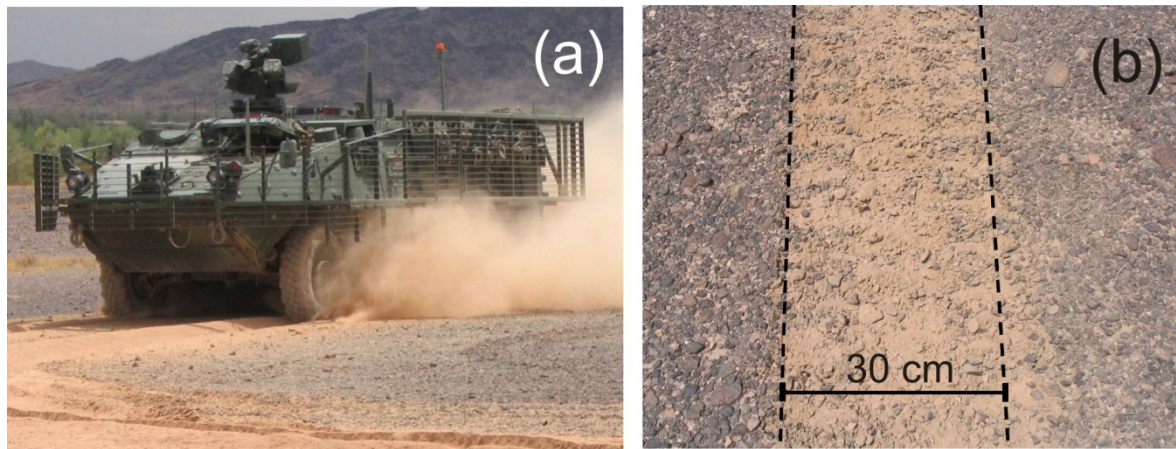
Figure 1. (a) The Stryker Light Armored Vehicle III used during the traffic experiment and (b) detail of rut at the soil surface after five passes.
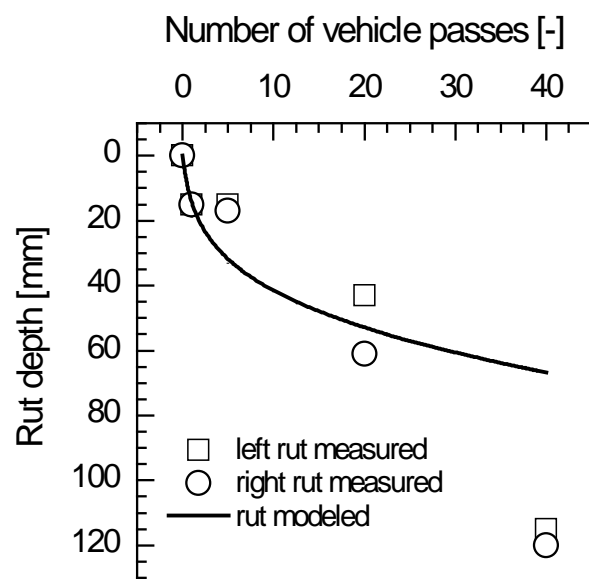
Figure 2. Measured versus calculated rut depths for up to forty passes by the Stryker.

1.3 Published manuscripts resulting from this work

Antinao, J.L., and McDonald, E.V., 2013, A reduced relevance of vegetation change for alluvial aggradation in arid zones: Geology.

Bacon, S.N., McDonald, E.V., Baker, S.E., Caldwell, T.G., and Stullenbarger, G., 2008, Desert terrain characterization of landforms and surface materials within vehicle test courses at U.S. Army Yuma Proving Ground, USA: Journal of Terramechanics, v. 45, p. 167-183.

Bacon, S.N., McDonald, E.V., Caldwell, T.G., and Dalldorf, G.K., 2010, Timing and distribution of alluvial fan sedimentation in response to strengthening of late Holocene ENSO variability in the Sonoran Desert, southwestern Arizona, USA: Quaternary Research, v. 73, p. 425-438.

Baker, S.E., Gosse, J.C., McDonald, E.V., Evenson, E.B., and Martinez, O., 2009, Quaternary history of the piedmont reach of the Rio Diamante, Argentina: Journal of South American Earth Sciences, v. 28, p. 54-73.

Berli, M., Caldwell, T.G., McDonald, E.V., and Gilewitch, D.A., In press, Desert pavement deterioration due to heavy vehicle traffic – soil mechanical measurements and model calculations: Journal of Terramechanics.

Boroda, R., Amit, R., Matmon, A., Team, A., Finkel, R., Porat, N., Enzel, Y., and Eyal, Y., 2011, Quaternary-scale evolution of sequences of talus flatirons in the hyperarid Negev: Geomorphology, v. 127, p. 41-52.

Bullard, T.F., Bacon, S.N., Canonne, P., Smith, J.N., Queen, C.R., Ruehlen, L., and Ormond, J., 2011, Geology, geomorphology, and the vertical dimension of the World War II battlefield, *in* Hausler, H., and Mang, R., eds., International Handbook of Military Geography, Volume 2: Vienna, Austria, Arbeitsgemeinschaft Truppendienst, Ministry of Defence and Sports, p. 99-106.

Caldwell, T.G., McDonald, E.V., Bacon, S.N., and Stullenbarger, G., 2008, The performance and sustainability of vehicle dust courses for desert military testing: Journal of Terramechanics, v. 45, p. 213-221.

Caldwell, T.G., McDonald, E.V., and Young, M.H., 2006, Soil disturbance and hydrologic reponse at the National Training Center, Ft. Irwin, California: Journal of Arid Environments, v. 67, p. 456-472.

Caldwell, T.G., McDonald, E.V., and Young, M.H., 2009, The seedbed microclimate and active revegetation of disturbed lands in the Mojave Desert: Journal of Arid Environments, v. 73, p. 563-573.

Caldwell, T.G., Wohling, T., Young, M.H., Boyle, D.P., and McDonald, E., In press, Characterizing disturbed desert soils using multiobjective inverse parameter optimization: Vadose Zone Journal.

Caldwell, T.G., Young, M.H., McDonald, E.V., and Zhu, J.T., 2012, Soil heterogeneity in Mojave Desert shrublands: Biotic and abiotic processes: Water Resources Research, v. 48.

Caldwell, T.G., Young, M.H., Zhu, J.T., and McDonald, E.V., 2008, Spatial structure of hydraulic properties

from canopy to interspace in the Mojave Desert Geophysical Research Letters, v. 35.

Enzel, Y., Amit, R., Dayan, U., Crouvi, O., Kahana, R., Ziv, B., and Sharon, D., 2008, The climatic and physiographic controls of the eastern Mediterranean over the late Pleistocene climates in the southern Levant and its neighboring deserts: Global and Planetary Change, v. 60, p. 165-192.

Enzel, Y., Amit, R., Grodek, T., Ayalon, A., Lekach, J., Porat, N., Bierman, P., Blum, J.D., and Erel, Y., 2012, Late Quaternary weathering, erosion, and deposition in Nahal Yael, Israel: An "impact of climatic change on an arid watershed"?: Geologic Society of America Bulletin, v. 124, p. 705-722.

Flerchinger, G.N., Caldwell, T.G., Cho, J., and Hardegree, S.P., 2012, Simultaneous Heat and Water (SHAW) Model: Model use, calibration, and validation: Transactions of the ASABE, v. 55, p. 1395-1411.

Goldsmith, Y., Stein, M., and Enzel, Y., In press, Geochemical mechanism of Mn accumulation in laminated rock varnish from the Negev Desert, Israel: Geochimica et Cosmochimica Acta.

Goldsmith, Y., Enzel, Y., and Stein, M., 2012, Systematic Mn fluctuations in laminated rock varnish developed on coeval early Holocene flint artifacts along a climatic transect, Negev desert, Israel: Quaternary Research, v. xxx-xxx.

Jacoby, Y., Grodek, T., Enzel, Y., Porat, N., McDonald, E.V., and Dahan, O., 2008, Late Holocene upper bounds of flood magnitudes and twentieth century large floods in the ungauged, hyperarid alluvial Nahal Arava, Israel Geomorphology, v. 95, p. 274-294.

Jayko, A.S., and Bacon, S.N., 2008, Late Quaternary MIS 6-8 shoreline features of pluvial Owens Lake, Owens Valley, eastern California: Geological Society of America Special Paper: Late Cenozoic drainage history of the southwestern Great Basin and lower Colorado River region: Geologic and biotic perspectives, v. 439, p. 185-206.

Lewis, C.J., McDonald, E.V., Sancho, C., Pena, J.L., and Rhodes, E.J., 2009, Climatic implications of correlated Upper Pleistocene glacial and fluvial deposits on the Cinca and Gallego Rivers (NE Spain) based on OSL dating and soil stratigraphy: Global and Planetary Change, v. 67, p. 141-152.

Matmon, A., Simhai, O., Amit, R., Haviv, I., Porat, N., McDonald, E.V., Benedetti, L., and Finkel, R., 2009, Desert pavement-coated surfaces in extreme deserts present the longest-lived landforms on Earth: Geologic Society of America Bulletin, v. 121, p. 688-697.

McAuliffe, J., and McDonald, E.V., 2006 Holocene environmental change and vegetation contraction in the Sonoran Desert: Quaternary Research, v. 65, p. 204-215.

Meadows, D., Young, M.H., and McDonald, E.V., 2005, A laboratory method for determining the unsaturated hydraulic properties of soil peds: Soil Science Society of America Journal, v. 69, p. 807-815.

Meadows, D., Young, M.H., and McDonald, E.V., 2006, Estimating the fine soil fraction of desert pavements using ground penetrating radar: Vadose Zone Journal, v. 5, p. 720-730.

Meadows, D., Young, M.H., and McDonald, E.V., 2008, Influence of relative surface age on hydraulic properties and infiltration on soils associated with desert pavements: Catena, v. 72, p. 169-178.

Shafer, D.S., Young, M.H., Zitzer, S.F., McDonald, E.V., and Caldwell, T.G., 2006, Coupled environmental processes in the Mojave Desert and implications for ET covers as stable landforms., *in* Miller, G.A., Zapata, C.E., Houston, S.L., and Fredlund, D.G., eds., Unsaturated Soils, American Society of Civil Engineers, p. 718-729.

Stevenson, B., McDonald, E.V., and Caldwell, T.G., 2009, Root patterns for Larrea tridentata in relation to soil morphology in Mojave desert soils of different ages, *in* Webb, R.H., Fenstermaker, L.F., Heaton, J.S., Hughson, D.L., McDonald, E.V., and Miller, D.M., eds., The Mojave Desert: Ecosystem Processes and Sustainability, University of Nevada Press, p. 312-338.

2. Acquiring Soil-Surface Data to Model Potential Dust Emission

2.1 Summary of overall accomplishments

Dust emission is a major soil-related hazard for military operations. Identifying dust source areas is a critical task for daily operations, for monitoring potential environmental health impacts to military personnel, and for mitigating abrasion and corrosion to military aircraft, vehicles, and equipment operating in desert regions. Therefore, considerable effort has been put into: (1) research to understand where in the geologic record high dust content deposits occur, with a focus on Israel and surrounding areas; (2) developing methods to measure and predict dust emission potential of various soil surfaces, and; (3) empirically measuring dust emission related to helicopter flight. All three of these areas of focus (described in more detail below) contribute greatly to our ability to predict dust-related hazards, as well as to the broader understanding of the role of dust in geomorphic processes and of its interactions with paleoclimate.

    a)   **Formation, sources, and role of desert dust**

The scientific community has now recognized that dust plays multiple roles in mediating physical and biogeochemical exchanges among the atmosphere, land and ocean. Yet, to estimate the past, current, and future impacts of dust (both fine dust and coarse dust, which can be termed as *loess*) on the climate and on the environment, quantitative data on the chemical, physical and optical properties of the dust particles and on their source location, are critical. However, even after decades of research, the sources and formation processes of dust and loess in deserts are still unclear. A component of this project was to track the sources of dust in Israel and its surroundings, and to suggest the most probable processes for the formation of the dust. Work was carried out at various spatial scales (from regional scale to soil profiles) using a wide range of tools (e.g., remote sensing, GIS, field surveys, laboratory analyses, OSL dating). Results have shed new light on the sources of dust and loess and have led to new ideas on the most probable formation process of these important sediments.

During the first stage of the project, hilltop loess sequences and their buried soils in several locations across the Negev were studied in detail and a unique remote-sensing technique for locating the primary loess deposits was developed. Results indicate that the source of coarse dust in the Negev's loess is the adjacent Sinai–Negev sand dunes, as opposed to previously suggested sources (Crouvi et al., 2008, 2009). Combining the results from these hilltop sequences with results from additional field-based research concentrated on ancient stable surfaces located farther south, suggests that the earliest occurrence of very high dust accumulation rates in the Negev is ~180 ka. (Amit et al., 2011). The absence of earlier Negev loess is not a result of interglacial erosion as previously proposed, but is due to the exposure of shallow offshore Nile delta sands (Amit et al.,

23

2011). Two projects are currently being finalized to further examine the sources of dust in Israel: one examines geochemical proxies (Sr and Nd isotopes) for changes in dust sources through time in the Negev, and the other examines buried soils as samplers of Quaternary dust in the central coastal plain of Israel.

The scarcity of fine dust grains in sand dunes suggests these finer grains form in situ in the dunes through eolian abrasion of sand grains. To test this preliminary idea, an additional field-based study was conducted in the Negev which verified our conclusions that the dunes are the sources of loess through breakage of sand grains (Enzel et al., 2010). This model was further tested in other desert loess areas worldwide: examination of desert loess in Africa and Arabia showed that similar to the Negev's loess, the loess in these regions are located downwind of nearby sand dunes, and exhibit temporal and mineralogical association with the dunes (Crouvi et al., 2010). Moreover, when the current dust hot spots are spatially correlated with a soil map of the Sahara, it is evident that 90% of the sources of dust storms are located in areas covered by sand dunes, leptosols (thin, rocky soils), calcisols, arenosols (sandy soils), and rock debris (Crouvi et al., 2012). In contrast to previous suggestions, it was found that only few dust storms originated from playas and dry lake beds. Land erodibility was estimated using additional wind data and showed that sand dunes are the most erodible landform. In summary, the results of this research lead to a paradigm shift from the previously proposed idea that the main sources of loess and fine dust are playas and fluvial deposits, towards a greater emphasis on the role of sand dunes as an important dust source, and on eolian abrasion as a key process for generating coarse and fine dust grains in deserts.

b) Development and application of new technology to measure dust emissions from soil surfaces

A major accomplishment of this project was the development, calibration, and extensive application of a new instrument for the measurement of dust emission potential from land surfaces. Previously, such measurements could only be carried out using a wind-tunnel, the setting up and operation of which is labor and time intensive and causes significant disturbance to the surface. The new instrument developed, named the Portable In-situ Soil Wind Erosion Laboratory (PI-SWERL), allows for more rapid measurements, is transportable to more remote places, and only requires a single operator. Calibration of the PI-SWERL with the University of Guelph's wind tunnel indicated that the results from the two instruments are highly comparable for desert surfaces. The PI-SWERL can measure PM_{10} emissions (particles <10 μm in diameter), $PM_{2.5}$ emissions (particles <2.5 μm diameter), and since more recently, TSP (total suspended particles up to 500 μm in diameter); it therefore has the capability of measuring the full range of grain sizes commonly made air borne by military activities.

After testing and calibration, the PI-SWERL has been used to measure dust emissions of a variety of desert landforms including fans, dry washes, sand dunes, playas, and lake features in many areas of the US southwest as well as in Israel. Testing has been completed on undisturbed as well as surfaces artificially disturbed to simulate anthropogenic impacts to the soils. Results have allowed

landform types to be ranked in order of dust emission potential in both disturbed and non-disturbed scenarios. Some interesting results include that: 1) playas, once thought to be major dust sources, actually have lower emission potentials than young alluvial landforms unless their surface crust is disturbed, which causes their propensity to emit dust to increase significantly; 2) due to their discontinuous and often disturbed crusting, playa margins can constitute major dust sources; and 3) textural analysis of the dust emissions reveals that the presence of a mixture of particle sizes that includes sand size grains correlates with high dust emission from surface soils.

c) **Empirical research on dust emissions caused by rotary-winged aircraft**

Experiments were performed at Yuma Proving Ground (YPG) to measure the dust emissions from desert surfaces caused by low level helicopter flight (for a range of speeds), landing and take-off, and hovering at two different elevations. In addition to measurements of the levels of dust emission and dust characteristics, data were acquired to assess the vertical and horizontal wind speeds (m s^{-1}) in the zone directly under the flight path, and the surface shear stress (N m^{-2}) created by the rotor downwash as it moved laterally from the flight path. These data were collected to test and validate a mechanistic helicopter dust emission model being developed as part of our research objectives. PI-SWERL measurements made on other desert surfaces at YPG will allow the helicopter dust emission results to be extrapolated to different desert surface conditions.

2.2 Published manuscripts resulting from this work

Amit, R., Enzel, Y., Crouvi, O., Simhai, O., Matmon, A., Porat, N., McDonald, E.V., and Gillespie, A.R., 2011, The role of the Nile in initiating a massive dust influx to the Negev in the middle Pleistocene: Geologic Society of America Bulletin, v. 123, p. 873-889.

Amit, R., Enzel, Y., Grodek, T., Crouvi, O., Porat, N., and Ayalon, A., 2010, The role of rare rainstorms in the formation of calcic soil horizons on alluvial surfaces in extreme deserts: Quaternary Research, v. 74, p. 177-187.

Amit, R., Enzel, Y., and Sharon, D., 2006, Permanent Quaternary hyperaridity in the Negev, Israel, resulting from regional tectonics blocking Mediterranean frontal systems: Geology, v. 34, p. 509-512.

Amit, R., Simhai, O., Ayalon, A., Enzel, Y., Matmon, A., Crouvi, O., Porat, N., and McDonald, E.V., 2011, Transition from arid to hyper-arid environment in the southern Levant deserts as recorded by early Pleistocene cummulic Aridisols: Quaternary Science Reviews, v. 30, p. 312-323.

Bacon, S.N., McDonald, E.V., Amit, R., Enzel, Y., and Crouvi, O., 2011, Total suspended particulate matter emissions at high friction velocities from desert landforms: Journal of Geophysical Research, v. 116, p. F03.

Bacon, S., McDonald, E., Dalldorf, G.K., Lucas, W., and Nikolich, G., In press, Recommendations for the development of a dust-suppressant test operations procedure (TOP) for U.S. Army materiel testing, *in* Harmon, R.S., and McDonald, E., eds., Reviews in Engineering Geology - Military Geoscience in the 21st Century: Denver, CO, Geological Society of America.

Crouvi, O., Amit, R., Enzel, Y., and Gillespie, A.R., 2010, Active sand seas and the formation of desert loess: Quaternary Science Reviews, v. 29, p. 2087-2098.

Crouvi, O., Amit, R., Enzel, Y., Porat, N., and Sandler, A., 2008, Sand dunes as a major proximal dust source for late Pleistocene loess in the Negev Desert, Israel: Quaternary Research, v. 70, p. 275-282.

Crouvi, O., Rivka, A., Porat, N., Gillespie, A.R., McDonald, E.V., and Enzel, Y., 2009, Significance of primary hilltop loess in reconstructing dust chronology, accretion rates, and sources; an example from the Negev Desert, Israel: Journal of Geophysical Research, v. 114.

Crouvi, O., Schepanski, K., Amit, R., and Gillespie, A.R., 2012, Multiple dust sources in the Sahara Desert: The importance of sand dunes: Geophysical Research Letters, v. 39, p. L13401.

Enzel, Y., Amit, R., Crouvi, O., and Porat, N., 2010, Abrasion-derived sediments under intensified winds at the latest Pleistocene leading edge of the advancing Sinai–Negev erg: Quaternary Research, v. 74, p. 121-131.

Etyemezian, V., Nikolich, G., Ahonen, S., Pitchford, M., Sweeney, M.R., Purcell, R., Gillies, J., and Kuhns, H., 2007, The Portable In-Situ Wind Erosion Laboratory (PI-SWERL): A new method to measure PM10

windblown dust properties and potential for emissions: Atmospheric Environment, v. 41, p. 3789-3796.

McDonald, E.V., and Caldwell, T.G., 2008, Geochemical characteristics of Iraqi dust and soil samples and related impacts to weapon malfunctions, *in* Nathanail, C.P., Abrahart, R.J., and Bradshaw, R.P., eds., Military Geography and Geology: History and Technology: Nottingham, Land Quality Press, p. 258-265.

Sweeney, M.R., Etyemezian, V., MacPherson, T., Nickling, W., Gillies, J., Nikolich, G., and McDonald, E.V., 2008, Comparison of PI-SWERL with dust emission measurements from a straight-line field wind tunnel: Journal of Geophysical Research, v. 113, p. Citation F01012.

3. Advancing Remote-Sensing Technologies and Applications, and Developing a GIS Platform for Terrain Predictions

3.1 Summary of overall accomplishments

Extensive effort has been put into developing methods of using remote sensing data to map terrain characteristics, a capability that adds to our ability to predict terrain in areas where limited on-the-ground data exists. Methods have been developed to map terrain parameters that directly relate to specific hazards, such as dust emission potential and surface roughness, as well parameters that may be fed into our global soils database to indirectly predict soil types with which certain hazards may be associated. Data types that fall into the latter category are soil parent material, landform age, and landform type. The main focus areas of this research are summarized below.

a) Parent material

Parent material type is one of the four main variables used to predict soil type by the overarching terrain prediction model developed as part of this project. Parent material type relates to the lithology of the bedrock at the actual site in the case of autochthonous soils, or in the source area in the case of soils developed in sediment (allocthonous soils). In some cases this information can be derived from published bedrock geology maps; however, in many locations this information does not exist or cannot be easily accessed. In such cases, automated mapping based on satellite imagery is the most efficient way of obtaining bedrock geology data.

An initial experiment was carried out to map the bedrock geology in the Inyo Mountains/Owens Valley area of California using NASA ASTER data. Over the course of two and a half days, an area of 3600 km^2 was mapped, with 16 lithologic classes differentiated. The algorithms developed during this test were then used to develop a parent material map for Cadiz Valley, California, where a whole different suite of rock types occur. This second test area was mapped 'blind' (i.e. with no consultation of other geologic data sources) and was expanded to include mapping of the allocthonous areas of the valley with the aim of distinguishing Quaternary landforms based on parent material lithology, as well as landform type and age. The method was then applied to a large area in the Carrizo Impact area where field validation and standard landform mapping showed that the method was a valuable tool to contribute to the overall success of a terrain mapping project.

b) Soil features (age, surface roughness, disturbances)

In addition to parent material type, landform/soil age comprises one of the four diagnostic parameters that may be used to predict soil surface and subsurface characteristics via our global soils database. It is therefore critical that we can accurately evaluate landform age from remote

sensing data. Using the series of different aged alluvial fans and their related soils at the Cibola Range – which were mapped, described in detail, and independently dated using the TCN method, all as part of this project – the specific surface characteristics of desert pavements of various ages and their related spectral signatures were analyzed. Results have indicated systematic differences including a higher spatial scale of variability on younger surfaces caused by a greater mean clast size which results in greater cast shadows; and a higher likelihood of rubified clasts on older surfaces. The assessment showed that spectral signatures can be used not only to map different aged pavement surfaces but to provide preliminary age estimates for the surfaces. Detailed observation and statistical analysis of the color (varnish and rubification) of surface clasts as part of this work has also contributed to understanding of desert pavement dynamics (clast deterioration and flipping over time).

Furthermore, LIDAR (Light Detection and Ranging) technology – which comprises an unparalleled method of detailed microtopographic analysis – was also applied to a range of landform types at YPG that represent good analogs for surfaces present in areas of SW Asia such as Afghanistan. LIDAR was used to create sub-centimeter digital elevation models (DEMs) of the landform surfaces. The goal of this microtopographic measurement exercise was to quantify surface roughness, which in desert landscapes is highly influential for vehicle trafficability, as well as dust trapping and entrainment during surface disturbance. As this application of the technology is unprecedented and no standard data processing or handling methods were available, a new set of algorithms were developed for quantifying and classifying surface roughness at both the microtopographic and landform scales, and are now available for rapid application to datasets collected in the future.

The use of remote sensing technology to detect surface disturbances has also been investigated. Specifically, a combination of Buckeye hyperspectral imagery, high resolution Electro-Optical (EO) images, and LIDAR data for selected geologic and geomorphic settings in the Carrizo Impact Area (CIA), Southern California, was processed to produce reflectance products that can be used to identify surface/sub-surface disturbances. One important application of this work is the detection of buried munitions (both UXO and IED).

c) **Mapping of dust emission potential**

Since dust emission potential is one of the most important substrate characteristics for terrain hazard prediction, work was done to determine a method of mapping this parameter over large areas from remote sensing data. Based on the well understood premise that the VIS/SWIR reflectivity of natural geologic substrates increases with decreasing particle size, MODIS image data was used to identify and map, based on their finer grain size, potential areas of high dust emissivity across the whole of Afghanistan. The analysis of the MODIS data was combined with the results of regional scale geomorphic analysis whereby a fifteen category arid landform classification was used to map the country based on Landsat 7 ETM imagery. Each landform category was given a ranking in terms of their dust emission potential. Areas identified in the MODIS data as having high

reflectance/albedo that also were identified during geomorphic mapping as one of the landform types with a 'Very High' dust source potential rating were ranked as most likely to constitute prominent dust sources. This two-pronged remote-sensing approach increases the accuracy and resolution of dust emission potential maps that can be produced for areas that lack field data.

Soft computing methods for modeling dust emission potential of desert landforms have also been developed and applied. Specifically, self-organizing map (SOM) and GIS models were used to estimate the dust emission from different soils across the Silver-Soda playa region in California. This modeling approach relies on relations in the underlying multivariate density function associated with a sparse local data set of dust emission potential values derived from field measurements, and a complete regional dataset of geomorphic parameters generated from DEM and ASTER-derived spectral data. Results indicate that the developed data-driven approach can provide a low-cost method of producing dust emission potential maps that are similar to those produced by more labor intensive expert-based mapping methods. During the last year, work was done to apply the soft computing method to the prediction of other soil properties in Cadiz Valley, in the Mojave Desert of California (see Section 3.2.1).

Another dust-related application of remote-sensing data explored is the mapping of dust storms using TIR (Thermal Infrared) satellite data. TIR data was acquired from MODIS and processed to investigate the dust plumes and their sources during five dust storms in Afghanistan. Soil mineral dust could be identified and quantified, with results highlighting that during dust storms there is a consistent pattern of dust plumes that relate to 1) the location of dust sources (of which there are two), 2) the prevailing wind direction, and 3) the topography. Detailed time-series analysis during a single dust storm also showed the detailed changes over time in the type and/or mass loading of the dust emitted from each dust source. Such monitoring provides a better understanding of the eolian transport system in an area, and helps to generate hazard maps of dust emission potential.

d) Landform

Mapping of landform type is usually carried out via interpretation of a combination of satellite images, photographs, topographic maps, and field surveys. While this is an invaluable technique, by the very virtue of it being expert-based, it retains a degree of subjectivity. To compliment this technique and add a degree of consistency, work was done to develop an automatic algorithm-based semi-quantitative model to extract landforms directly from a DEM. The data used was a 10 m horizontal resolution USGS DEM of Cadiz Valley. The model comprised five steps. At first, it identifies zones of highlands and lowlands based on a topographic roughness index (TRI) in a local scale. In the second step, the model uses an edge enhancement filter (high pass filter) in a local scale to map features that have sharp boundaries, such as deeply incised valleys, channels, sharp ridges and spurs of alluvial fans, and sand dunes. In the third step, the model maps landforms in medium and regional scales using a topographic position index (TPI). In the fourth step, the model differentiates dune fields from highly dissected alluvial fans. Finally, the model maps playa

boundaries using a landform position index (LPI). The preliminary results of this model showed that the model is capable of identifying the shapes and sizes of many desert landforms. During the last year, this model has been developed further to map various characteristics of alluvial fan surfaces based on their multiscale morphologies (see section 3.2.2). If based on high resolution data (such as 1m LIDAR DEM), this model ultimately allows the automated detailed differentiation of different generations of fan surfaces.

3.2 Accomplishments during FY2012

3.2.1 A soft computing approach for soil and landform characterization in desert environments

(Fabio Iwashita, Eric V. McDonald, Steven Bacon)

One of the main challenges in environmental sciences is to map landscape features and their properties when field measurements are limited in number, clustered or even impracticable to collect. To cope with potential problems, we propose a new approach, based on the self-organizing map (SOM) technique, to model soil properties by relating them to landform categories. This approach exploits underlying nonlinear relation of the steady-state geomorphic features and minerals spectral signatures (Table 1) to spatially limited soil textural data. The topographic and spectral features (Figure 5) are extracted and enhanced from the Advanced Spaceborne Thermal Emission and Reflectance Radiometer (ASTER) sensor; whereas soil texture (clay, silt, and sand) and potential dust emission were collected (0 to 6 inches depth) at ninety sites across an extensive area in the Mojave Desert (Figure 3). A categorical geomorphic map (Figure 4) was produce based on expert knowledge, fieldwork and imagery interpretation for Silver and Soda lake region. In contrast to traditional principal component analysis, the SOM identifies nonlinear relations among soil texture and spectral and relief features. Stochastic cross-validation indicates that the SOM is unbiased and provides a way to measure the magnitude of prediction uncertainty for all variables. The Spearman correlation index (Table 2) and SOM cross-component plots (Figure 6) of the soil texture and landforms reveals positive correlation between dust emission and playa margin and washes. The sand ratio is positively correlated to distal fans and dunes, and negatively correlated with desert pavement. Silt has a trend similar to clay, and both present a correlation to salt and silt playas. This approach, which estimates soil physical properties (Figure 7 and 8) by merging collected field data with continuous surfaces of explanatory variables and quantifying correlations between categorical maps and image band ratios, provides a robust alternative method for mapping soil properties in arid environments with limited soil data collection.
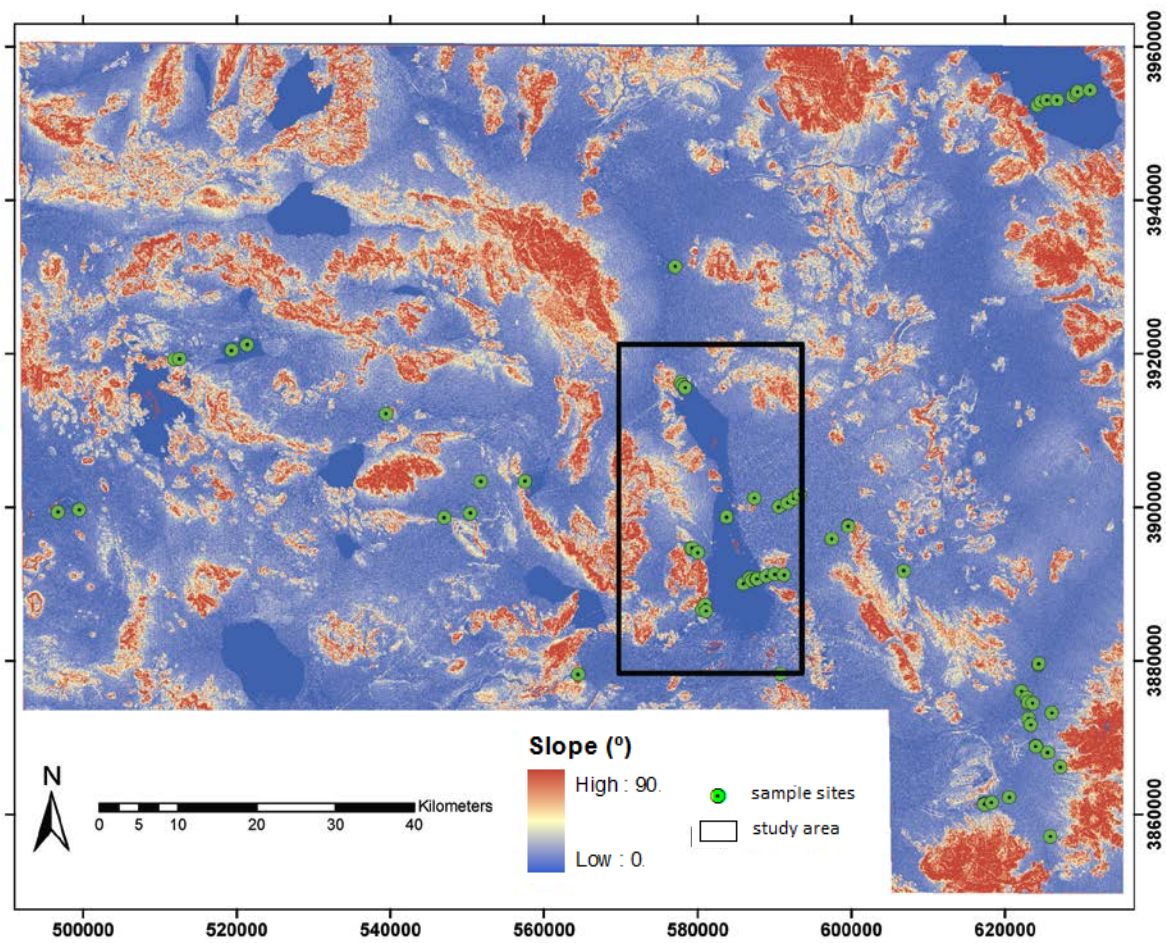
Figure 3. Slope map of the Mojave Desert, and sampling sites.
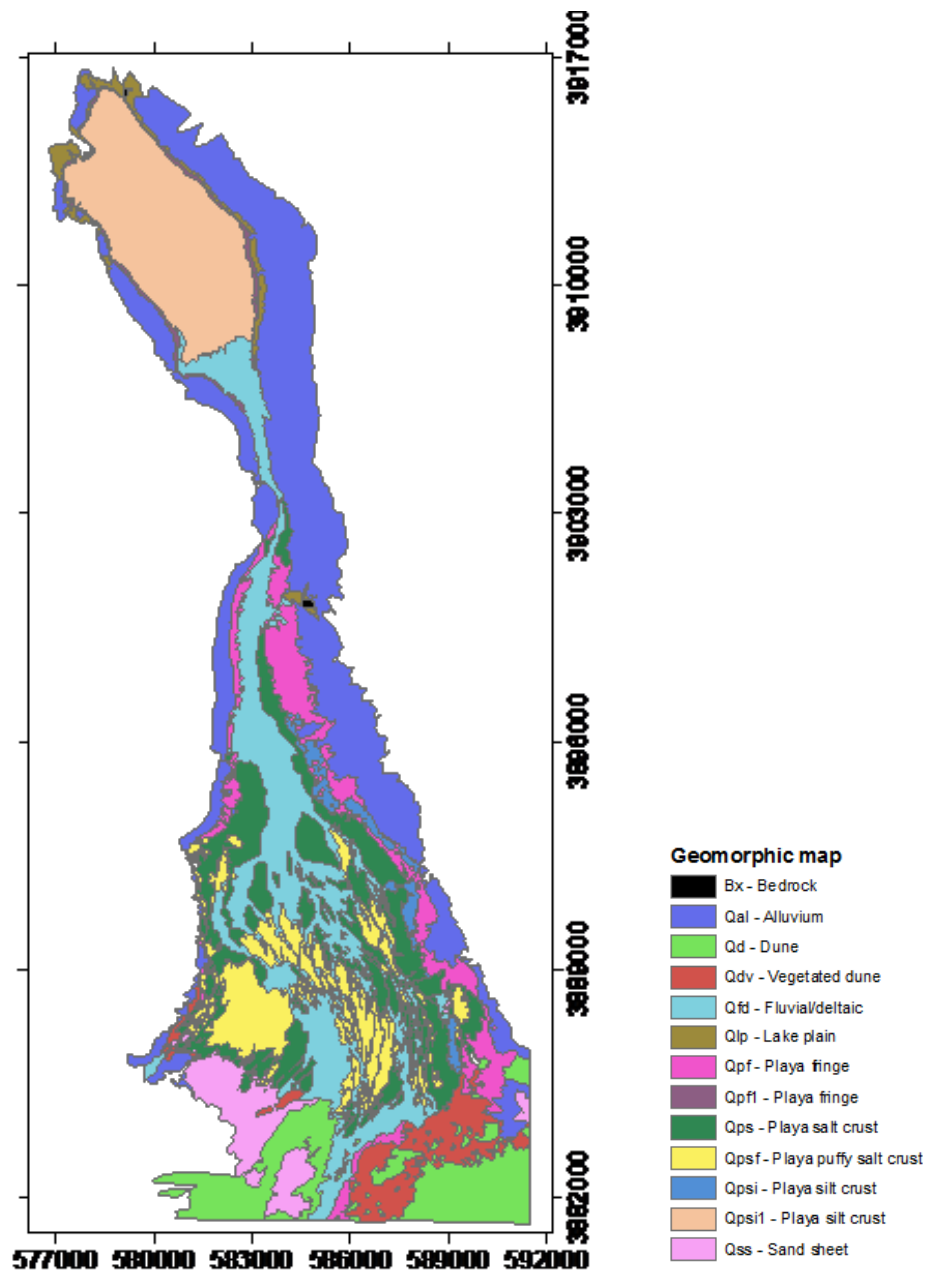
Figure 4. Landform map of Silver and Soda Lakes area, Mojave Desert, California.

Geomorphic map
- Bx – Bedrock
- Qal – Alluvium
- Qd – Dune
- Qdv – Vegetated dune
- Qfd – Fluvial/deltaic
- Qlp – Lake plain
- Qpf – Playa fringe
- Qpf1 – Playa fringe
- Qps – Playa salt crust
- Qpsf – Playa puffy salt crust
- Qpsi – Playa silt crust
- Qpsi1 – Playa silt crust
- Qss – Sand sheet

(a)   (b)
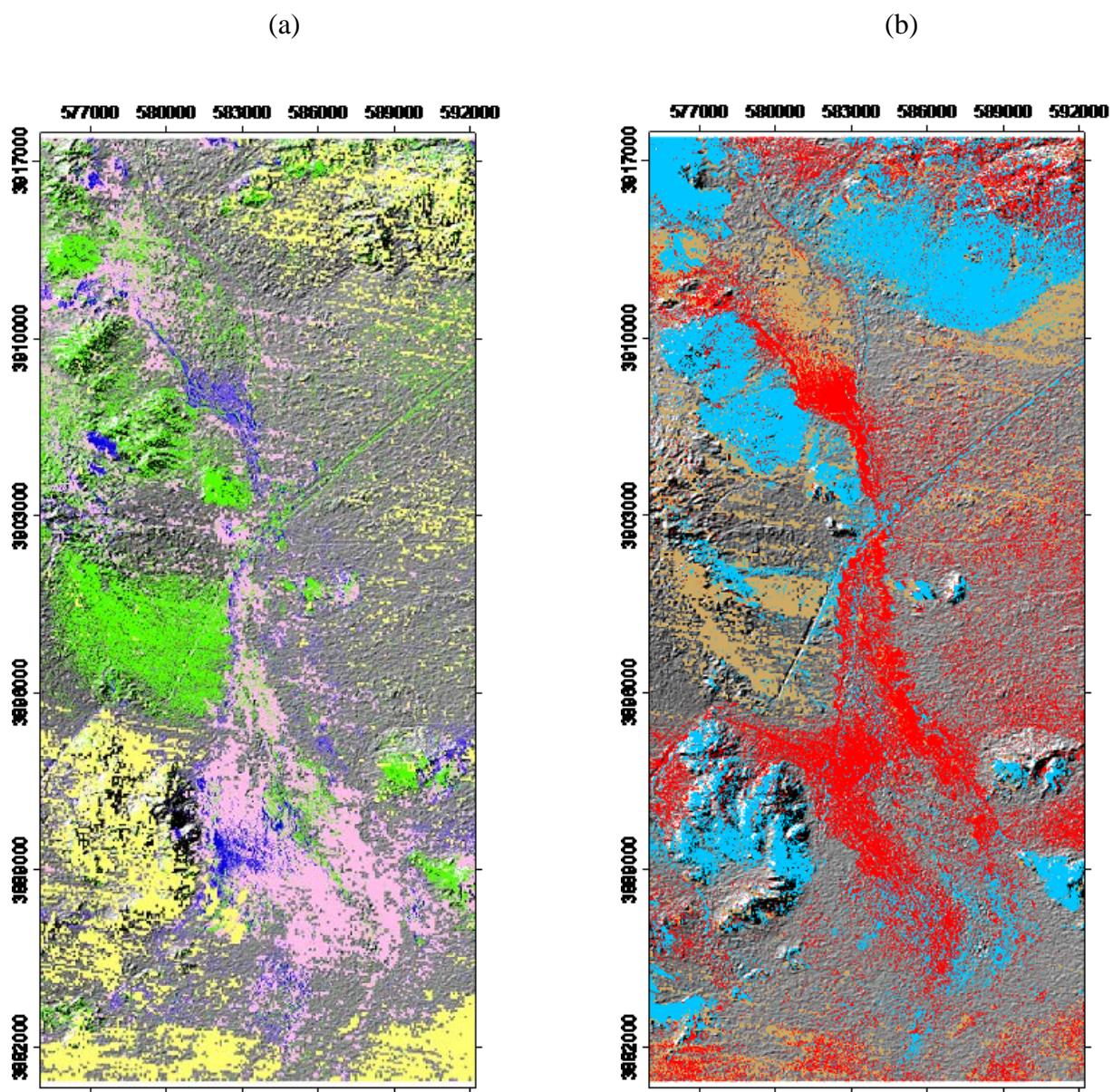
Figure 5. Band ratio images over shaded relied map. (a) Green – Sericite, muscovite, illite, smectite; Yellow – Kaolinite (TIR); Pink – Carbonate; Dark Blue – Alunite, Kaolinite, Pyrite. (b) Light Blue – Ferrous silica; Brown – Quartz; Red – Kaolinite (SWIR).
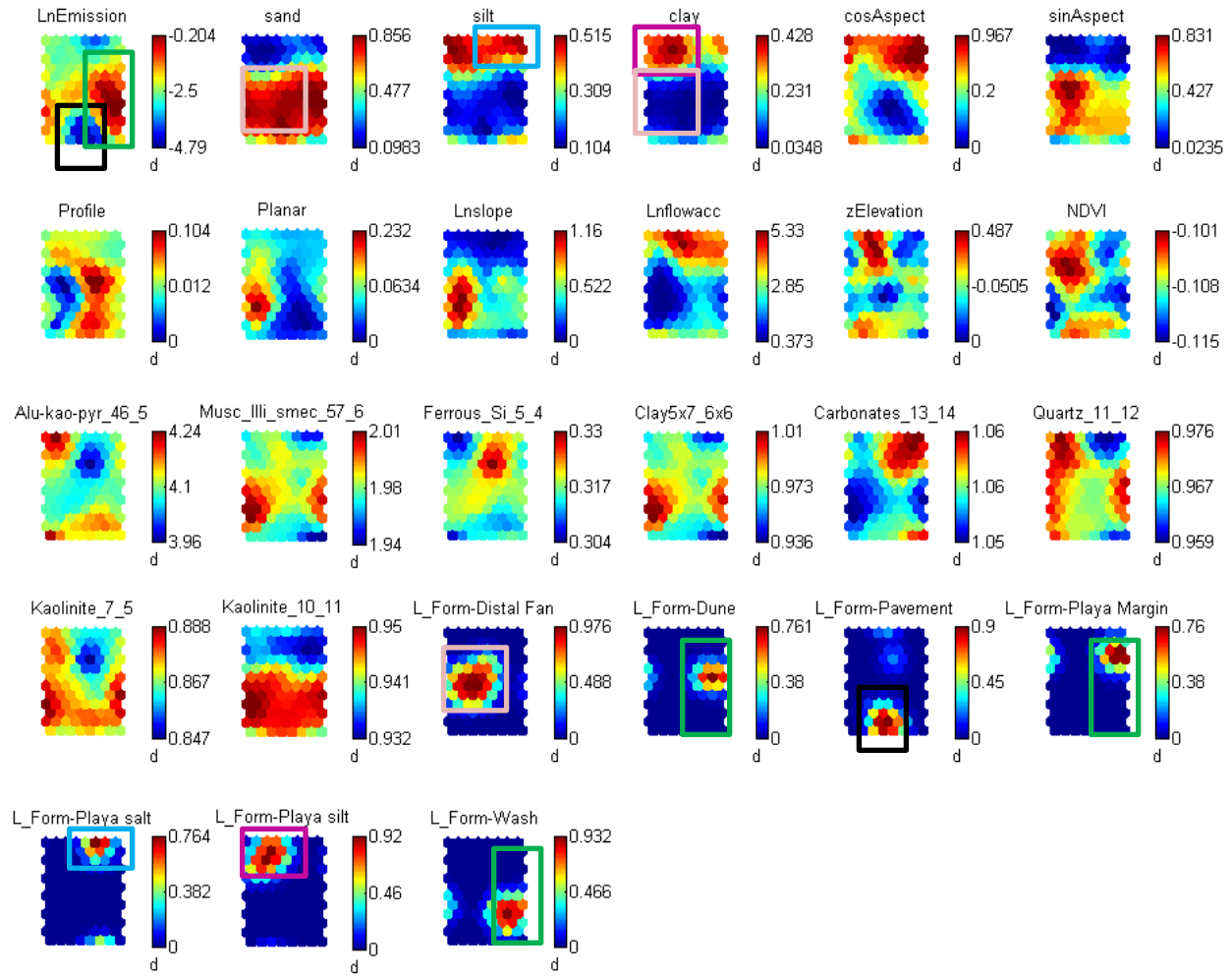
Figure 6. Component planes revealing underlying multivariate density function. Component planes plot of the Silver and Soda lakes SOM model variables (blue is low and red indicates high values). Same pattern and same color temperatures reveal positive correlation; for example, dust emission and desert pavement (black boxes), and clay with playa silt (purple boxes); and opposite color temperatures a negative correlation; for example, sand and clay (pink boxes). In many cases, the patterns among component planes are only partially similar. The reduced correlation is related to spatial heterogeneity. Similarly colored arrows reveal correlation among variables at adjacent locations in different categories.

Figure 7. Estimation of sand (left) and silt (right) using the self-organizing map.

Figure 8. Estimation of clay and potential dust emission using the self-organizing map.

38

Table 1. Description of band ratios used as explanatory variables.

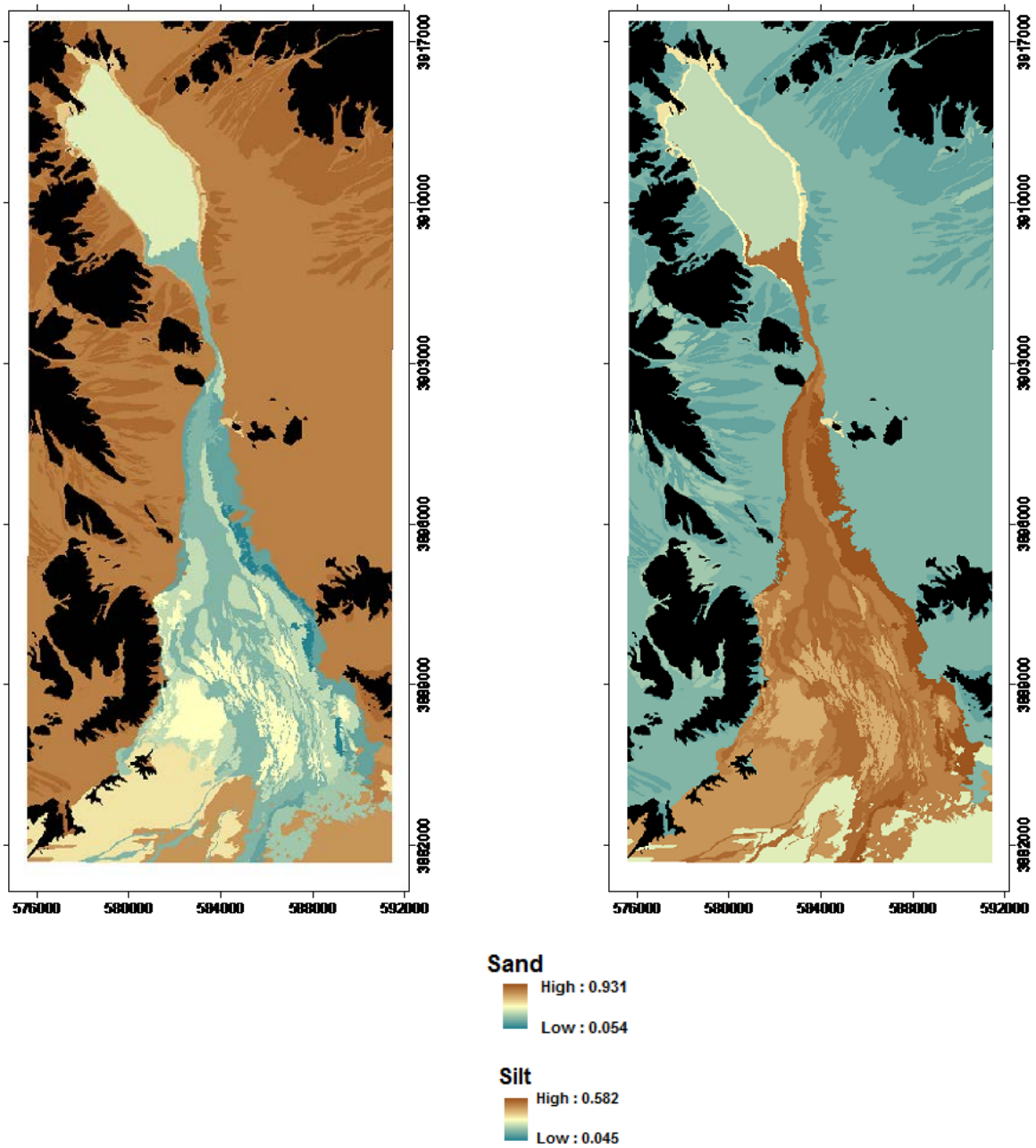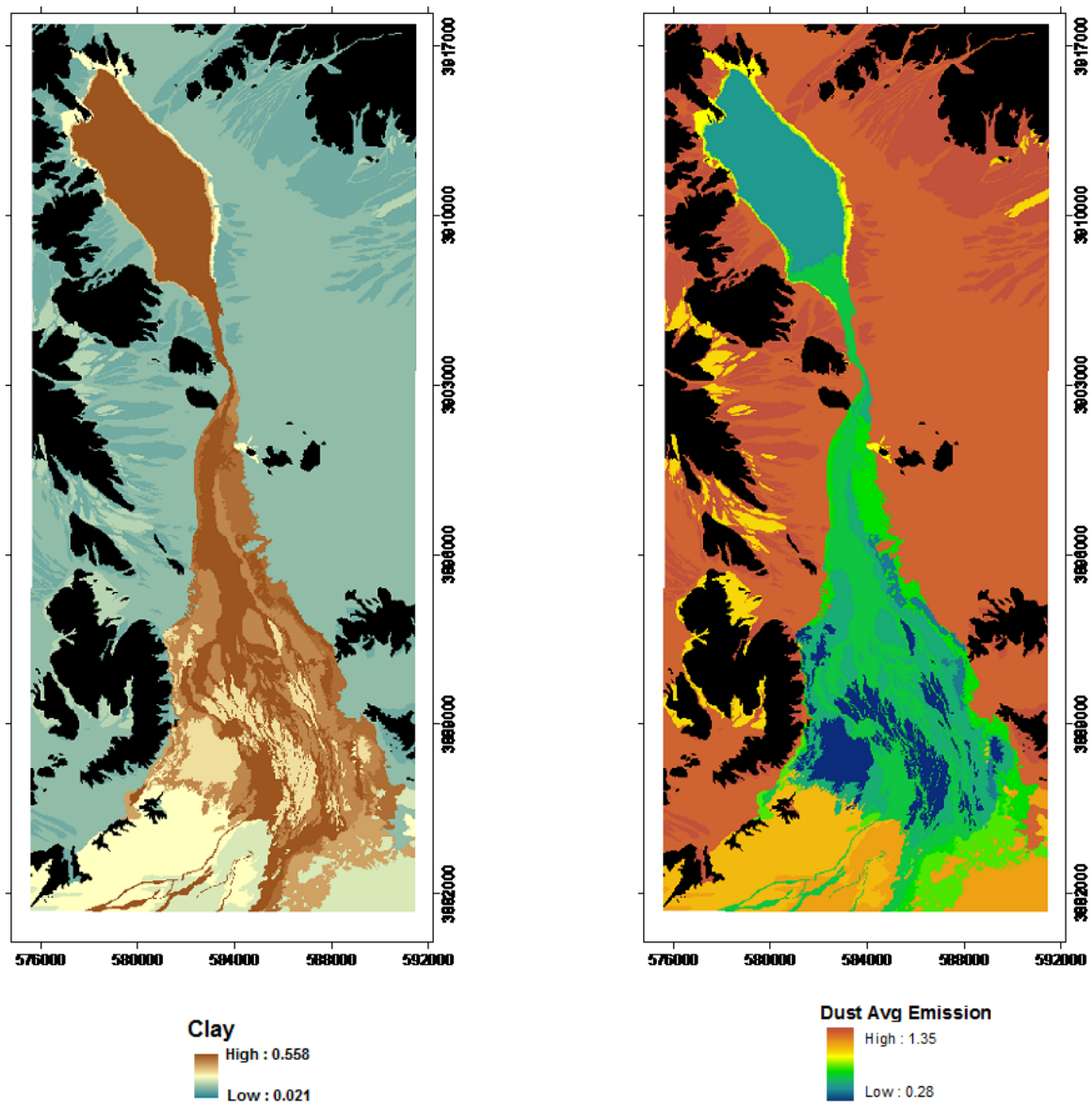| Feature	Band or Ratio	Comments	Reference
Ferrous silicates	5/4	Fe oxide Cu-Au bio, chl, amph) alteration	CSIRO
Sericite / muscovite / illite / smectite	(5+7)/6	Phyllic alteration	Rowan (USGS); Hewson (CSIRO)
Alunite / kaolinite / pyrophyllite	(4+6)/5	Rowan (USGS)	
Muscovite	7/6	Hewson	
Kaolinite	7/5	Approximate only*	Hewson
Kaolinite	10/11		
Carbonate	13/14	Exoskarn (cal/dolom)	Bierwith, Nimoyima, CSIRO
Clay	$(5x7)/6^2$		Bierwith
Silica	11/10		CSIRO
Silica	11/12		CSIRO
Silica	13/10		CSIRO
NDVI	(3-2)/(3+2)	Normalised difference vegetation index	

Table 2. Spearman correlation index for categorical variables and soil physical properties.

	Emission	*Sand*	*Silt*	*Clay*	*Distal Fan*	*Dune*	*Pavement*	*P. Margin*	*Playa salt*	*Playa silt*	*Wash*
Emission	1										
Sand	0.196	1									
Silt	-0.232	-0.932	1								
Clay	-0.124	-0.919	0.714	1							
Distal Fan	0.000	0.281	-0.214	-0.312	1						
Dune	0.206	0.226	-0.232	-0.183	-0.138	1					
Pavement	-0.397	0.266	-0.279	-0.211	-0.183	-0.094	1				
Playa Margin	0.041	-0.121	0.122	0.102	-0.150	-0.078	-0.103	1			
Playa salt	-0.210	-0.247	0.304	0.148	-0.125	-0.065	-0.086	-0.070	1		
Playa silt	-0.109	-0.605	0.477	0.648	-0.203	-0.105	-0.139	-0.114	-0.095	1	
Wash	0.355	0.307	-0.285	-0.285	-0.203	-0.105	-0.139	-0.114	-0.095	-0.154	1

3.2.2 Mapping Characteristics of Alluvial Fans Using a Digital Elevation Model

(Netra Regmi, Eric McDonald)

Introduction

Mapping of desert landforms is traditionally done via interpretation of satellite images, aerial photographs, topographic maps, and field surveys. These methods are slow, labor intensive and subjective. There is no guarantee of consistency of landform mapping between individual mappers. To overcome these limitations, utilization of a qualitative or quantitative analysis of a digital elevation model (DEM) will allow rapid collection, analysis, and mapping of large volumes of topographic data.

We developed an automatic quantitative method to extract various multi-scale characteristics of alluvial fans based on the analysis of a digital elevation model (DEM). We used a 1m LiDAR (Light Detection and Ranging) DEM, a 4m InSAR (Interferometric Synthetic Aperture Radar) DEM and a 10m NED (National Elevation Dataset) DEM data to map surface roughness, terrain roughness, and relative age of alluvial deposits in two different locations: the US Army Yuma Proving Ground (YPG) and the Providence Mountains in the southwestern United States (Figure 9).

The YPG study area is dominated by low gradient and broad alluvial fans that cover most of the lowland area between mountain highlands. The area is comprised of six distinct units of alluvial fan (Qf0 - Qf6, oldest to youngest) (Bacon et al., 2011). The Providence Mountains are a prominent feature in the Mojave Desert. The western margin of the Providence Mountains consisted of eight different units of alluvial fan (Qf1-Qf8, oldest to youngest) (McDonald et al., 2003) and three eolian sand units (Qe1-Qe3, oldest to youngest). The source of the fans in both study areas is mostly plutonic and volcanic rocks and lesser amount of sedimentary rocks (Richard et al., 2000, McDonald et al., 2003).The age of the alluvial fans in these areas vary greatly ranging from active wash to ~400 ka.
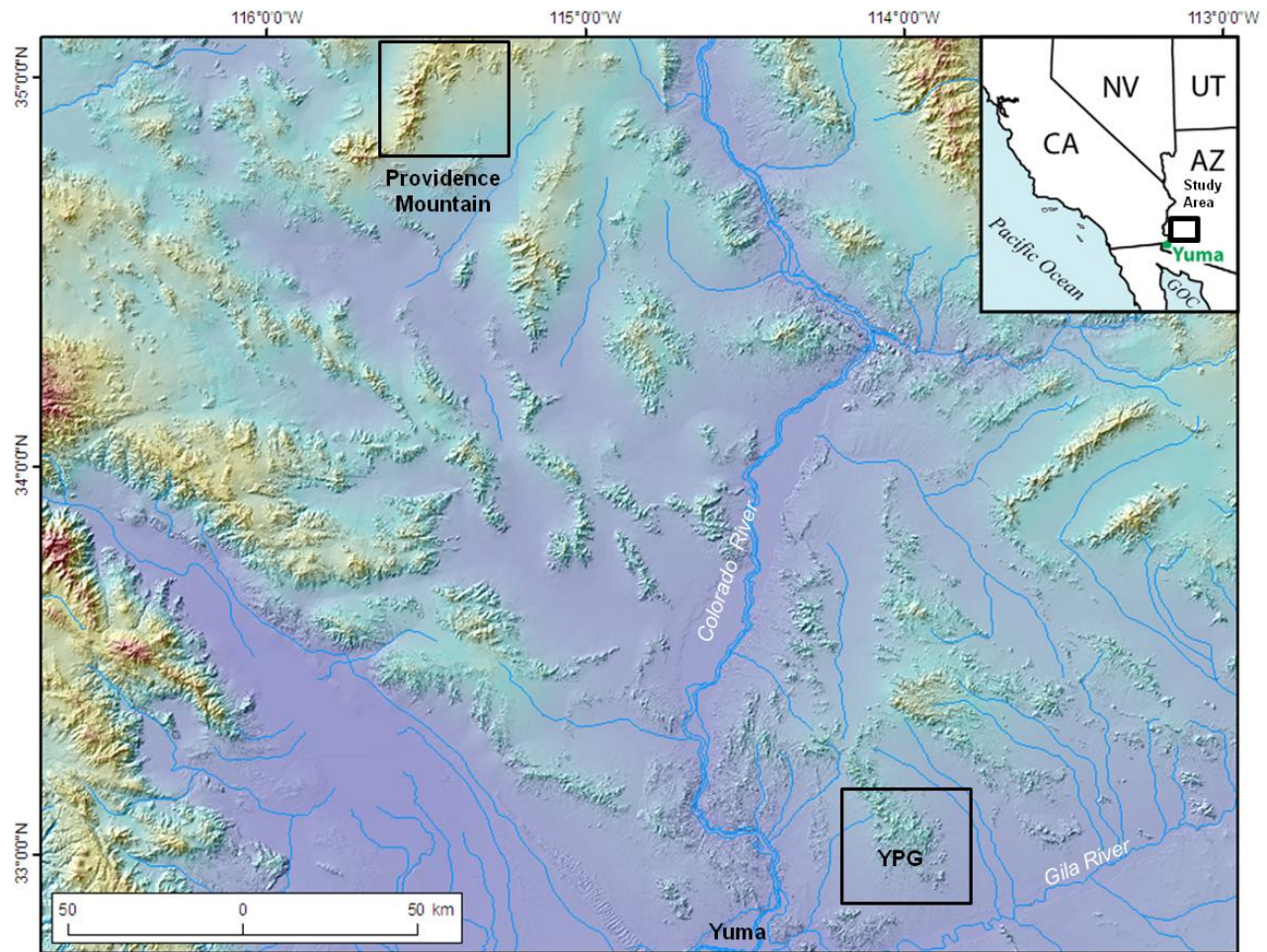
Figure 9. Location of the study area. 1m LiDAR and 4m InSAR elevation data were applied for Yuma Proving Ground (YPG) area and 10 m NED elevation data was applied for the Providence Mountains area.

Surface and terrain characteristics of the alluvial fans

Alluvial fan morphology is scale dependent. In a surface (local scale) observation the alluvial fans exhibit diverse morphology that is related to: (1) development of the desert pavement; (2) occurrence of bar and swale topography; (3) growth of vegetation and accumulation of the sediments around vegetation and obstructions; and (4) the frequency and the size of the sediments deposited by active channels. Older (Pleistocene) alluvial fan surfaces have well developed varnished desert pavement and lack vegetation and bar and swale topography. These fans are incised by the channels and graded to Holocene alluvial fans, alluvial plain terraces, and active washes (McDonald et al. 2003; Bacon et al., 2010). The younger (Holocene) alluvial fans have distinct bar and swale topography and lack well developed desert pavements. They feature sporadic vegetation in and around the active channels and wash. These fans also form bar and swale topography of variable size and contain sediments of all sizes ranging from boulders to pebbles. In general, the roughness of the alluvial fan surface decreases with the age of the alluvial deposit.

Similarly in a regional scale observation, the morphology of these fans is controlled by: (1) the magnitude of the channel incision; (2) the frequency of active channels; (3) the pattern of the drainage; and (4) large

41

scale bar and swale topography. These characteristics, primarily the response to Quaternary tectonics, climate events and the rate of sediment accumulation, vary among different fan units. The channels in the older alluvial fans have dendritic patterns, and have significantly greater depth of incision than the channels that have distributary patterns on younger alluvial fans. The frequency of the active channels on older fans is significantly lower than on younger fans. In general, the roughness of the alluvial fan terrain increases with the age of the alluvial deposit.

In this study, we assumed both local (surface) and regional (terrain) scale morphologies indicate the age of the alluvial deposit. We developed an algorithm to quantify these morphologies, in terms of roughness, based on the analysis of DEMs.

Roughness (surface and terrain) algorithm

The roughness contribution from the roughness elements at a defined scale of observation can be quantified in terms of the standard deviation (STD) of the variables (Eq. 1), such as slope, curvature, and aspect (Eq1). Previous researchers have used the STD of the slope (Frankel and Dolan, 2007). Here, we argue that the STD of slope only is not enough to define the roughness. Although the STD of slope provides variation in the magnitude (relief) of roughness elements in the vertical dimension, it is not sufficient to describe the variation in the curvature and the orientation of the roughness elements with respect to the horizontal dimension. In this regard, we propose that the integration of the standard deviations of slope, aspect and curvature better explains the surface as well as terrain roughness of an alluvial fan.

$$\sigma_v = \sqrt{\frac{\sum_{i=1}^{n}(v_i - \bar{v})^2}{n}} \qquad \text{.................................} 1$$

Where, σ_v = standard deviation of variable "v" within a defined window size, v_i = value of the variable in cell i in the window, $\bar{v}$ = mean value of the variable, and n = the number of the cells in the window.

The slope, aspect, and curvature for the central cell of a 3×3 moving window (Fig. 3) were determined using the following algorithms:

$$dz/dx = ((C_3 + 2C_6 + C_9) - (C_1 + 2C_4 + C_7))/8 \qquad \text{......................} 2$$

$$dz/dy = ((C_7 + 2C_8 + C_9) - (C_1 + 2C_2 + C_3))/8 \qquad \text{....................} 3$$

Slope = $\tan^{-1}(\sqrt{(dz/dx)^2 + (dz/dy)^2}) \times 180/\pi$ $\qquad \text{....................} 4$

Curvature = $-(C_2 + C_4 + C_6 + C_8 - 4C_5)/L^2$ $\qquad \text{..........................} 5$

Aspect = $\text{atan2}((dz/dx), -(dz/dy)) \times 180/\pi$ $\qquad \text{............................} 6$

Where, *dz/dx*, and *dz/dy* are the rates of change of the surface elevation in x and y directions, respectively.

L is the width of the cell and C_i is the elevation of the cell at the ith location (Figure 10). Atan2 is the arctangent function whose value ranges from π to $-\pi$.

The aspect map developed from equation 6 assigns 0º for east, 90º for north, -90º for south and ±180º for west compass directions. If this map is used to calculate the STD of aspect, data falling in west quadrants get a high STD value. To decrease this effect, another three aspect maps were derived (Fig. 2B). Next, to determine actual STD values of aspect, four STD maps were determined from the four maps of aspect using a 3×3 moving window, and then the maps were combined using Eq.7.

$\sigma_{asp} = min(\sigma_{asp1}, \sigma_{asp2}, \sigma_{asp3}, \sigma_{asp4})$..................7

where, σ_{asp} is the actual STD of aspect, and σ_{asp1}, σ_{asp2}, σ_{asp3}, and σ_{asp4} are the STDs of the aspect maps developed by the approach shown in Fig.3B.
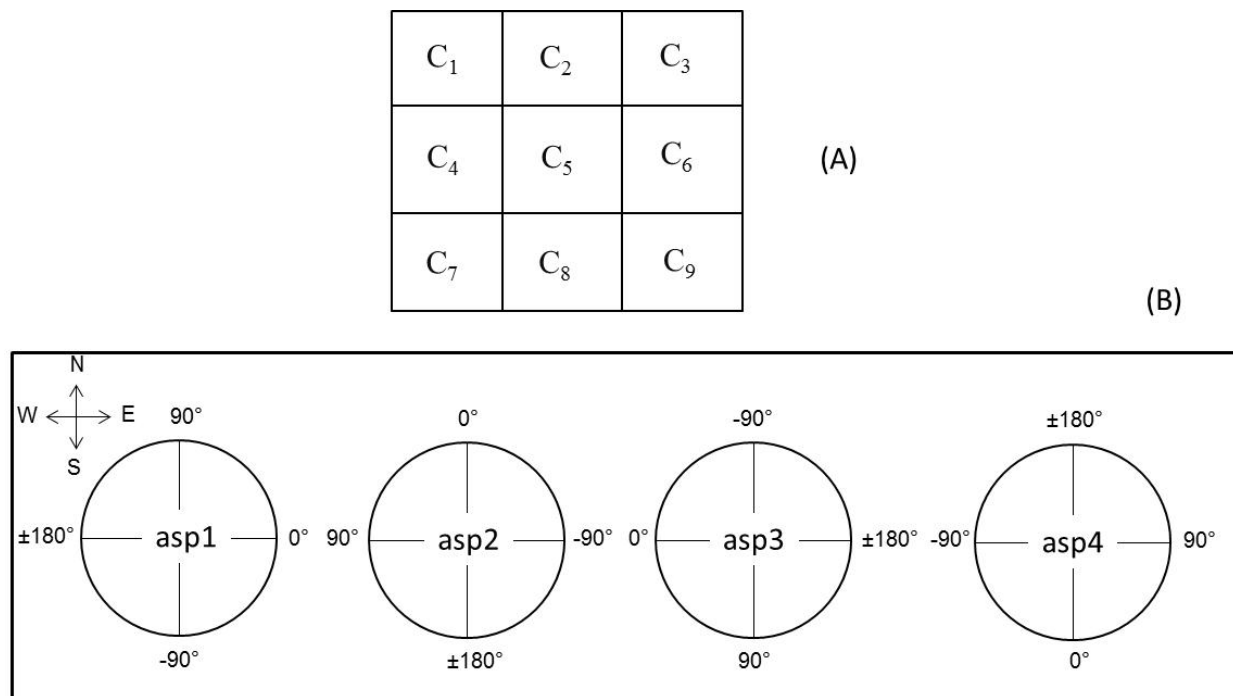

Figure 10. A) A schematic diagram showing a 3×3 moving window used to calculate slope, curvature, aspect, and roughness. These variables were computed for the central cell based on the data from all nine cells. B) A schematic diagram showing the nature of four aspect maps used.

An alluvial fan has roughness elements of different wavelengths, and the pattern of roughness is the function of their amplitudes (magnitude) and wavelengths (frequency) over which roughness values are calculated. For example, Figure 11 shows a schematic diagram of how the roughness depends on the size of observation scale, and the frequency and magnitude of the roughness elements. The shorter wavelength features (first order roughness elements), such as boulders, vegetation and vegetation scars, sediments accumulated around obstructions, very small bars and channels, and small undulations of the surface resulting from the process of diffusion or sheet erosion, have high frequency but low magnitude. The

higher wavelength features (higher order roughness elements), such as ridges and valleys developed by the incision of axial washes and large scale bars and channels have low frequency and high magnitude. The roughness in the scale of observation at higher wavelengths is always higher than the roughness contribution from the first order elements because of the influence of both first order and higher order elements. If the window size of observation is larger than the dominant wavelength of the highest order elements, the roughness remains constant, and is controlled by elements of all orders. Therefore it is necessary to determine the most appropriate scales at which the roughness controlled by surface roughness elements and or terrain roughness elements can be mapped from the DEM. This can be determined by using the elevation data of different resolutions and examining the nature of the relationships between observation scales (window sizes) and the roughness values. For example, the relation between scale and roughness shows an initial, rapid increase in roughness corresponding to an increase in the size of the moving window over which the roughness based on surface geometry is determined (Figure 11B). The observation scale at which surface roughness no longer changes rapidly defines the dominant topographic wavelengths of first order surface elements observed in the elevation data. We assumed that such roughness data determined from 1m LiDAR elevation data represents mostly the characteristics of the fan surface, and 4m InSAR and 10 m NED elevation data represents mostly the characteristics of alluvial fan terrain.
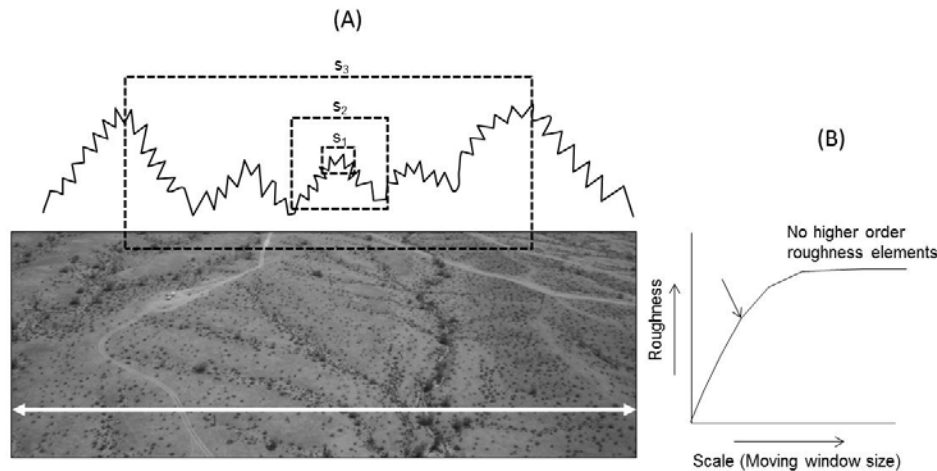

Figure 11. A schematic diagram showing how the signature of the different order roughness elements can be determined by plotting the surface roughness values against observation scale (the length of moving window). The rapid increase in the slope of the curve in smaller size windows is caused by the first order roughness elements (wavelength s1), such as vegetation, sediments, and small scale bar and swale topography. As the window size increases the roughness increases with lower rate because of the influence of the higher order roughness elements (wavelengths s2 and s3), such as ridges and valleys developed by the incised channels. If the terrain has no further higher order elements the roughness remains constant and the curve flattens.

In this study, the roughness values were calculated using roving windows of sizes ranging from 3m×3m to 150m×150m for LiDAR data analysis, 12m×12m to 600m×600m for InSAR data analysis and 30m×30m to 1500m×1500m for NED elevation data analysis. Then, the mean roughness values for each alluvial fan unit were plotted against the size of the moving window to determine the dominant wavelengths of the surface and terrain roughness elements.

Integration of slope, curvature and aspect based roughness

All roughness variables developed at scales corresponding to dominant wavelengths of surface and terrain roughness elements were standardized to a common measurement scale using fuzzy membership functions (Zadeh, 1965). Data standardization is needed because the DEM derived slope, curvature, and aspect based roughness values are independent from each other and are measured in different units. In addition, standardizing the data to a common scale allows comparisons between the data. All the roughness maps obtained at each scale of observation were standardized from 0 to 1 using a linear function (Eq. 8), where 0 represents the oldest alluvial fan surface and 1 represents the youngest alluvial fan surface.

$$r_m = (r - r_{min})/(r_{max} - r_{min}) \quad \text{............ 8}$$

Where, r_m is the membership value of roughness, r is the roughness value of each grid cell, r_{min} is the minimum roughness value and the r_{max} is the maximum roughness value of a roughness map.

Five fuzzy operators, namely: 1) fuzzy-OR, 2) fuzzy-AND, 3) fuzzy algebraic sum, 4) fuzzy algebraic product, and 5) fuzzy-gamma, were employed to combine fuzzy membership functions of slope, aspect and curvature:

$$r_{cm} = \max(r_{1m}, r_{2m}, r_{3m}....) \qquad\qquad \text{(Fuzzy OR)}...............9$$

$$r_{cm} = \min(r_{1m}, r_{2m}, r_{3m}....) \qquad\qquad \text{(Fuzzy AND)}.............10$$

$$r_{cm} = 1 - \prod_{i=1}^{n}(1 - r_{im}) \qquad\qquad \text{(Fuzzy algebraic sum)}....11$$

$$r_{cm} = \prod_{i=1}^{n} r_{im} \qquad\qquad \text{(Fuzzy algebraic product)}.........12$$

$$r_{cm} = \left[Fuzzy\ algebric\ sum\right]^{\gamma} \times \left[Fuzzy\ algebric\ product\right]^{1-\gamma} \qquad \text{(Fuzzy gamma)}.............13$$

Where, r_{im} is the fuzzy membership function for the ith map (i = 1, 2, ..., n), and r_{cm} is the combined output membership value.

Fuzzy-OR and fuzzy-AND operators are appropriate if the combined membership value at a location is controlled by the most suitable maps. In the fuzzy-OR operator (Eq. 9), the combined output membership value for any particular location is controlled by the maximum fuzzy-membership value of the input maps occurring at that location. In the fuzzy-AND operator (Eq.10), the output membership value for any particular location is controlled by the smallest fuzzy-membership value of the input maps occurring at that location. If the combination of fuzzy-membership values from two or more maps occurring at a location is more supportive than the membership value of a single map, then the fuzzy algebraic sum (Eq. 11), fuzzy algebraic product (Eq. 12), and fuzzy gamma (Eq. 13) operators are appropriate. The fuzzy-gamma

operation is defined in terms of the fuzzy algebraic sum, fuzzy algebraic product and a gamma value. The value of gamma ranges from 0 to 1.

We used the fuzzy OR operator to combine the roughness membership values derived from slope, and curvature. The resultant membership was then combined with the aspect membership using the fuzzy gamma operation. Nine roughness maps were prepared for each study with values of gamma ranging from 0.1 to 0.9.

The combined roughness maps were smoothed by using rectangular directional mean filters in eight directions (the aspect interval is 45º). The purpose of using a rectangular moving window rather than a square or a circle is that the shapes of the alluvial fans are elongated in one direction; therefore, a rectangle captures a larger area of the fan unit by decreasing the effect of the surface roughness of surrounding fan units. Then eight maps of smoothed surface roughness were combined at each grid cell by using fuzzy OR and fuzzy AND operators. The roughness maps were than classified into five categories in the case of the LiDAR study and three categories in the case of the InSAR and NED studies. These maps were compared with the observed maps of alluvial fans to estimate the accuracy of prediction.

Results for LiDAR and InSAR based mapping in YPG

LiDAR data was applied for mapping the surface roughness of a 60 km^2 area of the YPG. The roughness values of the alluvial fans were calculated based on the analysis of slope, aspect, and curvature at several observation scales (moving window size ranging from 3m×3m to 150m×150m). For each window size and for each variable included in this study, ~6,000,000 individual surface roughness values were derived from the elevation data. Roughness values of the steep slopes (>2.5º derived from 10m resampled LiDAR elevation data) formed by the incision of channels and small scale mass movement were excluded from the analysis. The excluded area is ~12% of the total area, and mostly comprised Qf1 and Qf5 channel walls. This removed anomalously high surface roughness values associated with steeper parts of the landscape.
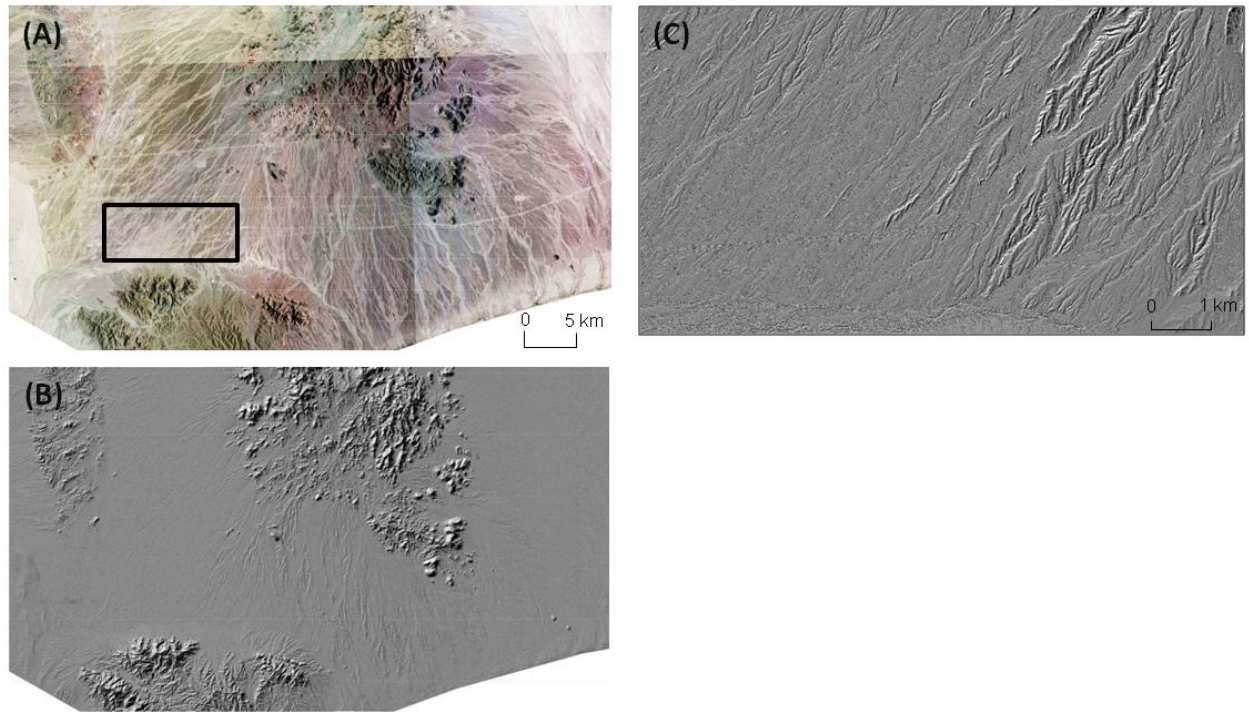
Figure 12. A) An aerial photograph of the YPG area. InSAR data is applied for the entire area and LiDAR data is applied for the area indicated by the rectangular box. The image shows different color of the alluvial fan surfaces. The color is the result of the varnish cover. B) A Hillshade map derived from InSAR elevation data. C) A Hillshade map derived from LiDAR elevation data.
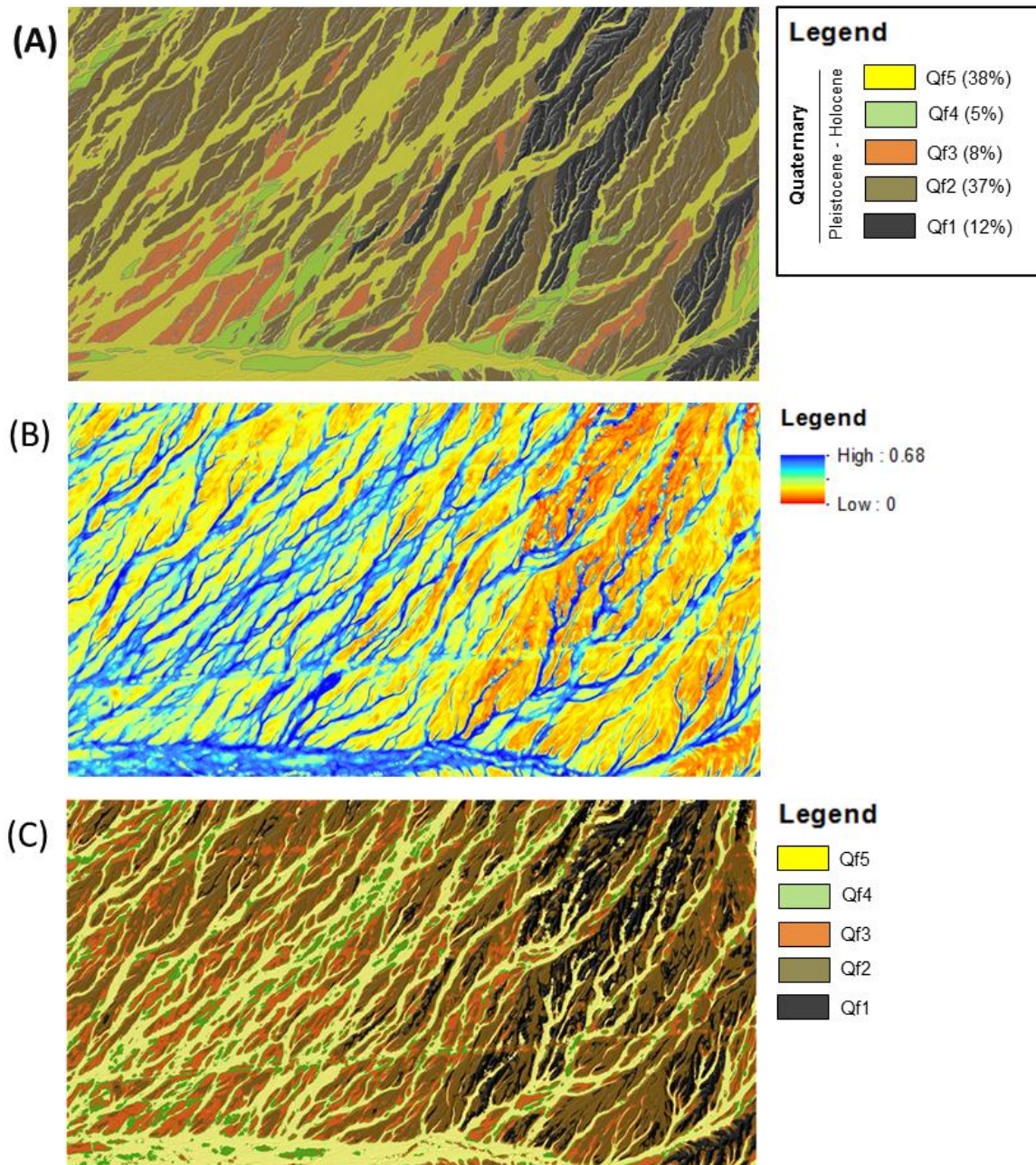
Figure 13. (A) A map of alluvial fans developed based on the analysis of aerial photographs and field survey. B) Smoothed combined surface roughness derived from 1m LiDAR elevation data. Roughness values are unitless. C) Categorized surface roughness.

The plots of the roughness value derived from slope, aspect, and curvature versus window size indicate that the dominant wavelength of the first order roughness elements observed in 1m LiDAR data is 7m. All three roughness maps at this scale were combined using fuzzy-logic operators, and the combined roughness data show that the average roughness of the alluvial fan surface decreases with the age of the alluvial deposit (Figure 13). The prediction accuracies of the individual maps and the combined map were

significantly different. The overall prediction accuracy of the combined roughness map is ~61%, while the prediction accuracies of the slope, curvature, and aspect based roughness maps are ~43%, 47% and ~53%, respectively. The percentage of the match is highest for the old (Qf1 and Qf2) and the young (Qf5) alluvial fans, and lowest for the intermediate aged fans (Qf3 and Qf4).

InSAR data was applied for mapping the terrain roughness of a 1,650 km^2 area of YPG. The roughness values of the alluvial fans were calculated based on the analysis of slope, aspect, and curvature at several observation scales (moving window size ranging from 12m×12m to 600m×600m). For each window size and for each variable included in this study, ~10.3×10^7 individual roughness values were derived from the elevation data. The plots of the roughness versus window size indicate that the dominant wavelength of the smallest roughness elements observed in InSAR data is 28m. Features contributing roughness at this scale are mostly the bar and swale topography in the case of younger alluvial fans and ridges and valleys developed by the incision of first order channels in the case of intermediate and old alluvial fans.

The slope, curvature, and aspect based roughness maps developed using a 28m×28m moving window were combined based on different fuzzy logic operators. The combined roughness data show that the average roughness of the alluvial fan surface increases with the age of the alluvial deposit. The observed map of the study area was categorized into four classes (Qf0-Qf1, Qf2, Qf3-Qf5, and mountain highland) and compared with the categorized roughness map. The prediction accuracy of the combined map was found to be better than the prediction accuracy of the individual maps. The overall prediction accuracy of the combined roughness map is ~70% (Figure 14). The match percentage is highest for the mountain highland and old alluvial fans (Qf0-Qf1).
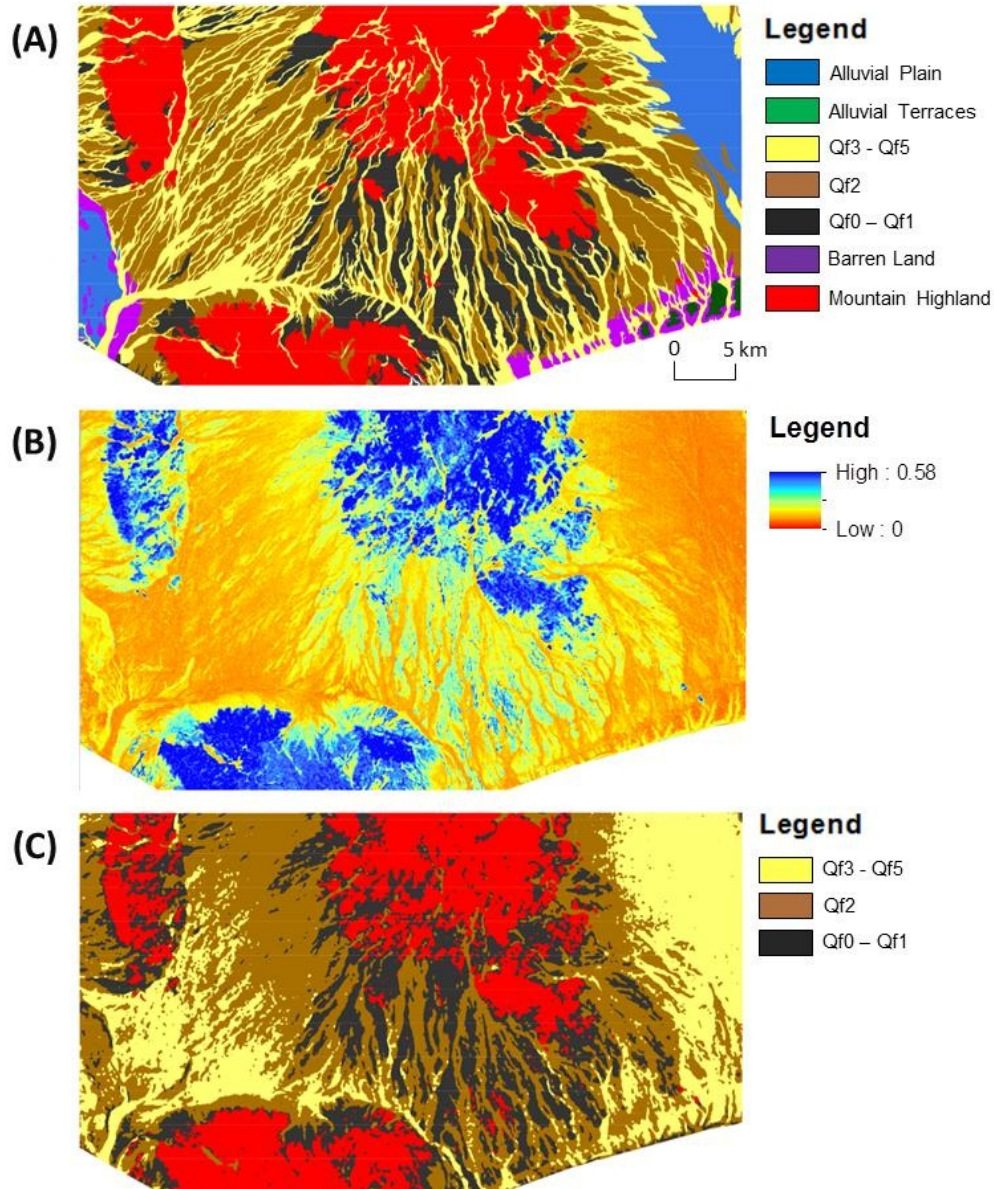
Figure 14. A) A map of alluvial fans developed based on the analysis of aerial photographs and field survey (modified after Bacon et al., 2010). B) Smoothed terrain roughness derived from 4m InSAR DEM. Roughness values are unitless. C) Categorized terrain roughness.

Results for NED based mapping in Providence Mountains

10m NED elevation data were applied for mapping the roughness of a 750 km^2 area of the western margin of the Providence Mountains (Figure 15). The roughness values of the alluvial fans were calculated based on the analysis of slope, aspect, and curvature at several observation scales (window size ranging from 30m×30m to 1500m×1500m). For each window size and for each variable included in this study, ~7.5×10^6 individual surface roughness values were derived from the elevation data. The plots of the roughness versus window size indicate that the dominant wavelength of the smallest roughness elements observed in NED data is 70m. Features contributing roughness at this scale comprised mostly the ridge and valley topography developed by the incision of first and second order stream channels.
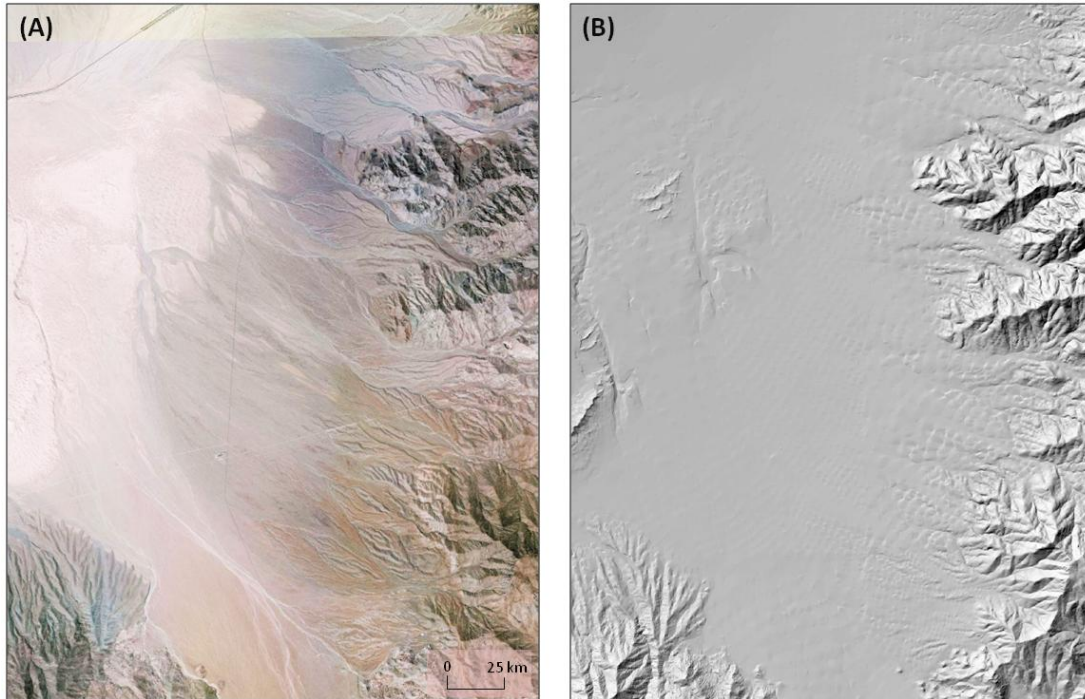
50

Figure 15. A) An aerial photograph of the Providence Mountain area. B) A Hillshade image developed from the analysis of the 10m NED elevation data.

The slope, curvature, and aspect based roughness maps developed at 70m×70m observation scale were combined using different fuzzy logic operators. The combined roughness data shows that the average roughness of the alluvial fan surface increases with the age of the alluvial deposit. The observed alluvial fan units of the Providence Mountains area were grouped into three major units as: old (Qf1-Qf3), intermediate (Qf4-Qf5), and young (Qf6-Qf8), and compared with the categorized combined roughness map. The prediction accuracy of the combined roughness map was better than the prediction accuracy of the individual maps. The overall prediction accuracy of the combined roughness map is ~66% (Figure 16). The match percentage is highest for the old alluvial fans (Qf1-Qf3).
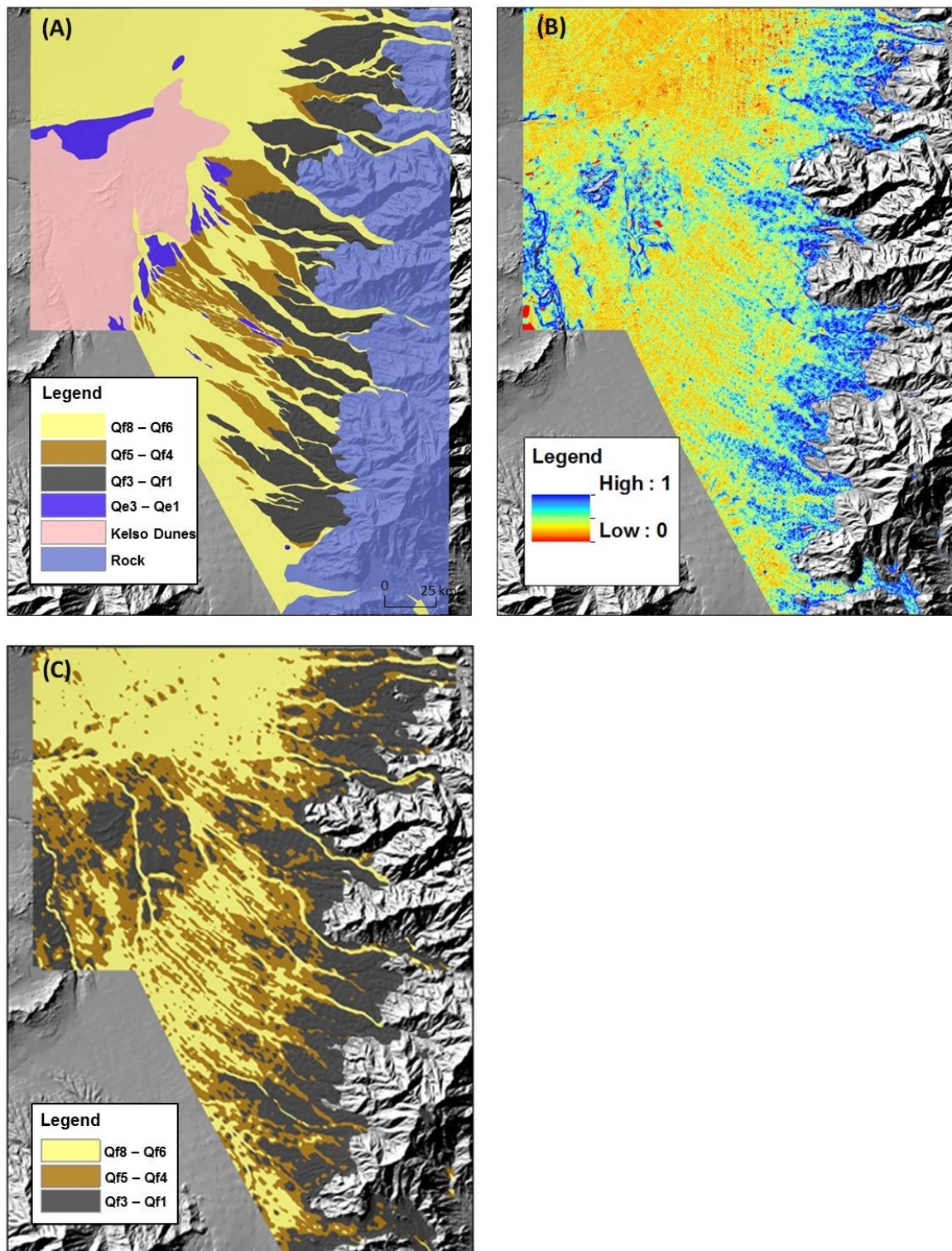
Figure 16. A) A map alluvial fans developed based on the analysis of aerial photographs and field-surveys (modified after McDonald et al., 2003). B) Combined terrain roughness. Roughness values are unitless and standardized from 0 to 1. C) Categorized terrain roughness.

Conclusions

The results suggest that the algorithm is very applicable for mapping various characteristics of alluvial fans based on their multi-scale morphologies. However, only high resolution datasets, such as 1m LiDAR DEM, are found suitable for mapping the detail surface roughness and relative age of the alluvial fans. Relatively low resolution datasets, such as 4m InSAR and 10 m NED data, capture only the terrain roughness and are therefore only suitable for mapping fans into a three-fold classification of age (i.e., old, intermediate and young).

References

Bacon, S.N., McDonald, E.V., Caldwell, T.G., Dalldorf, G.K., 2010. Timing and distribution of alluvial fan sedimentation in response to strengthening of late Holocene ENSO variability in the Sonoran Desert, southwestern Arizona, USA. Quaternary Research, 73: 425-438.

Frankel, K.L. and Dolan, J.F., 2007. Characterizing arid region alluvial fan surface roughness with airborne laser swath mapping digital topographic data. J. Geophys. Res., 112(F2): F02025.

McDonald, E.V, McFadden, L.D., Wells, S.G., 2003. Regional response of alluvial fans to the Pleistocene-Holocene climatic transition, Mojave Desert, California. Geological Society of America, Special Paper 368.

Richard, S.M., Reynolds, S.J., Spencer, J.E., and Pearthree, P.A., comps., 2000. Geologic map of Arizona: Arizona Geological Survey Map M-35, 1 sheet, scale: 1:1,000,000.

3.3 Published manuscripts resulting from this work

Crouvi, O., Ben-Dor, E., Beyth, M., Avigad, D., and Amit, R., 2006, Quantitative mapping of arid alluvial fan surfaces using field spectrometer and hyperspectral remote sensing: Remote Sensing of Environment, v. 104, p. 103-117.

Mushkin, A., and Gillespie, A.R., 2005, Estimating sub-pixel surface roughness using remotely-sensed stereoscopic data: Remote Sensing of Environment, v. 99, p. 75-83.

Regmi, N.R., McDonald, E., and Bacon, S.,Submitted, Mapping Quaternary Alluvial Fans in the Southwestern United States based on Multi-Parameter Surface Roughness of LiDAR Topographic Data: Journal of Geophysical Research - Earth Surface.

4. Developing a Database of Critical Global Soil and Terrain Data

4.1 Summary of overall accomplishments

An ongoing task during the course of this project was the development of the comprehensive soil database to catalog important desert soil and terrain properties and to provide searchable data for rapid mapping and prediction of terrain features. The final database was built in Oracle using PHP language, allowing multiple users to simultaneously access, edit, and add data through a webpage. Much work was put into configuring the data entry form so that complex soil data could be entered as consistently as possible. The data are entered in three tiers: the first holds information about the data source and the soil profile site (location, climate, landform); the second records information about the parent material deposit(s) in which the soil is formed; and the third holds detailed field and lab-derived data about each individual soil horizon. This structure allows data for complex soil profiles (those featuring buried/truncated soils and those formed in multiple parent material deposits) to be accommodated. Also, for as many fields as possible, dropdown lists of categories were developed so that parameters could be input in the most systematic way possible. In particular, a landform classification system was developed—including primary and secondary landform types (based on scale)—that aims to include all terrain features likely to be encountered. Furthermore, consistency of data representation within the database was maintained by the development of a detailed 'user's guide' that describes how different forms of data and nomenclature should be translated into the language and classification system of the data entry form.

The database was populated with soil profile data from a variety of sources including: field and lab data collected as part of this and related projects (see Section 1); data published in journal articles, theses, and books; and data harvested from other publically accessible soil databases, including the NRCS SSURGO, NCSS, and FAO databases (the last providing data for international sites). Soil profile data was prioritized for entry so as to ensure that all the feasible combinations of the four main environmental parameters of 1) parent material geology, 2) landform type, 3) climate, and 4) age (parameters that have predictable relationships with soil and terrain properties), were represented by soil sites in the database. To date, descriptions of over 800 georeferenced soil sites, amounting to more than 4000 soil horizons, have been entered. For soil sites for which local climate data was not available in the source reference or elsewhere, a GIS model was developed to estimate temperature and precipitation variables globally based on extrapolation of weather station data supplied by the National Climatic Data center (NCDC). Subsequently, this model was supplemented using publically available PRISM data.

A direct interface between the GIS platform used for terrain mapping and the database has been created, so that it may be used to directly attribute mapped polygons with soil data. This was achieved by developing a querying function, which allows the most representative soil profile for a mapped landform to be found by performing a search using the four main environmental parameters of the location, as well as six additional site descriptors (surface texture, deposit texture, slope class, and pavement development). This tool, called the Attribute Selector, can be used to view, sort, and analyze (using summary statistics) all

matching profiles; and to download representative data (stemming from either a specific chosen soil site or an amalgamated data set) to the attribute table of the shapefile of a mapped polygon.

The Attribute Selector tool can also be used to calculate the maximum, minimum, and standard deviation of certain soil parameters for a given landform type (based on all horizons entered into the database for that landform type). Furthermore, it can calculate profile depth indices (PDIs) for single soil profiles or a set of profiles. These synthesized values may be plotted against deposit age to portray soil development over time. The mass of data systematically recorded in the database, coupled with the querying and statistical analysis tools that can be developed to access and analyze it, has much potential for further research avenues.

5. Applying and Testing the Predictive Model

5.1 Summary of overall accomplishments

a) Testing the integrated predictive mapping approach at Cadiz Valley, California

A comprehensive test was conducted of the whole GIS-based predictive model system, including geomorphic mapping, remote sensing, and assignment of soil properties to geomorphic units using the global soil database to import data directly into the GIS data layers (Bacon et al., 2010). The specific aim chosen for this task was to test the model's ability to rapidly predict the soil attributes that control dust emission (those in the upper 50 cm of the soil). This test – a blind test – was performed at Cadiz Valley in the Mojave Desert, California, an area that features a variety of landforms including alluvial fans, sand dunes, and playa, and was previously unfamiliar to all involved personnel. The four soil-forming factors that comprise the model parameters used to make soil predictions were derived as follows: (1) Landform type and delineations were determined using office-based observational mapping based on DEM and multispectral satellite imagery at a scale of 1:40,000; (2) Surface age was estimated during geomorphic mapping based on cross-cutting relations and comparisons of topographic relief and surface roughness to areas where absolute chronological data exists; (3) Climate variables were derived from digital grid estimates of PRISM data; and (4) Parent material lithology was identified from ASTER multispectral data by the analysis of reflectance and emissivity of rock/soil compositions. These four data layers were used to query the global soil database by mean of the Attribute Selector tool, and representative soil properties were assigned to each mapped polygon.

Office based geomorphic mapping of the selected 335km^2 area and soil attribute assignment for each landform polygon was carried out by three people working independently. Although the exact locations of map unit boundaries showed some variation, each mapper determined the same basic suite of geomorphic units. The three resulting map-products were field-checked by describing and sampling test pits at eight sites that spanned all major mapped units, as well as reviewing the accuracy of the mapped unit boundaries. Lastly, the field data was compared with the predicted soil attributes using validation criteria consisting of soil texture (particle size distribution), genetic horizon designations, and age of soil. Of the 24 total possible validation criteria combinations, the three users had prediction accuracies of 79%, 83%, and 64%, respectively. Given that the time taken by the three users to make the predictive map was 8.5 hours, 14 hours, and 24 hours, respectively, this level of accuracy is promising considering that traditional soil mapping techniques would require at least several weeks of intensive field work.

The soil-forming model that comprises the foundation of this predictive mapping technique is geomorphic-based, and unlike most pedometric derived predictive soil mapping routines, considers soil age to be a significant factor in accurately predicting soil conditions in hyper arid to mildly arid

regions. This test showed the system developed during this project can be used to map shallow soil conditions associated with distinct geomorphic features, and will be capable of producing cost-effective and high resolution predictive soil maps to support dust emission models in remote and poorly characterized desert regions.

The Cadiz Valley has also been, and will continue to be, used as a field area for the more automated mapping routines that are spawning from this project. As discussed above (Section 3.2), while these soft computing and fuzzy logic algorithm-based models, (aimed at deciphering soil properties and landform type/age, respectively), are in their infancy, they are showing much potential, and having a test area that has previously been mapped by the first principles expert-based methods provides a useful test site for comparison and validation of their results.

a) **Applying the model**

Aspects of the integrative predictive mapping approach have been applied in various ways/capacities as part of this and associated projects. Geomorphic mapping and preliminary soil property prediction were used to guide comprehensive characterization of the soil hydraulic properties in several watersheds including Rainbow Watershed, Maricopa County, Arizona; Bunkerville watershed, Clarke County, Nevada; and Three Lakes Valley watershed, Nevada Test Site. Soil property characterization of these basins, facilitated by predictive landform and soil mapping, allowed the determination of parameters needed for hydrologic models of surface water behavior. The ultimate goals of these projects varied from flood prediction and mitigation, to understanding and planning for the potential spread of hazardous materials from testing activities at the Nevada Test Site. The rapid predictive mapping approach has also been applied to the development of cultural resource models that help guide and focus archaeological surveys so that areas where artifacts are likely to occur (based on depositional environment, surface age, surface preservation) may be prioritized to save time and expenses. Other ongoing applications include the integration of office-based geomorphic mapping, attribution of map polygons with particle size data from the global soils database, and other GIS layers for climate and parent material lithology data, to create maps of salt rich dust content for the country of Afghanistan (See Section 5.2.1), and to predict PM_{10} dust emission flux from undisturbed surfaces across all USCENTCOM countries (Section 5.2.2).

5.2 Progress during FY2012

5.2.1 Projection of salt-rich dust across Afghanistan and detailed geomorphic mapping of the southwestern portion of the country in support of dust emission models

(**Steven Bacon, Heather Green, and Eric McDonald)**

Summary

The occurrence of dust in arid environments is predominately controlled by proximity to dust-rich soils or surficial deposits related to specific landforms. Dust emission potential, however, is the amount of dust that *can* be released from a unit soil mass. Arid regions are often characterized by saline soils that are formed by a lack of precipitation, as well as influenced by surrounding and underlying geology. Identifying the source regions for soluble, salt-rich dust is a critical task for daily military operations, for monitoring potential environmental health impacts to military personnel, and for mitigating abrasion and corrosion to military aircraft, vehicles, and equipment operating in desert regions. This summary provides documentation of methods, approaches, and sources of information used to rapidly generate a regional-scale, predictive soluble salt-rich dust content map of Afghanistan that is based on soil-geomorphic principles, and is part of a larger mapping effort for all of CENTCOM. In addition, a brief description of on-going detailed geomorphic mapping of a dominant dust source area that spans the border of southeastern Iran and southwestern Afghanistan will be discussed.

Salt-rich Dust Content in Afghanistan

This study employed 15-meter resolution, compressed LANDSAT 7 TM+ imagery with 7-4-2 wavelength bands as a base for mapping. Major landform assemblages were then mapped visually at a scale of 1:750,000 across Afghanistan to evaluate and predict potential sources of regional salt-rich dust derived from desert soils (Figure 17). Four regional dust and salt content maps were produced: (1) projection of dust content for individual landforms based on the mean particle size distribution calculated from the global soils database, (2) estimates of salt content within the soil derived from gridded 1 km^2 average precipitation data, (3) geologic-based salt content developed from geologic maps (Figures 17-19), and then combined through an iteration process using factor ratings from the three aforementioned map products to produce (4) a predictive salt-rich dust content (Figure 18).

This study constitutes an initial step in the development of techniques to rapidly predict the dust and salt content of shallow soil conditions associated with distinct geomorphic features at relatively small (regional) map scales. The classification of Afghanistan by potential salt-rich dust content will provide spatial information to address dust-related hazards and the corrosion of military vehicles and equipment. Additionally, soil- and geomorphic-based data will aid in refining global atmospheric dust loading models.
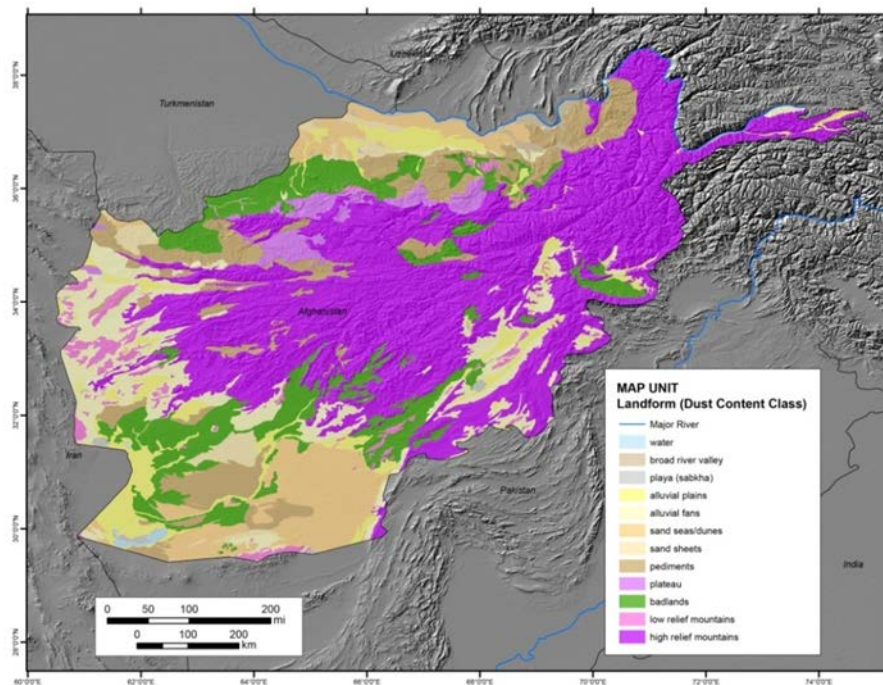
Figure 17. Landform map of Afghanistan based on 1:750,000-scale mapping using LANDSAT 7 TM+ imagery.
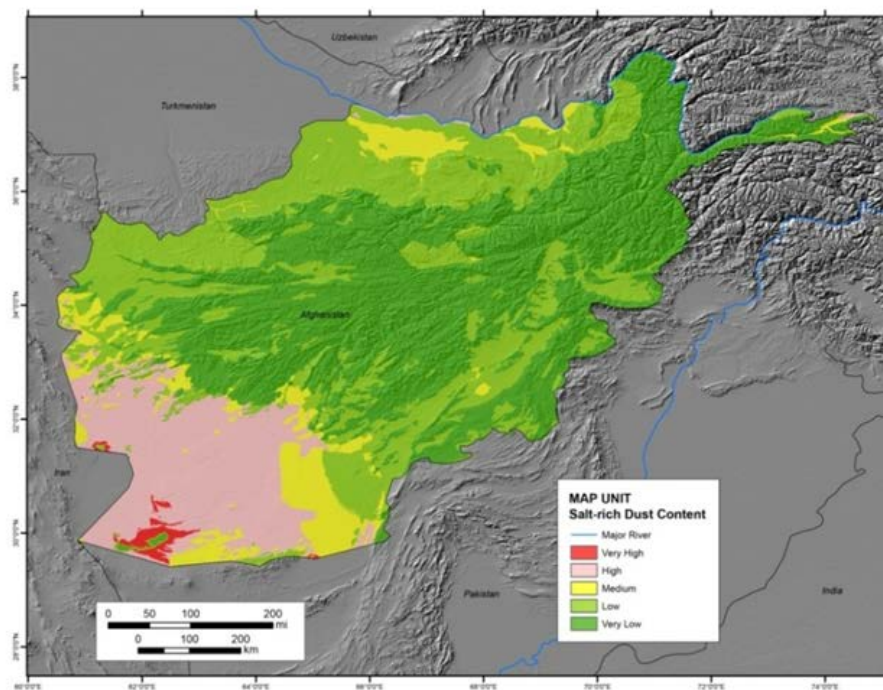

Figure 18. Salt-rich dust content map showing five-fold rating classes based on landform dust content, plus mean annual precipitation- and geologic-based salt content projections.

60

Detailed Geomorphic Mapping of the Dasht-i-Margo Desert, Southwestern Afghanistan

The methodology and approaches used to generate the small-scale (1:750,000) landform map was also applied at a much larger scale of 1:100,000, which has increased the accuracy of the delineation of landform boundaries, increased the number of landform unit types used to characterize the terrain in the area, and increased our understanding of the surface characteristics and dust potential related to specific soil-landform associations. A ~200 km^2 area encompassing the southern borders of Afghanistan and Iran and a large pluvial lake basin in the Dasht-i-Margo Desert was selected for the large-scale mapping, because it has been identified by the U.S. Air Force Weather Agency and Naval Research Laboratory as a significant source of dust in the region that affects both ground- and airborne-based military operations (Figure 19). The landform types in this area include playa, lake plain, alluvial plain, salt marshes and wetlands; sand dunes and sheets in areas distal to alluvial fans; and pediment (eroded surfaces), river terraces, and badlands in the relatively higher topographic positions in the basin (Figure 20). Each of the identified landform types was further differentiated into subunits based on relative surface age, thereby increasing the number of landform units (Figure 21). The geomorphic mapping has provided useful information to help validate salt-rich dust content projections performed in FY2011, as well as unit boundaries to perform a deterministic dust emission analysis for the same map area.
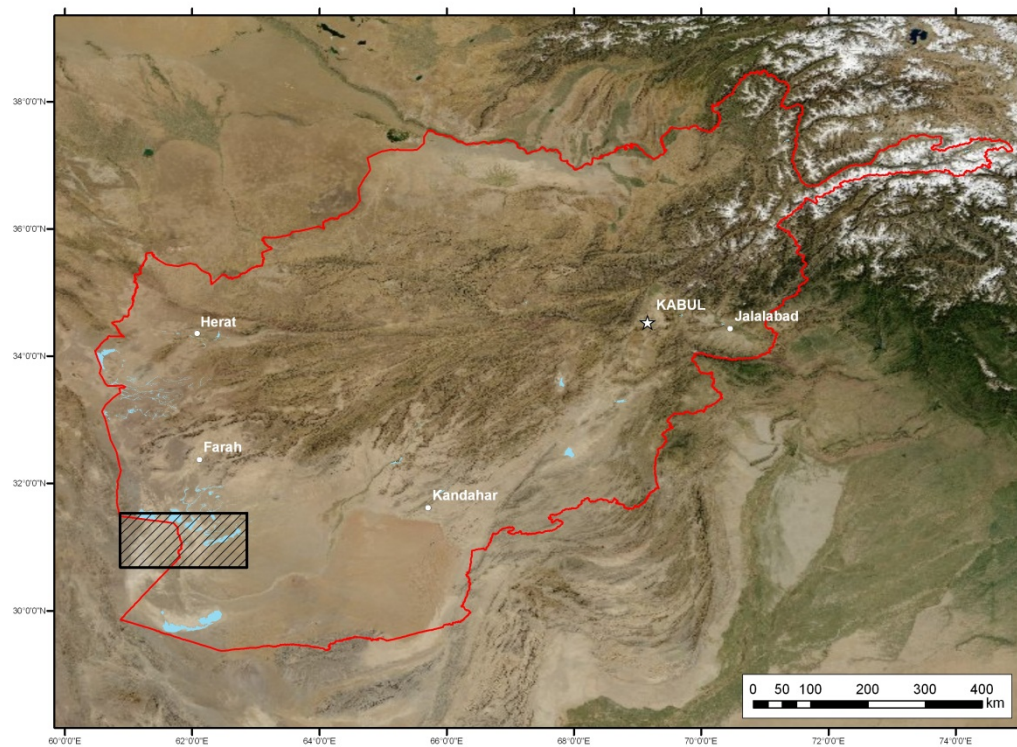

Figure 19. LANDSAT imagery of Afghanistan showing the ~200 km^2 area of 100,000-scale landform mapping that encompasses the Afghan-Iranian border and pluvial lake basin in the Dasht-i-Margo Desert (cross-hatched box).
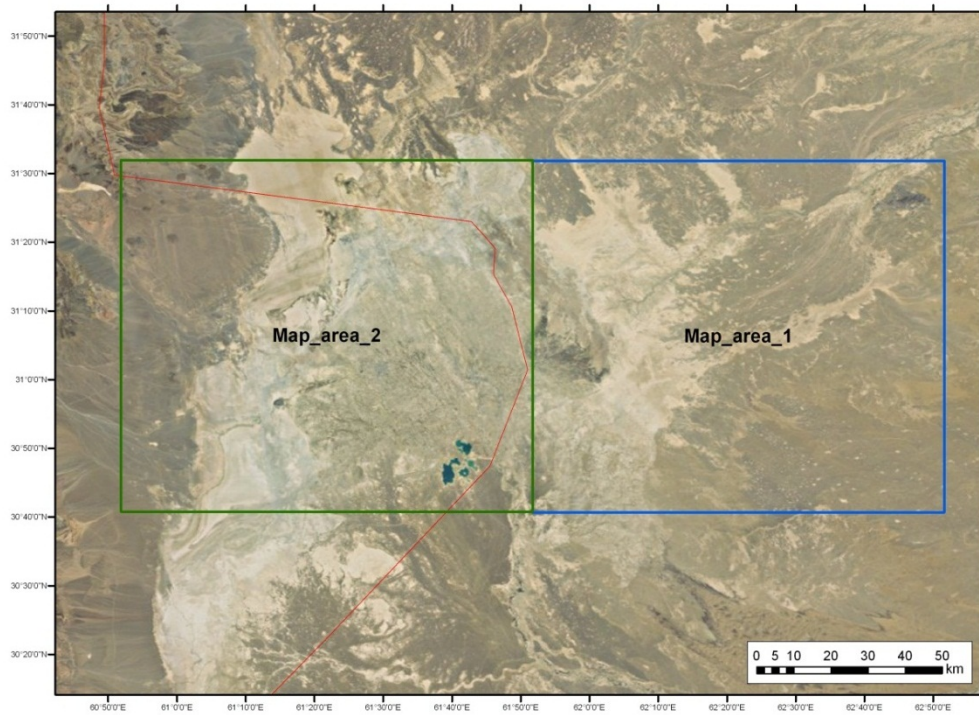
61

Figure 20. Spectral imagery of the ~200 km^2 map area of 100,000-scale landform mapping that shows a variety of desert terrain associated with the large pluvial lake basin that forms a significant source of dust to the region.
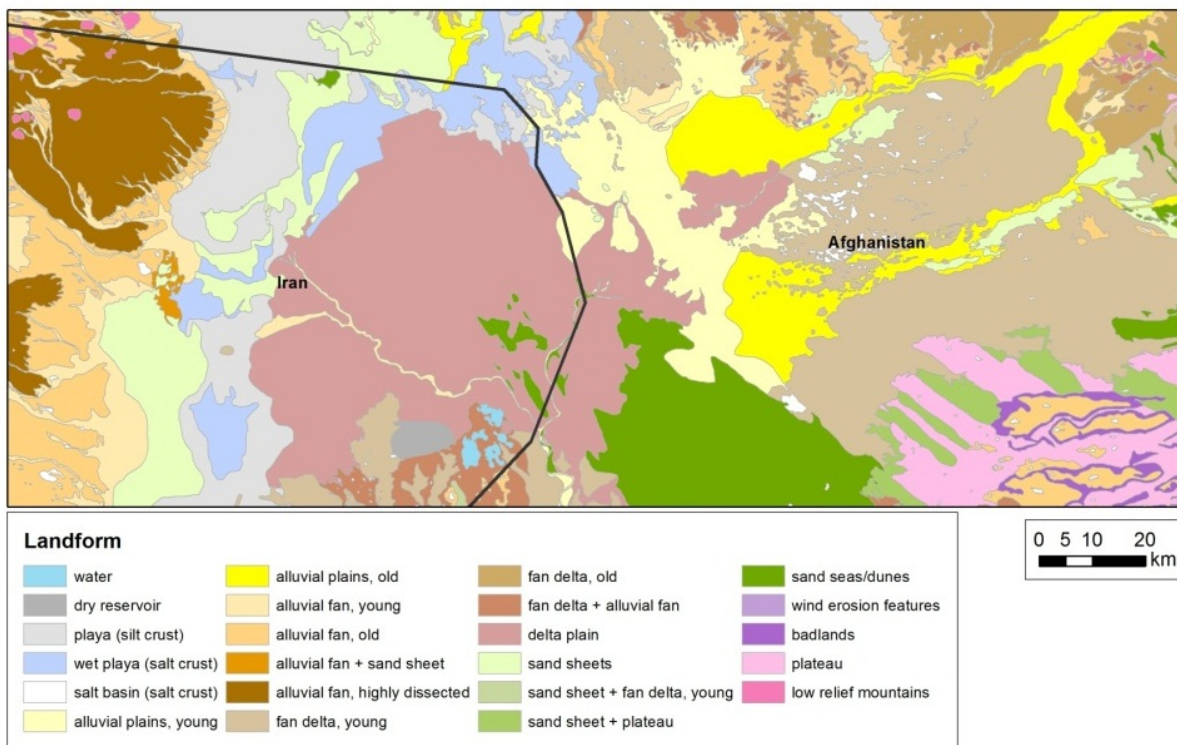

Landform

water	alluvial plains, old	fan delta, old	sand seas/dunes
dry reservoir	alluvial fan, young	fan delta + alluvial fan	wind erosion features
playa (silt crust)	alluvial fan, old	delta plain	badlands
wet playa (salt crust)	alluvial fan + sand sheet	sand sheets	plateau
salt basin (salt crust)	alluvial fan, highly dissected	sand sheet + fan delta, young	low relief mountains
alluvial plains, young	fan delta, young	sand sheet + plateau	

Figure 21. Landform map at 100,000-scale of ~200 km^2 area of southwestern Afganistan that encompasses the Afghan-Iranian border and pluvial lake basin in the Dasht-i-Margo Desert.

Conclusion and importance to DoD

This study constitutes an initial step in the development of techniques to rapidly predict dust and salt content associated with discrete landforms at both relatively small (regional) to large (tactical) map scales. The classification of areas in Afghanistan by potential for salt-rich dust will provide spatial information to address dust-related hazards and the corrosion of military vehicles and equipment. Additionally, soil- and geomorphic-based data will aid in refining global and regional atmospheric dust loading models used by DoD.

Further research will be directed towards: 1) estimating the quantitative dust emission potential of the region by considering how to integrate the salt-rich dust classes, detailed landform mapping, and predictive soil information, with modeled climatic and atmospheric variables responsible for the entrainment of particles required for major dust-raising events; and 2) producing deterministic dust emission maps based dust flux measurements of desert landforms in the western United States.

5.2.2 Deterministic PM$_{10}$ (Dust) Emission Flux from Undisturbed Surfaces across USCENTCOM and southwestern Afghanistan in support of dust loading models

(**Steven Bacon, Heather Green, and Eric McDonald**)

Summary

Understanding critical relationships between desert soils, their surface conditions (e.g., roughness, vegetation cover), and their potential for emission of PM$_{10}$ dust (airborne particulate matter less than 10 microns) as a result of military activities is critical to the successful execution of military operations in the desert. Information about the dust emission potential of desert soils is required to forecast terrain conditions and develop realistic ground-based models to support military operations. We have gathered critical field data on the dust characteristics (e.g., physical, chemical, hydrologic properties) and emission potential of desert soils from key locations across the southwestern U.S., the Middle East, and central Asia, that provide strong analogs to identified dust-producing soils in strategically sensitive areas in desert zones. Multiple field measurements across diverse desert soils have been conducted using DRI's Portable In-Situ Wind Erosion Laboratory (PI-SWERL): a small, portable, prototype wind tunnel for evaluating emissions created by aerodynamic forces. This instrument generates wind shear close to the ground. The shear induced causes soil particles to begin to move along the ground surface, causing PM$_{10}$ dust particles to be dislodged and emitted. These dust measurements have been important for assessing the relationship between the soil and surface properties of a landform and its dust emission potential, and have served to identify similarities and differences in the dust emission potentials of soils available for testing and training in the U.S. and those found within strategically sensitive areas outside the U.S., such as in southwest Asia.

This ongoing study has thus far produced two maps of deterministic PM$_{10}$ emission flux from undisturbed surfaces for USCENTCOM area of responsibility and southwestern Afghanistan. The purpose of this effort is to generate geomorphic- and field-based dust emission potential data sets for key desert landforms at strategic-and regional-scales to support DoD atmospheric dust-loading models. The deterministic data sets will be used to evaluate and validate 1-km grid numerical models of dust loading used by the U.S. Air Force Weather Agency. The methods used to generate the deterministic dust flux data sets and some preliminary results are described below:

Methods

- Performed 1:750,000-scale (1cm on map=7.5 km on land) geomorphic mapping of USCENTCOM to delineate 15 of the most common landform types in the region; and then resampled to 1 km-resolution (Figure 22);

- Performed 1:100,000-scale (1cm on map=1.0 km on land) geomorphic mapping of a portion of southwestern Afghanistan and southeastern Iran to delineate 22 landform types to evaluate point source regions; and then resampled to 500-m and 1-km resolution (Figure 23).

- Compiled unpublished and published PM$_{10}$ emission flux data (at u* = 0.69 m s^{-1}) from a variety of desert landforms in the southwestern U.S. and Israel that are analogous to landforms identified in

southwest Asia. These data were assigned to landforms mapped at 1:750,000- and 1:100,000-scales (Tables 3 and 4, respectively).

- Integrated continuous 1-km mean annual precipitation data to deterministic (1:750,000-scale) map units to limit emission flux in areas that may have high moisture content and vegetation (Figure 24); Also applied a linear function to decrease emission fluxes to 0 within semiarid (250-500 mm/yr) areas; Assigned a value of 0 emission flux to areas with mean annual precipitation of >500 mm/yr (Figure 25).

Results

- Assigned "representative" PM_{10} emission flux (mg m^{-2} s^{-1}) values to landforms identified at 1:750,000- and 1:100,000-scales (Figures 26 and 27, respectively).
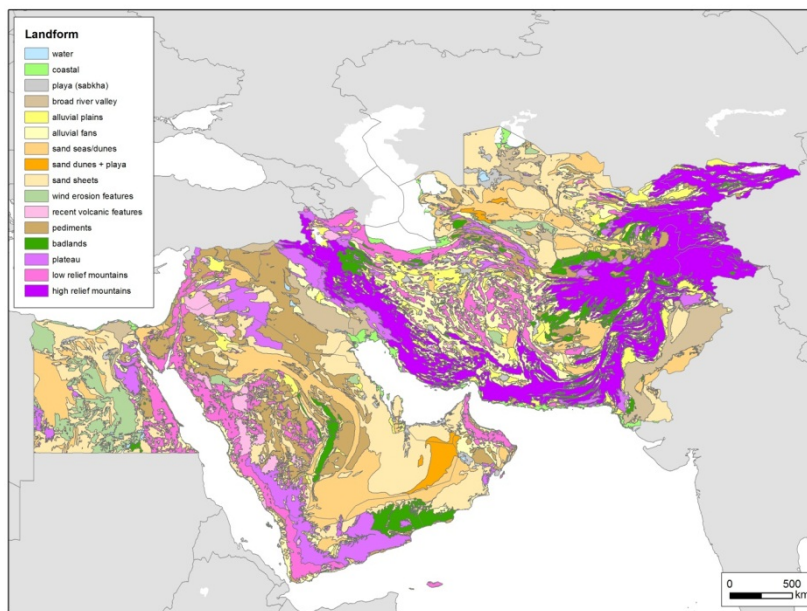
Figure 22. Landform map of southwestern Asia (USCENTCOM) based on 1:750,000-scale mapping using LANDSAT 7 TM+ imagery.
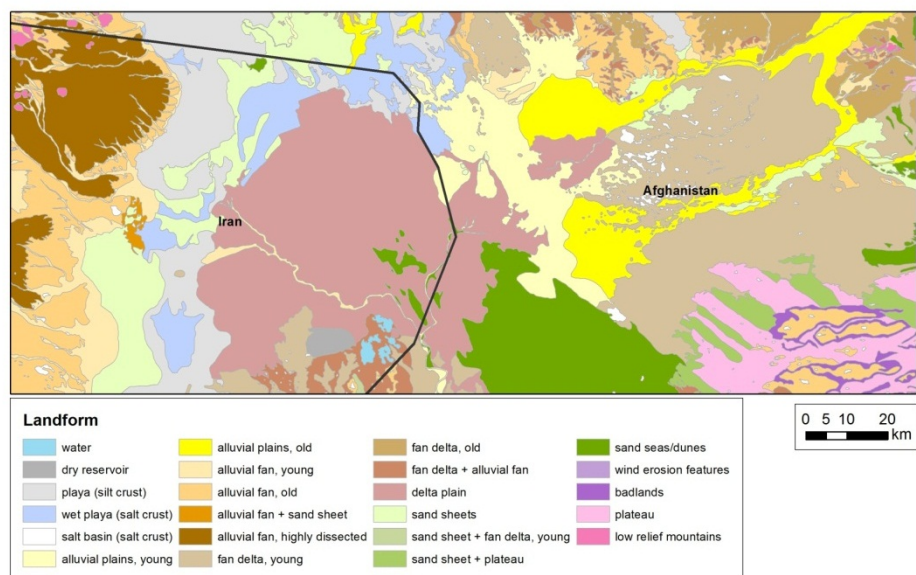
Figure 23. Landform map of border region between southwestern Afghanistan and southeastern Iran (USCENTCOM) based on 1:100,000-scale mapping using a variety of satellite imagery data sets.

Table 3. Undisturbed PM10 emission flux values assigned to analogous landforms mapped at 1:750,000 scale in southwest Asia

| Landform | PM$_{10}$ Emission Flux at $u^* = 0.69$ m s^{-1} (mg m^{-2} s^{-1}) | | |
| | Undisturbed Surface | | Source[a] |
	mean	stdv	
Broad river valley	2.824	1.275	Sweeney et al., 2011, Bacon et al., 2011; avg. of distal alluvial fan, playa (this study), alluvial plains (this study), sand sheet, sand dune.
Playa and Sabkha	0.360	0.665	Sweeney et al., 2011; playa salt and silt crusts
Badlands	0.360	0.665	Sweeney et al., 2011; playa salt and silt crusts
Alluvial plains	2.764	0.821	Sweeney et al., 2011, Bacon et al., 2011; avg. of distal alluvial fan and sand sheet
Alluvial fans	1.445	1.826	Sweeney et al., 2011; avg. distal alluvial fan, alluvial - desert pavement, wash
Pediments	0.285	0.069	Sweeney et al., 2011; alluvial - desert pavement
Sand sheet	4.700	0.629	Bacon et al., 2011; sandsheet
Sand seas/ dunes	3.472	2.987	Sweeney et al., 2011; sand dune
Sand seas/ dunes + playa	1.916	1.826	Sweeney et al., 2011; avg. sand dune and playa
Plateau	0.539	0.000	Bacon et al., 2011; loess plateau (silt-rich crust)
Coastal	3.732	0.725	Sweeney et al., 2011, Bacon et al., 2011; avg. sand dune and alluvial plain (this study)
Wind erosional features	1.916	1.826	Sweeney et al., 2011; avg. sand dune and playa (this study)
Recent volcanic features	0.000	0.000	Assumed none to negligible PM$_{10}$ emission
Low Relief Mountains	0.539	0.000	Bacon et al., 2011; loess plateau (silt-rich crust)
High Relief Mountains	0.000	0.000	Assumed none to negligible PM$_{10}$ emission
Salt domes	0.000	0.000	Assumed none to negligible PM$_{10}$ emission

[a] *PM$_{10}$ emission flux values from direct measurements using a Portable In Situ Wind Erosion Laboratory (PI-SWERL) on common desert landforms in southwestern U.S. and Israel.*

Table 4. Undisturbed PM10 emission flux values assigned to analogous landforms mapped at 1:100,000 scale in southwestern Afghanistan.

Landform	Undisturbed Surface mean	stdv	Source[a]
	PM_{10} Emission Flux at $u^* = 0.69$ m s^{-1} (mg m^{-2} s^{-1})		
Alluvial fan + sand sheet	2.492	0.349	Sweeney et al., 2011, Bacon et al., 2011; avg. of distal fan and sand sheet
Alluvial fan, highly dissected	0.322	0.367	Sweeney et al., 2011; avg. pavement and badlands (this study)
Alluvial fan, old	0.285	0.069	Sweeney et al., 2011; alluvial - desert pavement
Alluvial fan, young	2.025	1.694	Sweeney et al., 2011; avg. of distal fan and wash
Alluvial plains, old	2.764	0.821	Sweeney et al., 2011, Bacon et al., 2011; avg. of distal fan and sand sheet
Alluvial plains, young	3.961	2.513	Sweeney et al., 2011, Bacon et al., 2011; avg. of alluvial wash and sand sheet
Badlands	0.360	0.665	Sweeney et al., 2011; playa salt and silt crusts
Delta plain	2.161	1.589	Sweeney et al., 2011, Bacon et al., 2011; avg. playa salt crust, playa silt crust, alluvial wash, and sand sheet
Fan delta + alluvial fan	0.285	0.069	Sweeney et al., 2011; alluvial - desert pavement
Fan delta, old	0.285	0.069	Sweeney et al., 2011; alluvial - desert pavement
Fan delta, young	0.285	0.069	Sweeney et al., 2011; alluvial - desert pavement
Low relief mountains	0.539	0.000	Bacon et al., 2011; loess plateau (silt-rich crust)
Plateau	0.539	0.000	Bacon et al., 2011; loess plateau (silt-rich crust)
Playa (sabkha)	0.326	0.663	Sweeney et al., 2011; playa silt crust
Salt basin	0.394	0.666	Sweeney et al., 2011; playa salt crust
Wet playa	0.394	0.666	Sweeney et al., 2011; playa salt crust
Sand seas/dunes	3.472	2.987	Sweeney et al., 2011; sand dune
Sand sheet + fan delta, young	2.492	0.349	Sweeney et al., 2011, Bacon et al., 2011; alluvial - desert pavement and sand sheet
Sand sheet + plateau	2.619	0.314	Bacon et al., 2011; sand sheet and loess plateau (silt-rich crust)
Sand sheets	4.700	0.629	Bacon et al., 2011; sandsheet
Wind erosion features	1.916	1.826	Sweeney et al., 2011; avg. dune and playa
Dry reservoir	0.326	0.663	Sweeney et al., 2011; playa silt crust
water	0.000	0.000	No PM_{10} emission

[a] Original PM_{10} emission flux values from direct measurements using a Portable In Situ Wind Erosion Laboratory (PI-SWERL) on common desert landforms in southwestern U.S. and Israel.
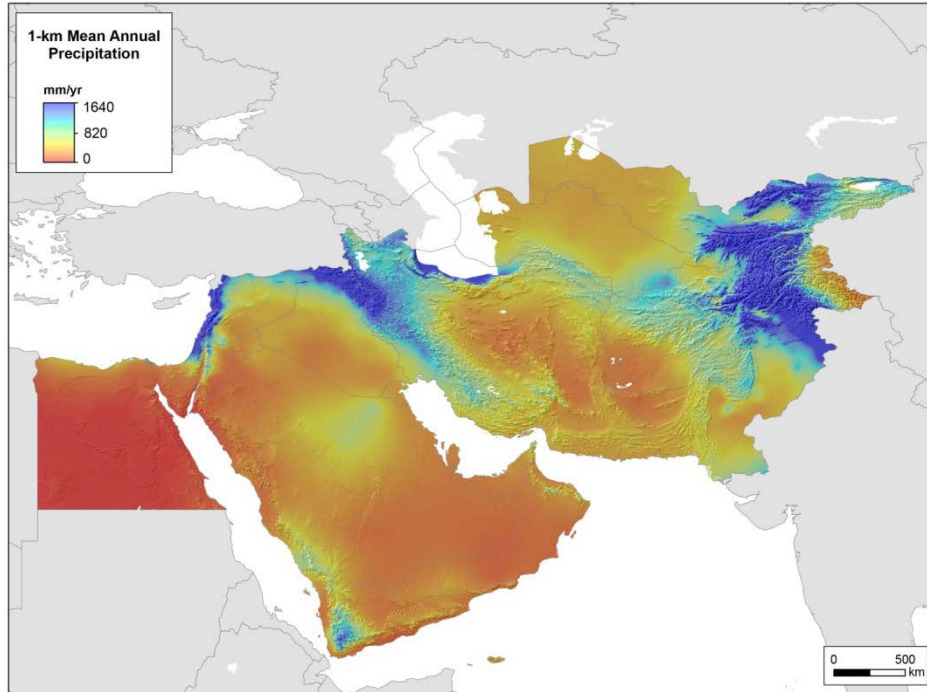
Figure 24. Continuous mean annual precipitation for USCENTCOM used to decrease potential dust flux.
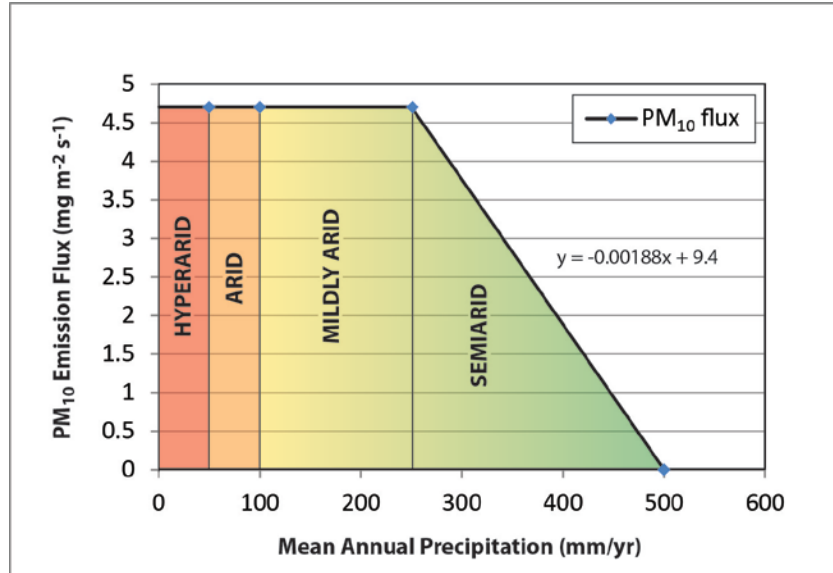

Figure 25. Example of how emission flux values were decreased to 0 using a linear function for the semiarid (250-500 mm/yr) class only. Emission flux values in hyperarid to mildy arid (0-250 mm/yr) areas were not changed. Emission flux values in areas with greater than 500 mm/yr of precipitation were assumed to have 0 emission.
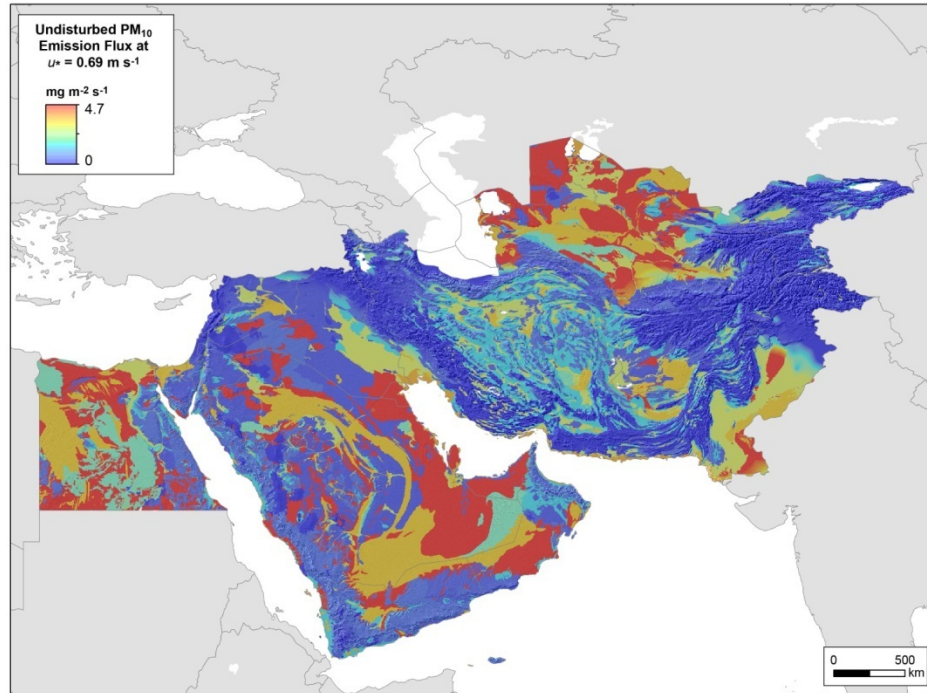
69

Figure 26. Deterministic mean PM$_{10}$ emission flux at 1km grid for USCENTCOM based on 1:750,000-scale landform mapping, the assignment of PI-SWERL data sets to analogous landforms, and integration of mean annual precipitation.
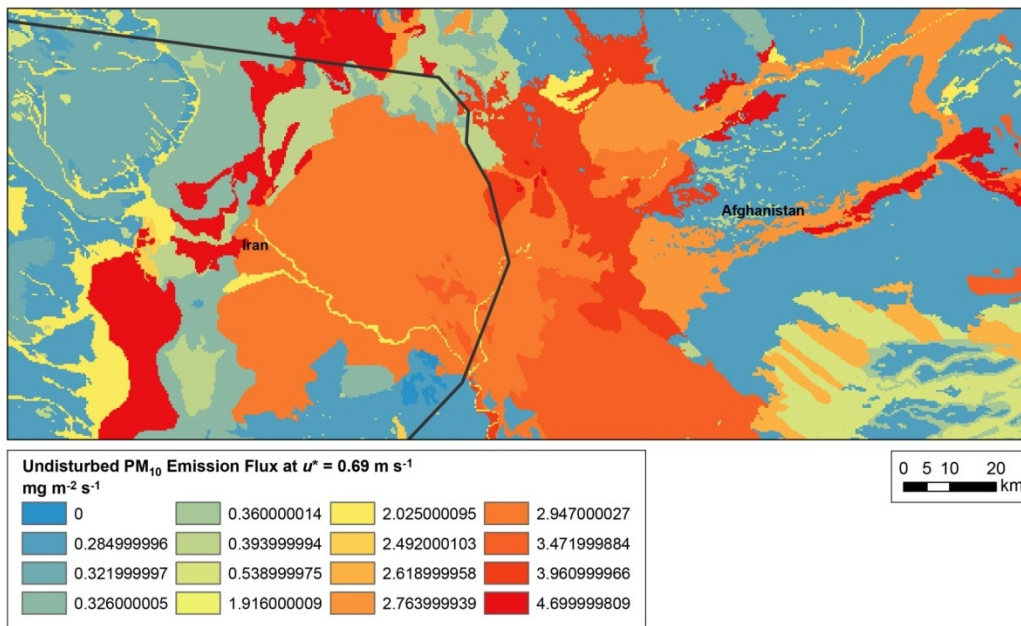
Figure 27. Deterministic mean PM$_{10}$ emission flux at 1km grid for border region between southwestern Afghanistan and southeastern Iran based on 1:100,000-scale landform mapping, the assignment of PI-SWERL data sets to analogous landforms, and integration of mean annual precipitation.

70

Conclusions

This study constitutes an initial step in the development of techniques to quantitatively determine the emission flux of PM_{10} from discrete landforms at both relatively small (strategic) to moderate (regional) map scales. The classification of PM_{10} emission flux in the USCENTCOM area of responsibility and southwestern Afghanistan will aid in validating and refining global and regional atmospheric dust loading models used by DoD.

5.3 Published manuscripts resulting from this work

Bacon, S., and McDonald, E., In press, Regional distribution of salt-rich dust across southwest Asia based predictive soil-geomorphic mapping techniques, *in* Harmon, R.S., and McDonald, E., eds., Reviews in Engineering Geology - Military Geoscience in the 21st Century: Denver, CO, Geological Society of America.

Bacon, S.N., McDonald, E.V., Dalldorf, G.K., Baker, S.E., Sabol, D.E., Minor, T.B., Bassett, S.D., MacCabe, S.R., and Bullard, T.F., 2010, Predictive soil maps based on geomorphic mapping, remote sensing, and soil databases in the desert southwest, *in* Boeettinger, J., Howell, D., Moore, A., Hartemink, A., and Kienast-Brown, S., eds., Digital soil mapping: bridging research, production, and environmental application: The Netherlands, Springer, p. 409-419.

McDonald, E.V., Bullard, T.F., Britt, T., and O'Ruiz, M.O., 2004, Development of archeological predictive model for management of military lands - Identification of geological variables in desert terrain, *in* Caldwell, D.R., Ehlen, J., and Harmon, R.S., eds., Studies in Military Geography and Geology, Kluwer Academic Publishers, p. 259-270.

6. Advanced Environmental Modeling and Visualization

6.1 Summary of overall accomplishments

The modeling group was tasked with the development of tools to forecast dust emissions from rotary aircraft operating over desert terrain. The main objectives of the group may be summarized as follows:

a) To develop a dust-emission parameterization scheme for rotorcraft in low-level flight;

b) To develop a local dust entrainment and dispersion scheme to simulate the transport of dust; and

c) To use the developed air quality modeling tools to build risk assessment tools for visibility and air quality impacts.

Modeling group members assisted with the collection of meteorological and helicopter-wake wind data during the Joint DRI Helicopter Dust Entrainment Experiment conducted at the U.S. Army Proving Grounds in Yuma, Arizona in May 2007 (hereafter referred to as the "Yuma experiment"). The data collected during this experiment was critical for fulfilling the model development objectives. The datasets were used to develop model parameters and to validate modeling results. An important result of this work was the confirmation of observed wake flow structure under a defined range of rotorcraft advance ratio at full scale. These ranges had been observed previously in scaled wind tunnel studies but never confirmed at the full scale in the literature. Figure 28 includes a plot of the observed wake detachment length (front of the frontal recirculation zone) and observed wake structure under a range of advance ratios (speed of the helicopter normalized by rotor parameters).
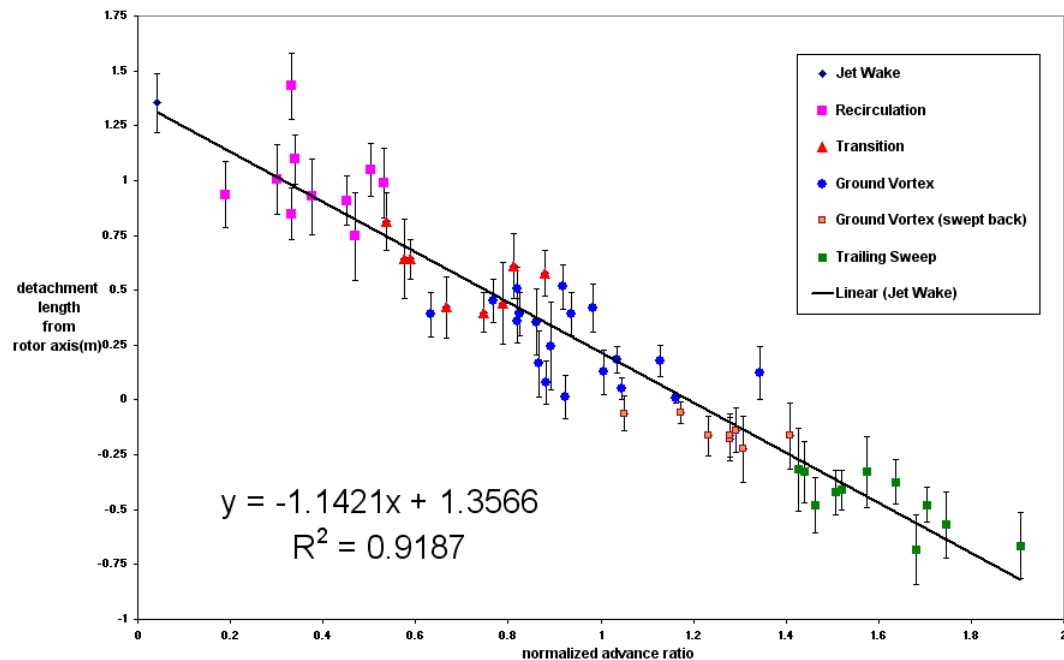

Figure 28. CFD modeling results superimposed over photographs of the helicopter low-level flights from the Yuma experiment (red/orange indicate higher velocity wind).

Video data collected by the group was used in conjunction with dust concentration data to define the impacts of dust on visibility as reported in McAlpine et al. (2007). This was an important result because it was shown that brown-out potential could be directly related to downwind measurements of dust concentration in the atmospheric surface layer. The model developed in McAlpine et al. (2007) was shown to closely predict the correct visibility deterioration when compared to visuals from the Yuma experiment, illustrated in Figure 29.

Initial helicopter wake modeling was conducted using a computational fluid dynamics (CFD) model and rotor disk parameterization scheme. The method was utilized in an attempt to define the mean wake structure for input into a dust entrainment and dispersion model. The modeling results were shown to adequately predict elements of the wake structure as measured during the Yuma experiment, under a certain range of operating conditions. Wake recirculation zones and surface shear stress were produced that qualitatively appeared physically realistic, as illustrated in Figure 30.
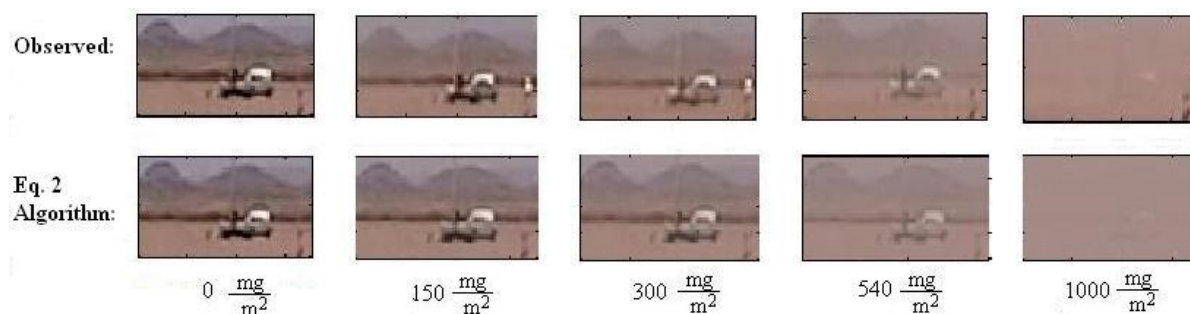

Figure 29. Simulated (bottom) and observed (top) visual impacts from helicopter dust entrainment using the model developed by the group.

The limitations of the modeling approach were defined as well as reported in McAlpine et al. (2010). This paper demonstrated also how well the CFD method used was able to estimate the forward detachment length of the helicopter wake, as shown in Figure 31, despite its shortcomings at simulating other wake features. Examples of the CFD-generated windfields superimposed on photographs from the Yuma experiment are included in Figure 32, demonstrating the capabilities of the method.

The helicopter wake fields generated with CFD were used in conjunction with a dust entrainment and dispersion model in further work. Shear-stress fields generated with CFD, an example of which is included in Figure 29, were used to estimate the flux of PM_{10} dust particles during low-level flight of the rotorcraft. A Lagrangian Stochastic Particle Dispersion Model (LSPDM) was developed by the group in order to limit instability prevalent in strong rotational flows. The LSPDM was used to model the movement of dust within and downstream of the helicopter wake: an example is included in Figure 33. This modeling method was used to simulate the entrainment of dust using the conditions observed during the Yuma experiment. The magnitudes of dust concentration downwind of the wakes were shown to compare well to experimental measurements (McAlpine, 2009). A qualitative example is included in Figure 34.
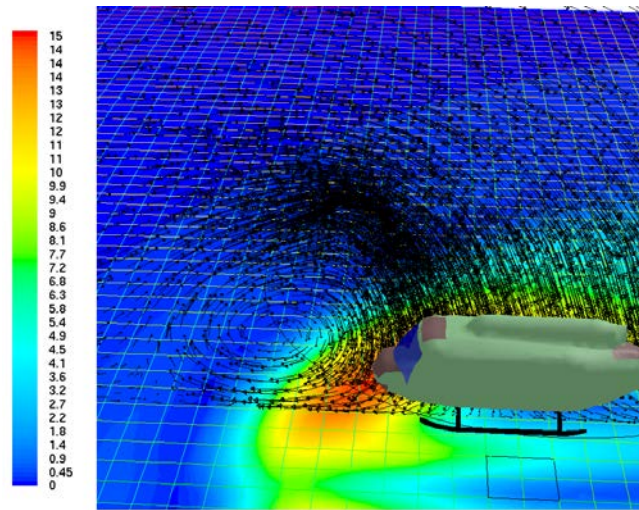
Figure 30. CFD modeling results of a rotorcraft operating near the ground: wind vectors are illustrated as well as surface shear stress.
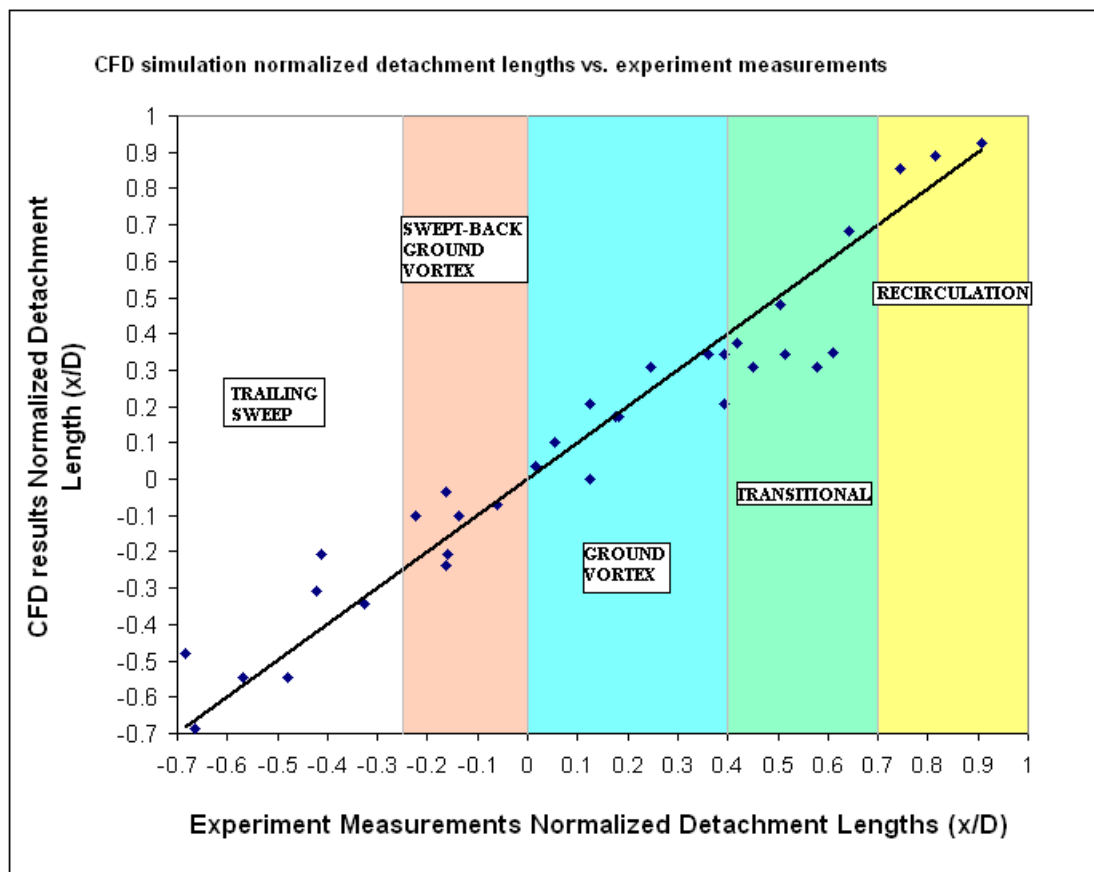

Figure 31. CFD modeling results vs. experimental estimates of normalized wake detachment length, x/D, where x is the detachment length and D is the rotor diameter.
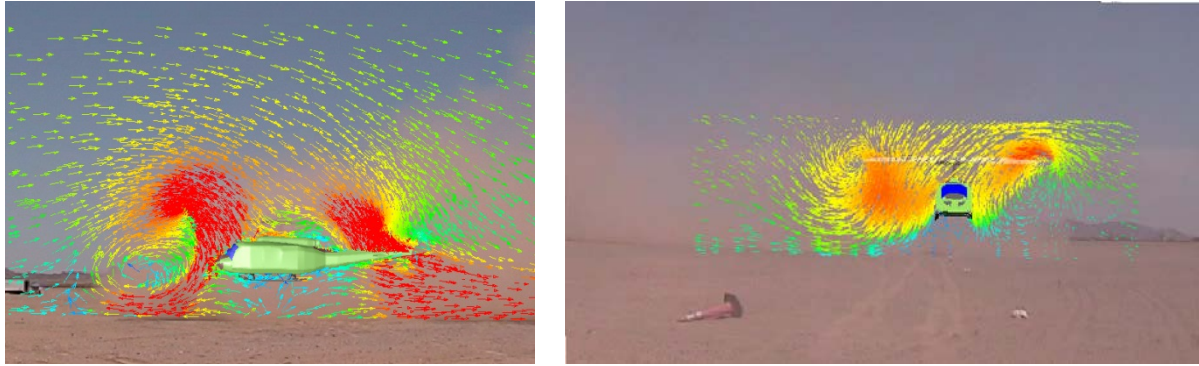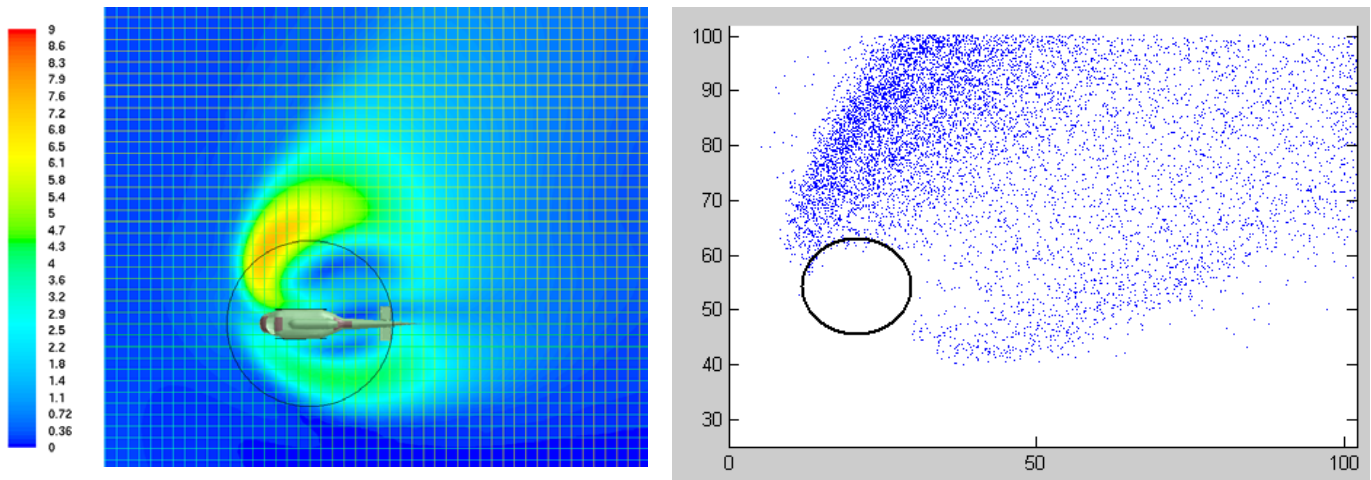
Figure 32. CFD modeling results superimposed over photographs of the helicopter low-level flights from the Yuma experiment (red/orange indicate higher velocity wind).

Figure 33. Shear-stress field used to simulate dust entrainment (left) and LSPDM dust dispersion modeling of dust in the helicopter wake (right).
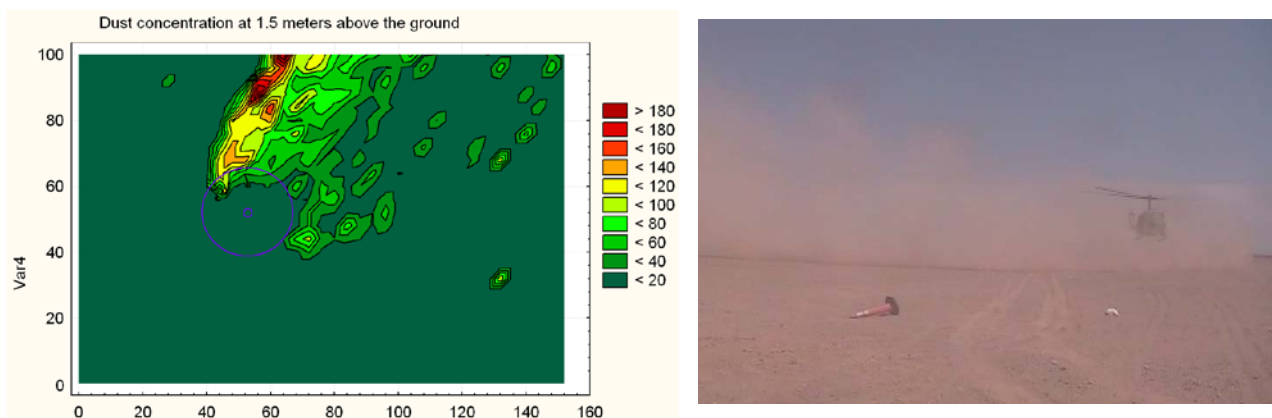

Figure 34. Snapshot of simulated dust concentrations (left) from the CFD-LSPDM model compared to the experiment case being simulated (right).

Despite some success with the coupled CFD-LSPDM approach, the modeling group altered strategy in 2011 to develop a more practical statistical parameterization scheme. The purpose of this was for easier implementation into existing air quality models and for development of a statistical risk-assessment tools. From this approach, a statistical model was developed referred to as the ROtorcraft Dust Emission Risk-assessment tool (RODER), described fully in McAlpine et al. (submitted (a)).

RODER uses a U.S. Dept. of Defense momentum-theory model, combined with a wake-structure model developed using data from the Yuma experiment, to estimate the surface shear-stress field in the wake of the rotorcraft. A state-of-the-art dust emission model is utilized to predict the volume of PM_{10} dust particles emitted from the surface. The model was shown to adequately predict the magnitude of dust emission measured using PI-SWERL at the U.S. Army Proving Grounds in Yuma as illustrated in Figure 35. Example results of this model for a full helicopter simulation are included in Figure 36 for a model run of conditions measured for a flight pass during the Yuma experiment (Day 1 [desert pavement surface], Pass 1 [6.1 m/s]).

RODER modeling of each flight pass using measured conditions from the Yuma experiment was conducted. These results were compared to the wake emission rate estimates from the experiment. Overall, the RODER model is shown to predict the magnitude of the wake dust emission rate quite satisfactorily; the comparison is included in Figure 37.
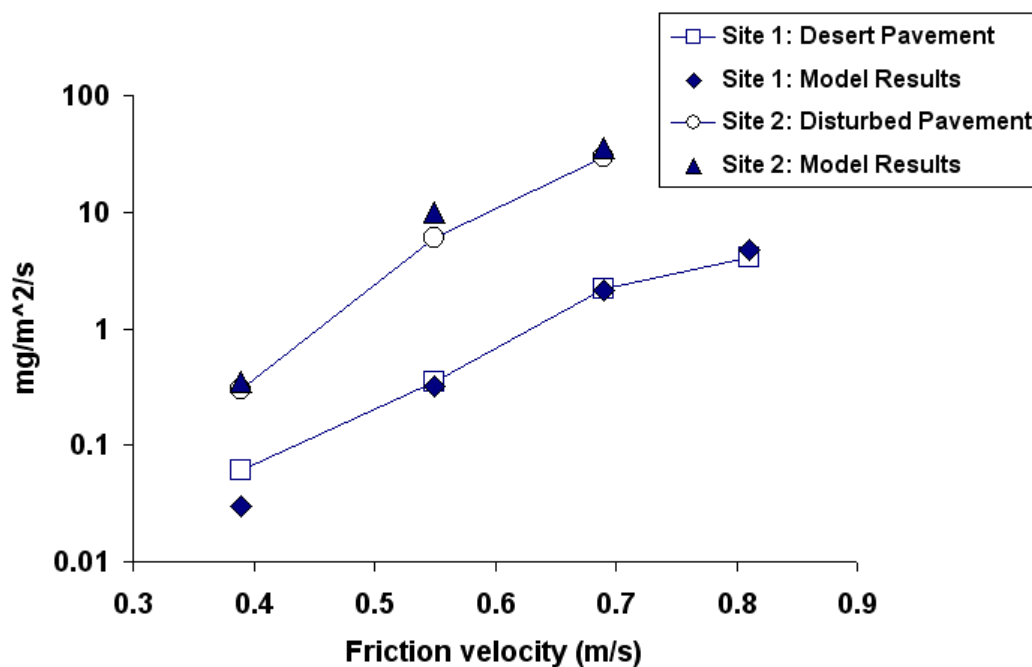

Figure 35. RODER model validation: results vs. PI-SWIRL emission rate measurements at the 2 helicopter dust experiment sites at the Yuma Proving Grounds.
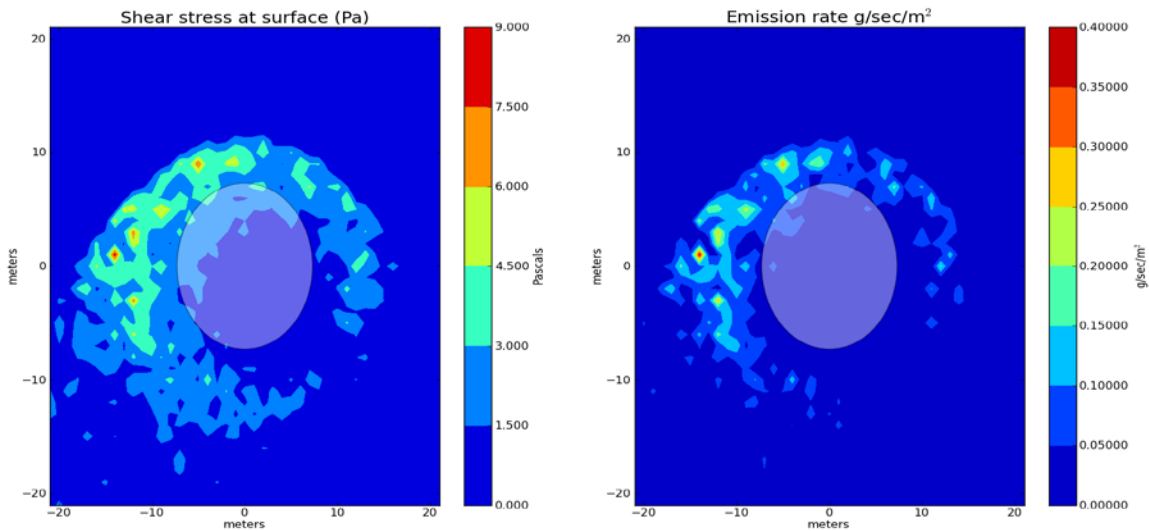
Figure 36. RODER model results: wake shear stress estimate (left) and dust emission rate (right) of a UH-1 rotorcraft operating near the surface at a low ground speed.
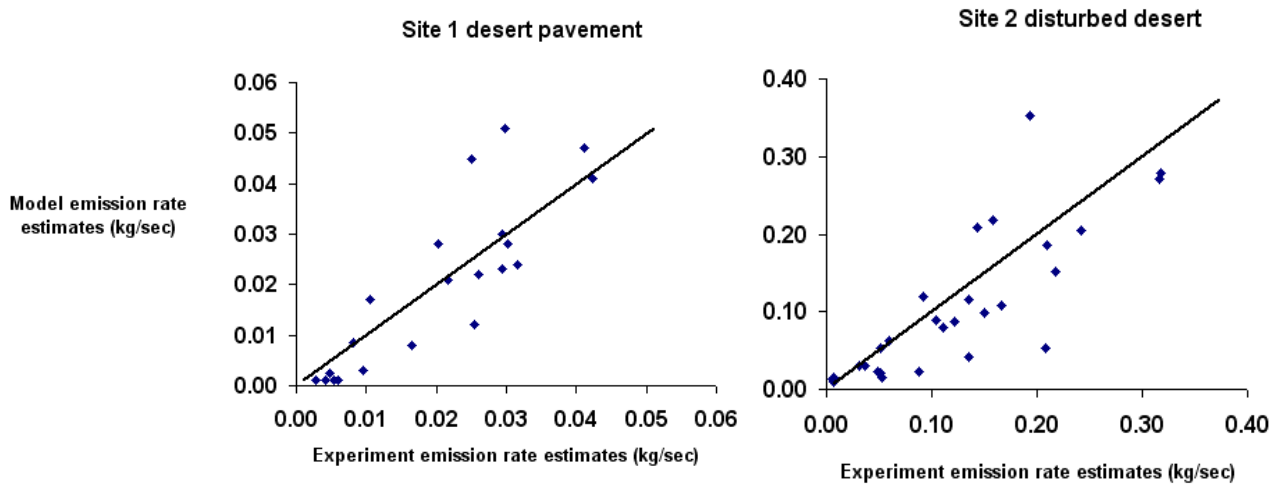

Figure 37. RODER model results for all Yuma experiment flight passes vs. emission rate estimates developed using dust concentration measurements.

The wake emission rates estimated with this model can be utilized by other tools, such as an air quality model or visibility risk-assessment tool. RODER itself contains a visibility risk-assessment tool developed using visibility impacts observed during the Yuma experiment. RODER produces a histogram of possible visibility impacts within the wake to help estimate the probability of brownout. The RODER brown-out risk assessment for the helicopter flight modeled above in Figure 36 (Yuma experiment, Day 1, Pass 1) is included in Figure 38: the model estimates average brown-out risk at moderate to high. Figure 38 includes photographs of the visibility impacts observed during the experiment for the Day 1, Pass 1 flight for

78

comparison. The development and capabilities of the RODER model were summarized in McAlpine et al. (Submitted (a)).

The RODER emission estimates are also a main component of the helicopter dust source parameterization scheme developed by the modeling group, summarized in McAlpine et al. (Submitted (b)). The parameterization scheme is the culmination of all work by the modeling group and can be adopted for use in any air quality model. The scheme itself consists of two parts:

a)   RODER to estimate the wake emissions; and

b)   An emission distribution tool that specifies the distribution of dust emitted from the source area.

Instead of directly modeling the advection of dust within the helicopter wake itself, the scheme describes the probabilistic spatial distribution of dust leaving a defined volume that encapsulates the wake (refer to Figure 32 for demonstration).

Visibility impact risk assessment using RODER was shown to be useful for predicting the spatial distribution of emission risk over a region for a rotorcraft operating under certain conditions. Figure 39 includes impact risk maps developed using estimates from RODER.

To determine the spatial distribution of dust leaving the source area, McAlpine (Submitted (b)) utilized inverse Lagrangian stochastic particle modeling to estimate the distribution of dust emission. An example of the inverse modeling results is included in Figure 40. Distribution modeling was conducted using conditions from Yuma experiment flight passes to relate changes in the distribution pattern to different helicopter operation parameters. A spatial probability density function scheme was developed relating the speed of the helicopter to the distribution of emission from the wake.

The final helicopter dust parameterization scheme is used in conjunction with a boundary-layer LSPDM in McAlpine (Submitted (b)) using the conditions observed during the Yuma experiment. Simulated dust concentrations will be compared to experimental measurements to analyze the effectiveness of the scheme.
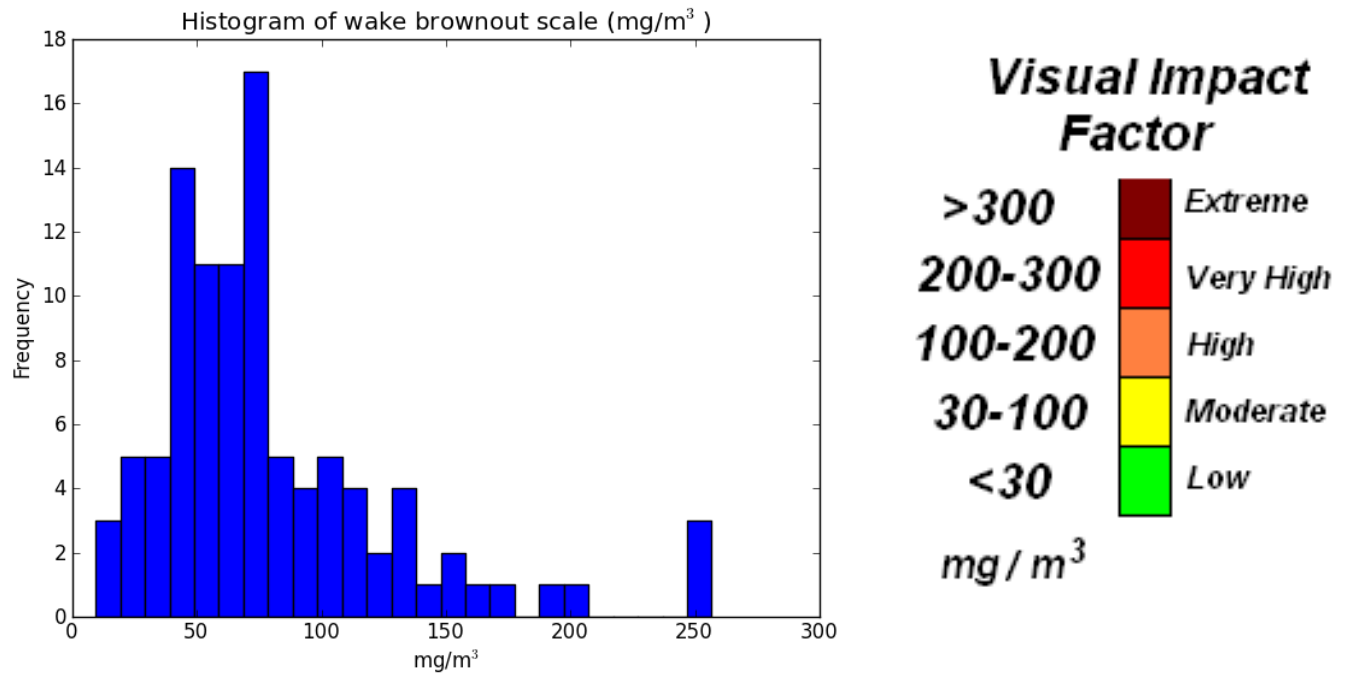
Figure 38. RODER visibility impact risk estimate histogram (top) compared to the actual visual impacts observed for the flight pass modeled.
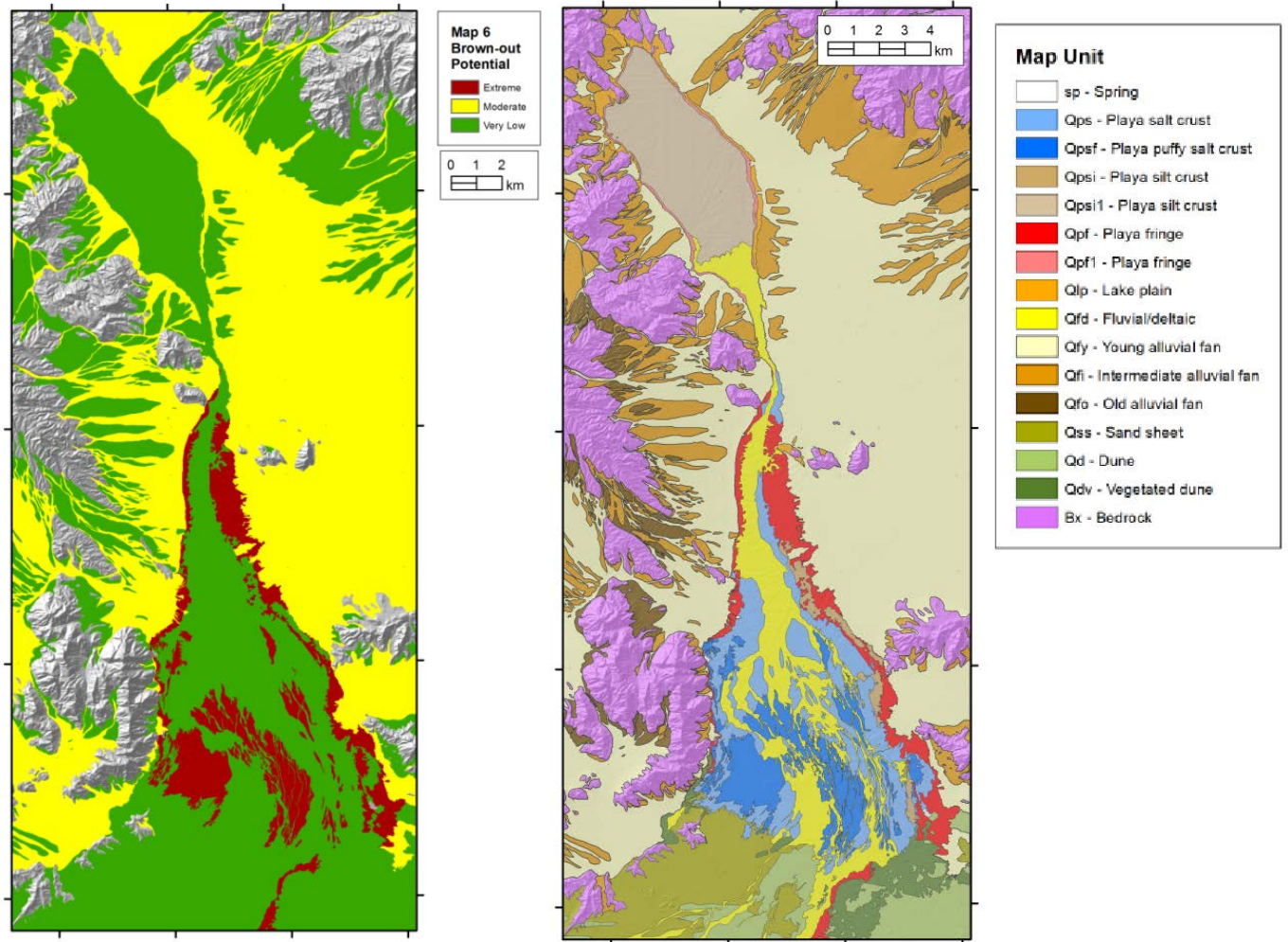
Figure 39. Brown-out potential risk map for a helicopter operating near the surface given specified operation parameters and weather conditions (left). Emission potential is strongly dependent on landform and soil type (right).
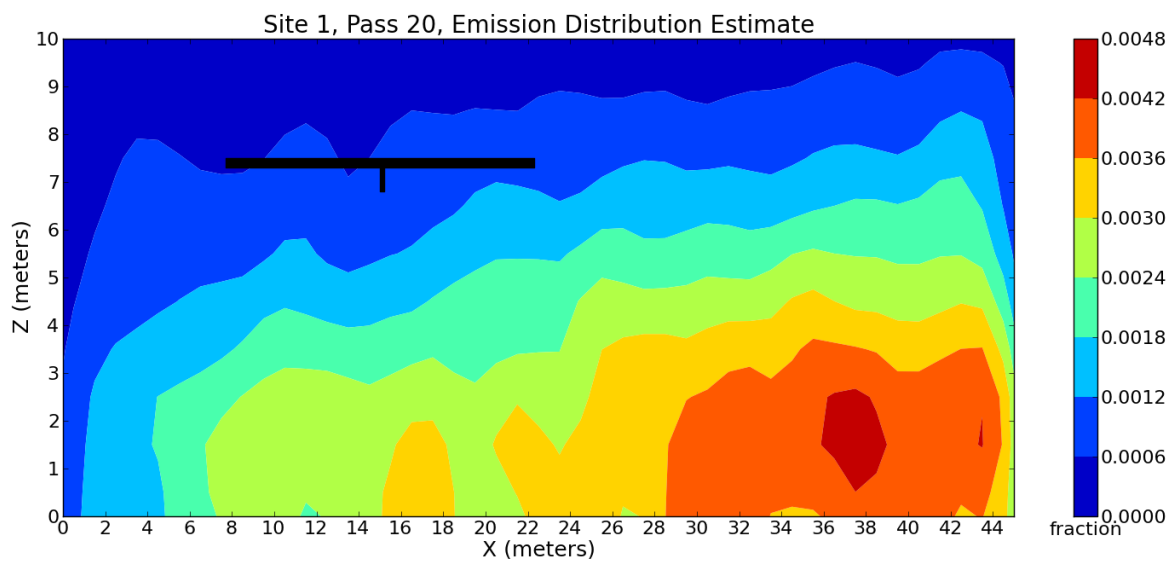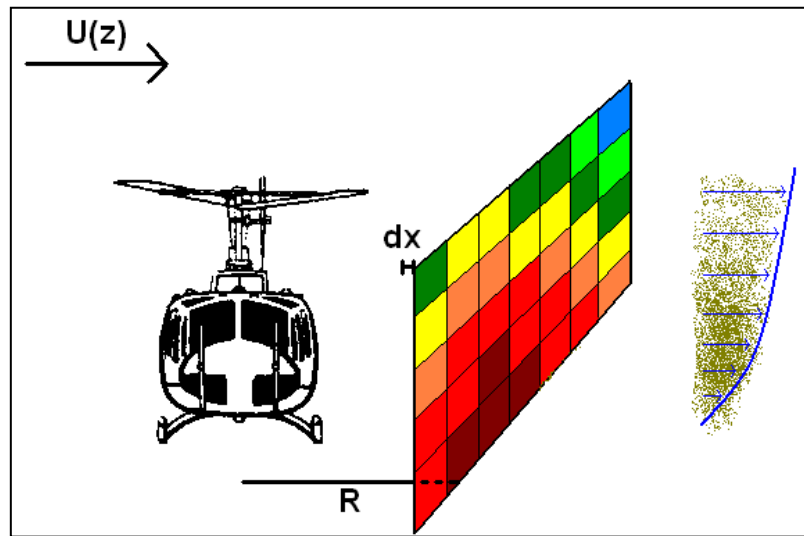
Figure 40. Inverse LSPDM: demonstration of the method (top), dust emission spatial distribution on the down-wind plane representing the boundary of the helicopter wake. Inverse LSPDM modeling results from the Day 1 (Site 1), Pass 20 helicopter flight Pass (bottom). U(z) represents the incoming wind and R is the rotor radius.

6.2 Published manuscripts resulting from this work

McAlpine, J.D., Koracin, D., Veropoulos, K., Boyle, D., McDonald, E.V., and Lamoray, G., 2007, Determining atmospheric dust concentrations during strong flow perturbations using a digital-optical technique: Lecture notes in Computer Science, v. 4841/2007, p. 393-402.

McAlpine, J.D., Koracin, D., Bacon, S., and McDonald, E., Submitted (a), Development of a rotorcraft dust-source parameterization for air-quality modeling: Atmospheric Environment.

McAlpine, J.D., Koracin, D., and McDonald, E., Submitted (b), Simulation and parameterization of atmospheric surface flow with computational fluid dynamics: Computers and Fluids.

McAlpine, J.D., Koracin, D.R., Boyle, D.P., Gillies, J.A., and McDonald, E.V., 2010, Development of rotorcraft dust-emission parameterization using a CFD model: Environmental Fluid Mechanics, v. 10, p. 691-710.

APPENDIX 1: TECHNOLOGY TRANSFER, FY2012

1) **Emission Flux Characterization of Disturbed Landform Surfaces (U.S. Air Force Weather Agency (AFWA) 16th Weather Squadron Dust and Aerosols Team Offutt Air Force Base, NE)**: DRI provided geomorphic-based dust emission data to support the evaluation of atmospheric dust-loading models that AFWA currently uses to forecast weather conditions and dust storm activity within the USCENTCOM area of responsibility. Project results have been integrated in AFWA models used to predict regional dust storm activity and have been demonstrated by AFWA to dramatically increase AFWA's forecasting efficiency.

2) **Yuma Proving Ground, Advance Technology Directorate (ATD)**: DRI provided ATD with a variety of datasets (soil, geomorphic mapping, dust chemistry data) to assist in developing web-accessible terrain data to support test operations of military equipment.

3) **Joint Improvised Explosive Device Defeat Organization (JIEDDO) Test Board**: DRI provided soil and terrain characterization support and data to investigate possible ground effects on near-surface radio frequency propagation. Results indicate that the soil properties will results in large deviations of signal strength in certain settings.

4) **Briefings Conducted at Army Laboratories, installations, and other DoD Organizations:**

> DoD Locations of technical briefings that have presented results from this project:
> - US Military Academy, West Point
> - ERDC-Topographic Engineering Center
> - ERDC-Geotechnical and Structures Lab
> - ERDC-Cold Regions and Engineering Lab
> - ERDC-Construction and Engineering Lab
> - ERDC Edgewood Chemical Biologic Center
> - Yuma Proving Ground, AZ
> - National Training Center, Ft. Irwin, CA
> - Ft. Carson, CO
> - Ft. Greely, AK
> - AFRL, Wright-Patterson AFB, OH
> - Offutt AFB, Omaha, NB
> - National Geospatial-Intelligence Agency, Bethesda, MD
> - Army Research Laboratories, Bethesda, MD
> - NVESD (Night Vision and Electronic Sensors Directorate), Ft. Belvoir, VA